MEASURING, UNDERSTANDING AND MODELING ECOHYDROLOGICAL SEPARATION

A Thesis Submitted to the College of
Graduate Studies and Research
In Partial Fulfillment of the Requirements
For the Degree of Doctor of Philosophy
In the School of Environment and Sustainability
University of Saskatchewan
Saskatoon

By

JAIVIME EVARISTO

PERMISSION TO USE

In presenting this thesis/dissertation in partial fulfillment of the requirements for a Postgraduate degree from the University of Saskatchewan, I agree that the Libraries of this University may make it freely available for inspection. I further agree that permission for copying of this thesis/dissertation in any manner, in whole or in part, for scholarly purposes may be granted by the professor or professors who supervised my thesis/dissertation work or, in their absence, by the Head of the Department or the Dean of the College in which my thesis work was done. It is understood that any copying or publication or use of this thesis/dissertation or parts thereof for financial gain shall not be allowed without my written permission. It is also understood that due recognition shall be given to me and to the University of Saskatchewan in any scholarly use which may be made of any material in my thesis/dissertation.

DISCLAIMER

The software and platforms (ArcGIS, statistical analyses) were used to meet the thesis and/or exhibition requirements for the degree of Doctor of Philosophy at the University of Saskatchewan. Reference in this thesis/dissertation to any specific commercial products, process, or service by trade name, trademark, manufacturer, or otherwise, does not constitute or imply its endorsement, recommendation, or favoring by the University of Saskatchewan. The views and opinions of the author expressed herein do not state or reflect those of the University of Saskatchewan, and shall not be used for advertising or product endorsement purposes.

Requests for permission to copy or to make other uses of materials in this thesis/dissertation in whole or part should be addressed to:

Executive Director

School of Environment and Sustainability

University of Saskatchewan

Room 323, Kirk Hall

117 Science Place

Saskatoon, Saskatchewan S7N 5C8 Canada

ABSTRACT

My dissertation sought to answer some of the fundamental questions on how subsurface water may be partitioned between root water uptake and streamflow. I explored a phenomenon called *ecohydrological separation* – plants using water of a character different from the mobile water found in soils, groundwater and streams. The generality of ecohydrological separation, however, remained wanting; and, possible controls in both space and time was elusive. I began with testing the generality of ecohydrological separation, first at two sites in the tropics with contrasting moisture conditions, and then at the global scale. Using a global database of water stable isotopes, I then quantified the degree of groundwater use by vegetation. Finally, I unscrambled the possible process controls behind the partitioning of subsurface water between root water uptake, groundwater recharge, and streamflow generation by conducting controlled drought-rewetting experiments in a tropical mesocosm. Key results of these research efforts were: (1) ecohydrological separation was widespread across biomes of the world, providing clues to fundamental controls; (2) groundwater use by vegetation globally was not as widespread as increasingly assumed in the literature; and, (3) transpiration flux was older than groundwater recharge flux, supporting a perceptual model whereby transpiration and groundwater recharge fluxes were sourced from separate storage volumes and sampled at markedly different average sampling flux. Because determining the ages and sources of water that supply transpiration and groundwater recharge was a major challenge in ecohydrology, these findings are ground-breaking. Indeed, I was the first to measure and quantify what was referred heretofore as the "missing exit age" of transpiration. The mechanisms underlying the phenomenological manifestations of ecohydrological separation, as explored and uncovered in my dissertation, have direct implications for how we measure and model the transport of water, nutrients, and pollutants at various scales in space and time.

ACKNOWLEDGEMENTS

First, to my PhD supervisor and mentor, Dr. Jeffrey J. McDonnell, for the intellectual inspiration and motivation, for constantly and creatively challenging paradigms, and for nurturing a culture of excellence. “It is never too early to pose a question, write and be published”, Jeff would say. Second, to my collaborators – Dr. Scott Jasechko (U Calgary), Martha Scholl (US Geological Survey), Dr. Sampurno Bruijnzeel (King’s College London), Dr. Kwok P. Chun (Hong Kong Baptist U), Dr. Joost van Haaren (U Arizona), Dr. Peter Troch (U Arizona), Minseok Kim (Johns Hopkins U), Dr. Ciaran Harman (Johns Hopkins U), and Dr. Luke Pangle (Georgia State U) – for the exchange of ideas and synergy of expertise that led to the completion of manuscripts embodied in this dissertation. Third, to the Global Institute for Water Security, School of Environment and Sustainability, and Saskatchewan Innovation and Opportunity Scholarship, for the range of financial support extended that made my research possible. Fourth, to Kim Janzen and Cody Millar for lab and logistical support in water extractions and isotopic analyses; and to other members of McDonnell Lab (Anna Coles, Chris Gabrielli, Dyan Pratt, Willemijn Appels, Natalie Orlowski, Veva McDonnell) for promoting vibrant group discussions. Finally but not least, to members of my PhD Committee – Dr. Saman Razavi, Dr. Sina Adl, Dr. Bingcheng Si, Dr. Yanping Li – for the guidance and support from inception of research chapters that constitute this dissertation through to its implementation. Thank you.

PERMISSION TO REPRODUCE

Permission to reproduce two published manuscripts in this dissertation was acquired from the following publishers:

1. Evaristo, J., S. Jasechko, and J. J. McDonnell (2015), Global separation of plant transpiration from groundwater and streamflow, *Nature, 525*, 91-94.

   Publisher: Springer Nature

   Copyright: Jaivime Evaristo (Author)

2. Evaristo, J., J. J. McDonnell, M. A. Scholl, L. A. Bruijnzeel, and K. P. Chun (2016), Insights into plant water uptake from xylem-water isotope measurements in two tropical catchments with contrasting moisture conditions, *Hydrol. Process., 30*, 3210-3227.

   Publisher: John Wiley and Sons

   Copyright: John Wiley and Sons

   License number: 3934361399581

   License date: Aug 22, 2016

DEDICATION

For Mama, Papa, Yepyep, and Greanne, forthcoming daughter, Zeneva Isabelle, and Myla

TABLE OF CONTENTS

page

LIST OF TABLES

LIST OF FIGURES

LIST OF ABBREVIATIONS

AET	actual evapotranspiration
ANPP	above-ground net primary productivity
B2-TRF	Biosphere 2 Tropical Rainforest
BNPP	below-ground net primary productivity
$C_{M,i}$	dimensionless mixing coefficient
CRDS	cavity ring-down spectroscopy
DBH	diameter at breast height
d-excess	deuterium excess
DREAM	DiffeRential Evolution Adaptive Metropolis
e_0	evaporation rate
EL	evaporation line
erf	error function
ET	evapotranspiration
E_w	wet-canopy evaporation rate
GMWL	global meteoric water line
GPP	gross primary productivity
GW	groundwater
IAEA/WMO	International Atomic Energy Agency / World Meteorological Organization
IRIS	isotope ratio infrared spectroscopy
IRMS	isotope ratio mass spectrometry
K_{eff}	effective soil hydraulic conductivity
L_C	stage 1 evaporation characteristic length
LCE	line-conditioned excess
LEL	local evaporation line
L_G	gravity characteristic length

LGR OA-ICOS	Los Gatos Research off-axis integrated cavity output spectroscopy
LMWL	local meteoric water lines
LTER-LUQ	Long term Ecological Research Luquillo
LUQ	Luquillo
MAP	mean annual precipitation
MAT	mean annual temperature
MCMC	Markov Chain Monte Carlo
MTT	mean transit time
NCBI	National Center for Biotechnology Information
NPP	net primary productivity
P	precipitation
PBM	process-based mixing
PET	potential evapotranspiration
RH	relative humidity
RWU	root water uptake
SIAR	Stable Isotope Analysis in R
SIRFER	Stable Isotope Ratio Facility for Environmental Research
SLM	simple linear mixing
SMOW	standard mean ocean water
S_U	root zone actual storage
S_{Umax}	root zone actual storage
SUS	Susua
SWP	soil water potential
T	transpiration
TEF	trophic enrichment factor
TT	transit time
TTD	transit time distribution
USDA NRCS	United States Department of Agriculture Natural Resources Conservation Service

USGS	United States Geological Survey
VPD	vapor pressure deficit
V-SMOW	Vienna standard mean ocean water
VWA	volume weighted average
VWC	volumetric water content

CHAPTER 1

INTRODUCTION

Water uptake by vegetation (i.e. transpiration) returns almost half of terrestrial precipitation to the global water cycle (Schlesinger and Jasechko, 2014). The partitioning of terrestrial precipitation between transpiration, interception, soil water evaporation, soil and groundwater recharge and streamflow generation under different physiographic characteristics, however, is poorly understood (Vivoni *et al*., 2008; Gouet-Kaplan *et al*., 2012). Environmental tracers, particularly water stable isotopes ($\delta^{18}O$ and $\delta^{2}H$ or δD), are powerful tools for partitioning the different components of the ecohydrological cycle (Ehleringer and Dawson, 1992). The utility of water stable isotopes in ecohydrological investigations is built on the assumption that root water uptake is generally considered a non-fractionating process (Dawson and Ehleringer, 1991). That is, the isotopic composition of xylem (i.e. stem or sap) water represents an integrated signal of its sources in the subsurface.

Investigations in humid continental and arid/semi-arid environments have demonstrated the variable temporal and spatial responses of trees to antecedent climate histories. White *et al*. (1985) reported that depending on the recent history of precipitation events, eastern white pine (*Pinus strobus*) switches water extraction between deep and surface soil layers, as well as between groundwater and heartwood water. In a semi-arid setting, however, Dawson and Ehleringer (1991) showed that mature trees growing in or near a perennial stream used little or none of that stream's water, while small streamside individuals and small non-streamside individuals used stream water and recent precipitation, respectively, as their primary water sources. The authors explained that this behavior by mature riparian trees allowed the species to avoid interspecies competition with more shallow-rooted shrub and herb species within the same site, particularly in periods when availability of moisture in upper soil layers was limited. These findings were supported by investigations in other riparian ecosystems along the Colorado River

in the western United States (Busch *et al*., 1992) and along the floodplains of River Murray in Australia (Thorburn *et al*., 1993).

To examine more closely how vegetation responds to summer precipitation in climates where both winter, spring and summer precipitation are received, Flanagan & Ehleringer (1991) surveyed the water uptake patterns of two dominant tree species (rabbitbrush and Utah juniper) and two dominant shrub species (pinyon pine and sagebrush) in a pinyon-juniper ecosystem site in southern Utah. They found that rabbitbrush and Utah juniper did not utilize summer precipitation during the year of study; xylem sap remained close to that of the groundwater, indicating winter recharge precipitation. In contrast, pinyon pine and sagebrush utilized summer precipitation. The apparent differential species response was also demonstrated by Valentini *et al.* (1992) in a study of a Mediterranean macchia ecosystem. Moreover, Ehleringer and Dawson (1992) argued that while a general physiological response is evident in environments where summer-winter bimodality is strong, and where precipitation input, or the lack of it, is predictable. Some plants can develop a dimorphic root system to hedge against the risks of a variable moisture input in some environments. This was illustrated by Pate and Dawson (1999) in an investigation of phraetophytic plants of dimorphic root morphology in Australia. They reported that during the dry season, plants derived the majority of their water from deeper sources while in the wet season, most of the water they used was derived from shallower sources supplied by lateral roots in the upper soil layers. These results pointed to a process called "hydraulic lift" (Richards and Caldwell, 1987), which refers to the nocturnal movement of water from deep, hydric soil layers through roots to upper, more xeric soil layers (Dawson 1993). The occurrence of hydraulic lift has been shown in arid and semi-arid environments (Caldwell and Richards 1989) as well as in more mesic regions (Dawson 1993), with the latter investigator illustrating how plants that were situated close to trees that conducted hydraulic lift could use a significant proportion of this water.

In the tropics, one of the most important drivers of soil-plant hydrology research has been in the context of forest harvesting and replanting with exotics. The introduction of fast-growing exotic tree species has caused some concerns among academics and resource managers alike (Pohjonen

and Pukkala 1990; McJannet *et al*. 2000). For example, Fritzsche *et al*. (2006) reported that the growth of an exotic species, *Eucalyptus globulus* Labill., in south Ethiopia was largely independent of topsoil water content, giving it the potential to cause substantial dry-season groundwater depletion. Lachniet and Patterson (2002), on the other hand, examined the spatial variation in $\delta^{18}O$ and δD of surface waters and precipitation in Costa Rica. They postulated that recycled moisture in certain regions of the country was an important component of the water budget. Although results, among others, showed weak relationships between the $\delta^{18}O$ of surface waters and latitude, longitude, elevation, and distance from the Caribbean Sea, they found some distinct geographic trends such as the inverse relationship of $\delta^{18}O$ and δD values in the leeward side of the mountain ranges in relation to the altitude that the air masses traversed. These local, aspect-scale variations in $\delta^{18}O$ and δD values may have some practical implications for water budgets, particularly in temporal and spatial upscaling of these results from catchment to continental scales (Bowen and Wilkinson, 2002).

A majority of investigations using water stable isotopes in tropical ecohydrology, however, has centered on soil-water partitioning objectives. Soil-water partitioning patterns have been explored and linked to their relationships to leaf phenology, differences in rooting patterns, and root activity (Meinzer *et al*. 1999) among others (Jackson *et al*. 1995; Stratton, Goldstein, & Meinzer 2000; Andrade *et al*. 2005; Lambs, Muller, & Fromard 2008; Gutierrez-Soto and Ewel 2008). In a study during a four-month dry season of several diverse canopy species in a lowland tropical forest in Panama, Meinzer *et al*. (1999) reported a species independent behavior and a strong positive relationship between tree size (diameter at breast height, DBH) and xylem water δD. That is, smaller trees tapped deeper sources of soil water (more negative δD) than larger trees. The seasonal variation of this trend, moreover, was demonstrated to have a strong association with leaf phenology. The influence of species-specific attributes like leaf phenology to water use was supported by Gutierrez-Soto and Ewel (2008) who, in a study of soil water use patterns of four model plant associations in Costa Rica, reported that temporal factors were important in determining the competition and complementary relations among plant associations. They illustrated that species-specific attributes, such as biomass allocation to fine roots, phenology, and canopy structure, determined the water use in the plant associations investigated.

While the use of water stable isotopes in ecohydrological studies has improved our understanding of the role of vegetation in modifying seasonal macroclimates (Troch *et al*., 2009; Lee *et al*., 2005; Bonan, 2002) and local microclimates (Green *et al*., 2015; Simonin *et al*., 2013), the prevailing assumption is that vegetation draws water from the same subsurface stocks that eventually reach the stream (i.e. green vs. blue water flows in D'Odorico *et al*., 2010). If that were universally the case and knowing that root water uptake is generally a non-fractionating process, then subsurface water pools contributing to groundwater recharge and streamflow should have similar stable water isotope ratios as some of the subsurface water stocks that are available for root water uptake. However, work by Brooks *et al*. (2010) and Goldsmith *et al*. (2012) in Mediterranean and seasonally dry tropical settings, respectively, has suggested that there may be *ecohydrological separation*..Ecohydrological separation (also known colloquially as the *two water worlds* hypothesis; McDonnell, 2014) posits that the water used by vegetation is different from the "more mobile" water in soils, groundwater and streams. A similar phenomenon was also recently reported using nitrate isotopes (*two nitrate worlds*) (Hall *et al.*, 2016), thereby supporting the idea that water/nutrient uptake by vegetation and groundwater recharge/nutrient export to streams are separated. Indeed, if ecohydrological separation is real, then the implications, among others, for quantifying transit times in streams using current approaches that assumed a well-mixed subsurface are profound, since ecohydrological separation is synonymous with an acutely non-well mixed subsurface.

Recent satellite-based global isotope mass balance work (Good *et al*. 2015) shows that ecohydrological separation is more likely the rule than the exception, and that water contributing to groundwater recharge is often (but not always) isolated from water used in plant transpiration (Jasechko and Taylor, 2015; Jasechko *et al*., 2014). Nevertheless, the need to test for ecohydrological separation under different physiographic settings persists; its implications for the role of groundwater (saturated zone or phreatic water) in sustaining vegetation at the global scale are yet to be established; and, the possible controls underlying these phenomenological observations have yet to be unraveled.

1.1 Objectives and Hypotheses

The overarching objective of my PhD research work was to understand some of the outstanding fundamental questions on how subsurface water might be partitioned between root water uptake and groundwater recharge or streamflow. In particular and at the center of this objective was the phenomenological observation called *ecohydrological separation* which, heretofore, remained poorly understood. In achieving the overarching objective, I systematically organized my research work into chapters that independently addressed the following outstanding questions surrounding ecohydrological separation:

1. Is ecohydrological separation a phenomenon unique to highly seasonal settings where hydrologic input is temporally "out of phase" with primary productivity?
2. Is ecohydrological separation widespread?
3. What is the degree of groundwater use by vegetation at the scale of the globe?
4. What are the possible mechanisms that control ecohydrological separation?

I began with testing the generality of ecohydrological separation (Chapters 2 and 3). Although not mutually exclusive, ecohydrological separation has implications for the role of groundwater in sustaining vegetation. A synthesis of groundwater-vegetation work, however, remained wanting. It was against this backdrop that I embarked on a meta-analysis to be able to quantify the degree of groundwater use by vegetation at the global scale (Chapter 4). Having established the generality of ecohydrological separation and quantified the magnitude of dependence of groundwater use by vegetation, I conducted a controlled drought and rewetting experiment to be able to unscramble the possible process controls behind ecohydrological separation, that is, the partitioning of subsurface water between root water uptake, groundwater recharge, and streamflow generation (Chapter 5).

Specifically, in Chapter 2, my main objective was to test for ecohydrological separation in less seasonal semi-arid and humid tropics. Following the original work on ecohydrological separation by Brooks *et al*. (2010), it was suggested that ecohydrological separation may be explained by a site's wetness-dependent interconnectivity. Phillips (2010) described wetness-dependent interconnectivity as a precondition for ecohydrological separation whereby the timing of

vegetation activity (e.g. primary productivity) is "out of phase" with hydrological activity (e.g. precipitation input) – the boundary conditions that broadly described the study system of Brooks *et al*. (2010) in Oregon, USA. At the ecosystem scale, such a precondition for ecohydrological separation might pertain to sites with high seasonality as the case was in Goldsmith *et al*. (2012) in the seasonally dry tropical climate in Veracruz, Mexico. At the scale of flow systems in the soil, such a precondition supports a mechanistic interpretation whereby the exchange between soil-matrix water (contributing to transpiration) and preferential flow path water (contributing to groundwater recharge and streamflow) is negligible; thus, supporting an observation consistent with ecohydrological separation. If wetness-dependent interconnectivity is indeed a precondition for ecohydrological separation then the latter should not be evident in settings where wetness-dependent interconnectivity is high, that is, in less seasonal systems. To this end, I posed this as a null hypothesis to test in two less seasonal semi-arid and humid sites in Puerto Rico. My null hypothesis was that ecohydrological separation is an observation that is specific to Mediterranean and seasonally dry tropical climates, and therefore absent in settings where hydrologic input is temporally in-phase with primary productivity. To demonstrate temporal phasing between hydrologic input and primary productivity, I performed a time-series analysis on 8.5-yr rainfall amount, rainfall isotope ($\delta^{18}O$), and gross primary productivity (GPP) data. I then tested for ecohydrological separation using xylem (stem) water of mahogany (*Swietenia* spp.), soil water, groundwater, and stream water isotopes collected during two contrasting moisture periods. Finally, I explored the utility of a simple linear mixing model, implemented in a Bayesian inference framework, to quantify source water contributions at both sites and moisture periods. This study was submitted for peer review in July 2014 and was accepted for publication in March 2016 [Citation: Evaristo, J., J. J. McDonnell, M. A. Scholl, L. A. Bruijnzeel, and K. P. Chun (2016), "Insights into plant water uptake from xylem-water isotope measurements in two tropical catchments with contrasting moisture conditions", *Hydrol. Process., 30*, 3210-3227].

In Chapter 3, my main objective was to test the generality of ecohydrological separation at the scale of the globe. Following the site-level studies that provided evidence consistent with ecohydrological separation (Brooks *et al*., 2010; Goldsmith *et al*., 2012; Evaristo *et al*., 2016), I

embarked on a meta-analysis of published literature for water stable isotopes in ecology and hydrology. To this end, my null hypothesis was that ecohydrological separation is an observation that is specific to a few sites, and therefore not generalizable across biomes and diverse physiographic settings of the world. Because prior work on ecohydrological separation was based on the "offset" of a water sample (xylem water, soil water, groundwater, stream water) from the local meteoric water line, I included only dual-isotope studies and excluded papers that used only δ^2H or $\delta^{18}O$ alone. I extracted groundwater isotope data either from compiled papers or from a comprehensive groundwater database. I then conducted a sensitivity analysis to support the use of groundwater data within an optimal radius around each study site. Appropriate statistical techniques were used to demonstrate ecohydrological separation between xylem/soil water and groundwater/stream water, from site- to biome-level. This study was submitted for peer review in September 2014 and was accepted for publication in July 2015 [Citation: Evaristo, J., S. Jasechko, and J. J. McDonnell (2015), "Global separation of plant transpiration from groundwater and streamflow", *Nature, 525*, 91-94.].

In Chapter 4, my main objective was to quantify the degree of groundwater (saturated zone or phreatic water) use by vegetation at the global scale. One corollary implication of ecohydrological separation is the supposition that groundwater use by vegetation may not be as widespread as increasingly being suggested in the literature (e.g. Fan, 2015). That root water uptake does not result in isotopic fractionation underlies the utility of stable isotopes in plant water uptake investigations. While many site-based studies have now been completed, a global synthesis of these data has not yet been made. To this end, I developed two testable hypotheses: (1) groundwater use by vegetation is significant, that is, greater than 50% of the world's vegetation; (2) groundwater use by vegetation is not significant, that is, less than 50% of the world's vegetation. I searched the published literature for water stable isotope papers in ecology and hydrology. Where single isotope (δ^2H or $\delta^{18}O$) was used in a source paper, I compiled percent groundwater use by vegetation either from direct interpolation method or from reported mixing model results. Where dual isotopes were used in a source paper, I used the line-conditioned excess parameter (Landwehr and Coplen, 2006) to calculate the "offset" (to quantify xylem-groundwater connectivity) of a xylem water value from the groundwater line. The

groundwater line was calculated from measurements of $\delta^{18}O$ and $\delta^{2}H$ of groundwater at a site. I then defined upper and lower bounds of groundwater use if a xylem-groundwater connectivity value fell within the 10^{th} and 90^{th} percentiles and within the 25^{th} and 75^{th} percentiles of groundwater nonparametric data density space, respectively. I employed species-level accounting for establishing groundwater use by vegetation. This approach enabled me to test for effects not only at a site level but also at other categories of interest (e.g. species, genus, biome, etc.). This study was submitted for peer review in March 2016 and is presently in revision [Citation: Evaristo, J., and J. J. McDonnell (In Revision), "Groundwater use by plants not widespread globally". *Nature (Scientific Reports)*].

In Chapter 5, my main objective was to identify the possible mechanisms that control ecohydrological separation – the partitioning of subsurface water between root water uptake, and groundwater recharge – during and after an extended period of drought. One outstanding research question surrounding ecohydrological separation is whether or not the latter is a separation between transpiration and mobile soil water in time or a separation in space (Bowen, 2015). Earlier research on ecohydrological separation carried the implicit suggestion that transpiration flux is older than the more mobile water pool. This runs counter to most catchment modeling studies that suggest that evapotranspiration fluxes are younger (Hrachowitz *et al*., 2013, 2015; Harman, 2015). This time aspect involves quantifying the mean transit time (MTT) and corresponding transit time distribution (TTD) of soil water and transpiration. MTT is the ratio between storage volume (L^3) and average water flux ($L^3\,T^{-1}$). Catchment transit time is the time that a water parcel spends from input as rainfall to output as streamflow or transpiration water (also known as "exit age").

Nonetheless, no studies have yet quantified the transit time of transpired water or the transit time of the low mobility water. Beyond time, the space aspect of ecohydrological separation entails quantifying the source proportions of the isotopic signal that is integrated in the xylem (i.e. plant stem) water. Evaluating and quantifying these time- and space-based components of ecohydrological separation, however, are difficult when boundary conditions in natural catchments are unknown and largely unknowable. Experiments that allow for high degree of

control over environmental variables at useful space and time scales are ideal but rare. In general, the degree of control over experiments spans extremes in spatial scales: growth chamber experiments allow for high degree of control but scalability is an issue; field experiments satisfy scale requirements (i.e. being the natural system) but control over experimental variables is nearly impossible. In Chapter 4 I took advantage of the 27 m tall, 1936 m^2 mesocosm Biosphere 2-Tropical Rainforest (B2-TRF) biome with a total volume of 35000 m^3. The B2-TRF biome represents the ideal scale at which to address fundamental aspects of ecohydrological separation, enabling controlled experiments to be designed and implemented at the biome scale, but with complete boundary controls.

I conducted a 10-week experiment whereby water stress was induced (drought) in four tree species (n=8). After the drought, I then added deuterated water as a label in rainfall distributed over four precipitation events. Followed by 13 rainfall events without a label spaced every 2-3 days, I tracked the evolution of the label over the course of this 6 months. I tested the null hypothesis that the ecohydrological system is tightly connected in that water forming groundwater recharge and plant transpiration is from a common pool. Alternatively, if labelled water is taken up by vegetation via roots is the same as the water that contributes to groundwater recharge (and eventual routing to streams), then their "ages" (i.e. mean transit times) and by extension sources in the subsurface, should be the same. Results of this study form Chapter 4 and will be submitted for peer review in *Water Resources Research* [Evaristo, J., J.J. McDonnell, M. Kim, J. van Haren, L. Pangle, C. Harman, P. Troch, "Source apportionment in the critical zone: Characterizing the fluxes and age distribution of soil water, plant water and deep percolation"].

1.2 References

1. Andrade, J. L., F. C. Meinzer, G. Goldstein, and S. A. Schnitzer (2005), Water uptake and transport in lianas and co-occurring trees of a seasonally dry tropical forest, *Trees-Structure and Function, 19*, 282-289.

2. Bonan, G. B., S. Levis, L. Kergoat, and K. W. Oleson (2002), Landscapes as patches of plant functional types: An integrating concept for climate and ecosystem models, *Global Biogeochem. Cycles, 16*, 5-1.

3. Bowen, G. J. and B. Wilkinson (2002), Spatial distribution of delta O-18 in meteoric precipitation, *Geology, 30*, 315-318.

4. Bowen, G. (2015), HYDROLOGY The diversified economics of soil water, *Nature, 525*, 43-44.

5. Brooks, J. R., H. R. Barnard, R. Coulombe, and J. J. McDonnell (2010), Ecohydrologic separation of water between trees and streams in a Mediterranean climate, *Nature Geosci., 3*, 100-104.

6. Busch, D. E., N. L. Ingraham, and S. D. Smith (1992), Water uptake in woody riparian phreatophytes of the southwestern United States: a stable isotope study, *Ecol. Appl., 2*, 450-459.

7. Caldwell, M. M. and J. H. Richards (1989), Hydraulic Lift - Water Efflux from Upper Roots Improves Effectiveness of Water-Uptake by Deep Roots, *Oecologia, 79*, 1-5.

8. Dawson, T. E. (1993), Hydraulic lift and water use by plants: implications for water balance, performance and plant-plant interactions, *Oecologia, 95*, 565-574.

9. Dawson, T. E. and J. R. Ehleringer (1991), Streamside Trees that do Not use Stream Water, *Nature, 350*, 335-337.

10. D'Odorico, P., F. Laio, A. Porporato, L. Ridolfi, A. Rinaldo, and I. Rodriguez-Iturbe (2010), Ecohydrology of terrestrial ecosystems, *Bioscience, 60*, 898-907.

11. Ehleringer, J. R. and T. E. Dawson (1992), Water uptake by plants: perspectives from stable isotope composition, *Plant, Cell Environ., 15*, 1073-1082.

12. Evaristo, J., J. J. McDonnell, M. A. Scholl, L. A. Bruijnzeel, and K. P. Chun (2016), Insights into plant water uptake from xylem-water isotope measurements in two tropical catchments with contrasting moisture conditions, *Hydrol. Process., 30*, 3210-3227.

13. Fan, Y. (2015), Groundwater in the Earth's critical zone: Relevance to large-scale patterns and processes, *Water Resour. Res.*, *51*, 3052-3069.

14. Flanagan, L. B. and J. R. Ehleringer (1991), Stable Isotope Composition of Stem and Leaf Water - Applications to the Study of Plant Water-use, *Funct. Ecol.*, *5*, 270-277.

15. Fritzsche, F., A. Abate, M. Fetene, E. Beck, S. Weise, and G. Guggenberger (2006), Soil-plant hydrology of indigenous and exotic trees in an Ethiopian montane forest, *Tree Physiol.*, *26*, 1043-1054.

16. Goldsmith, G. R., L. E. Muñoz-Villers, F. Holwerda, J. J. Mcdonnell, H. Asbjornsen, and T. E. Dawson (2012), Stable isotopes reveal linkages among ecohydrological processes in a seasonally dry tropical montane cloud forest, *Ecohydrology*, *5*, 779-790.

17. Good, S. P., D. Noone, and G. Bowen (2015), Hydrologic connectivity constrains partitioning of global terrestrial water fluxes, *Science*, *349*, 175-177.

18. Gouet-Kaplan, M., G. Arye, and B. Berkowitz (2012), Interplay between resident and infiltrating water: Estimates from transient water flow and solute transport, *Journal of Hydrology*, *458-459*, 40-50.

19. Green, M. B., B. K. Laursen, J. L. Campbell, K. J. McGuire, and E. P. Kelsey (2015), Stable water isotopes suggest sub-canopy water recycling in a northern forested catchment, *Hydrol. Process.*, *29*, 5193-5202.

20. Gutierrez-Soto, M. V. and J. J. Ewel (2008), Water use in four model tropical plant associations established in the lowlands of Costa Rica, *Rev. Biol. Trop.*, *56*, 1947-1957.

21. Harman, C. J. (2015), Time-variable transit time distributions and transport: Theory and application to storage-dependent transport of chloride in a watershed, *Water Resour. Res.*, *51*, 1-30.

22. Hrachowitz, M., H. Savenije, T. A. Bogaard, D. Tetzlaff, and C. Soulsby (2013), What can flux tracking teach us about water age distribution patterns and their temporal dynamics?, *Hydrology and Earth System Sciences*, *17*, 533-564.

23. Hrachowitz, M., O. Fovet, L. Ruiz, and H. H. G. Savenije (2015), Transit time distributions, legacy contamination and variability in biogeochemical 1/f(alpha) scaling: how are hydrological response dynamics linked to water quality at the catchment scale?, *Hydrol. Process., 29*, 5241-5256.

24. Jackson, P. C., J. Cavelier, G. Goldstein, F. C. Meinzer, and N. M. Holbrook (1995), Partitioning of Water-Resources among Plants of a Lowland Tropical Forest, *Oecologia, 101*, 197-203.

25. Jasechko, S. (2014), The pronounced seasonality of global groundwater recharge, *Wat. Resour. Res., 50*, 8845-8867.

26. Jasechko, S. and R. G. Taylor (2015), Intensive rainfall recharges tropical groundwaters, *Environmental Research Letters, 12*, 24015-24015.

27. Lachniet, M. S. and W. P. Patterson (2002), Stable isotope values of Costa Rican surface waters, *Journal of Hydrology, 260*, 135-150.

28. Lambs, L., E. Muller, and F. Fromard (2008), Mangrove trees growing in a very saline condition but not using seawater, *Rapid Communications in Mass Spectrometry, 22*, 2835-2843.

29. Landwehr, J. and T. Coplen (2006), Isotopes in Environmental Studies, 132-135.

30. Lee, J. -., R. S. Oliveira, T. E. Dawson, and I. Fung (2005), Root functioning modifies seasonal climate, *Proc. Natl. Acad. Sci. U. S. A., 102*, 17576-17581.

31. McDonnell, J. J. (2014), The two water worlds hypothesis: ecohydrological separation of water between streams and trees?, *WIREs Water, 1*, 323-329.

32. McJannet, D. L., R. A. Vertessy, and C. A. Clifton (2000), Observations of evapotranspiration in a break of slope plantation susceptible to periodic drought stress, *Tree Physiol., 20*, 169-177.

33. Meinzer, F. C., J. L. Andrade, G. Goldstein, N. M. Holbrook, J. Cavelier, and S. J. Wright (1999), Partitioning of soil water among canopy trees in a seasonally dry tropical forest, *Oecologia, 121*, 293-301.

34. Pate, J. S. and T. E. Dawson (1999), Assessing the performance of woody plants in uptake and utilisation of carbon, water and nutrients: Implications for designing agricultural mimic systems, *Agrofor. Syst., 45*, 245-275.

35. Phillips, F. M. (2010), Hydrology: Soil-water bypass, *Nature Geoscience, 3*, 77-78.

36. Pohjonen, V. and T. Pukkala (1990), Eucalyptus-Globulus in Ethiopian Forestry, *For. Ecol. Manage., 36*, 19-31.

37. Richards, J. H. and M. M. Caldwell (1987), Hydraulic Lift - Substantial Nocturnal Water Transport between Soil Layers by Artemisia-Tridentata Roots, *Oecologia, 73*, 486-489.

38. Schlesinger, W. H. and S. Jasechko (2014), Transpiration in the global water cycle, *Agric. For. Meteorol., 189*, 115-117.

39. Simonin, K. A., P. Link, D. Rempe, S. Miller, J. Oshun, C. Bode, W. E. Dietrich, I. Fung, and T. E. Dawson (2013), Vegetation induced changes in the stable isotope composition of near surface humidity, *Ecohydrology*.

40. Stratton, L. C., G. Goldstein, and F. C. Meinzer (2000), Temporal and spatial partitioning of water resources among eight woody species in a Hawaiian dry forest, *Oecologia, 124*, 309-317.

41. Thorburn, P. J., T. J. Hatton, and G. R. Walker (1993), Combining measurements of transpiration and stable isotopes of water to determine groundwater discharge from forests, *Journal of Hydrology, 150*, 563-587.

42. Troch, P. A., G. F. Martinez, V. R. N. Pauwels, M. Durcik, M. Sivapalan, C. Harman, P. D. Brooks, H. Gupta, and T. Huxman (2009), Climate and vegetation water use efficiency at catchment scales, *Hydrol. Process., 23*, 2409-2414.

43. Valentini, R., G. E. S. Mugnozza, and J. R. Ehleringer (1992), Hydrogen and Carbon Isotope Ratios of Selected Species of a Mediterranean Macchia Ecosystem, *Funct. Ecol., 6*, 627-631.

44. Vivoni, E. R. et al. (2008), Vegetation controls on soil moisture distribution in the Valles Caldera, New Mexico, during the North American monsoon, *Ecohydrology, 1*, 225-238.

45. White J.W.C., E.R. Cook, J.R. Lawrence, and W.S. Broecker (1985), The deuterium to hydrogen ratios of sap in trees: implications for water sources and tree ring deuterium to hydrogen ratios. *Geochim. Cosmochim. Acta* 49:237-46.

CHAPTER 2

INSIGHTS INTO PLANT WATER UPTAKE FROM XYLEM-WATER ISOTOPE MEASUREMENTS IN TWO TROPICAL CATCHMENTS WITH CONTRASTING MOISTURE CONDITIONS

Status: Published

Citation: Evaristo, J., J. J. McDonnell, M. A. Scholl, L. A. Bruijnzeel, and K. P. Chun (2016), Insights into plant water uptake from xylem-water isotope measurements in two tropical catchments with contrasting moisture conditions, *Hydrol. Process., 30*, 3210-3227.

2.1 Abstract

Water transpired by trees has long been assumed to be sourced from the same subsurface water stocks that contribute to groundwater recharge and streamflow. However, recent investigations using dual water stable isotopes have shown an apparent ecohydrological separation between tree-transpired water and stream water. Here we present evidence for such ecohydrological separation in two tropical environments in Puerto Rico where precipitation seasonality is relatively low and where precipitation is positively correlated with primary productivity. We determined the stable isotope signature of xylem water of 30 mahogany (*Swietenia* spp.) trees sampled during two periods with contrasting moisture status. Our results suggest that the separation between transpiration water and groundwater recharge/streamflow water might be related less to the temporal phasing of hydrologic inputs and primary productivity, and more to the fundamental processes that drive evaporative isotopic enrichment of residual soil water within the soil matrix. The lack of an evaporative signature of both groundwater and streams in the study area suggests that these water balance components have a water source that is transported quickly to deeper subsurface storage compared to waters that trees use. A Bayesian mixing model used to partition source water proportions of xylem water showed that groundwater contribution was greater for valley-bottom, riparian trees than for ridge-top trees.

Groundwater contribution was also greater at the xeric site than at the mesic-hydric site. These model results (1) underline the utility of a simple linear mixing model, implemented in a Bayesian inference framework, in quantifying source water contributions at sites with contrasting physiographic characteristics, and (2) highlight the informed judgment that should be made in interpreting mixing model results, of import particularly in surveying groundwater use patterns by vegetation from regional to global scales.

2.2 Introduction

The partitioning of infiltrating water between plant transpiration, soil water evaporation, groundwater recharge and streamflow generation under different physiographic characteristics is poorly understood (Vivoni *et al*., 2008; Gouet-Kaplan *et al*., 2012). While advances in terrestrial ecohydrology have improved our appreciation of the role of vegetation in modifying seasonal macroclimates (Troch *et al*., 2009; Lee *et al*., 2005; Bonan, 2002) and local microclimates (Green *et al*., 2015; Simonin *et al*., 2013), the prevailing assumption is that vegetation draws water from the same subsurface stocks that eventually reach the stream, i.e. green water flows and blue water flows (D'Odorico et al., 2010) originate from the same homogeneous source. If that were universally the case (knowing plant-water uptake is generally a non-fractionating process; Zimmermann *et al*., 1966; Ehleringer and Dawson, 1992), then subsurface water pools contributing to groundwater recharge and streamflow should have similar stable water isotope ratios to plant xylem water. However, work by Brooks *et al*. (2010) and Goldsmith *et al*. (2012) in Mediterranean and seasonally tropical settings, respectively, has suggested that there may be ecohydrological separation of the water sources for streams and trees, in that plants typically use matrix soil water not contributing to streamflow, while the water contributing to streamflow is not accessed by the plants (McDonnell, 2014). More recently, global-in-scale investigations (Good *et al*. 2015; Evaristo *et al*. 2015) have shown that a poorly-mixed (i.e. ecohydrological separation) conceptualization of soil water pools is more likely the rule than the exception, and that water contributing to groundwater recharge is often (but not always) isolated from water used in plant transpiration (Jasechko and Taylor, 2015; Jasechko *et al*., 2014).

Evaristo *et al*. (2015) showed that ecohydrological separation was greatest in tropical and Mediterranean biomes. Most of the tropical studies in the meta-analysis of Evaristo *et al*. (2015), however, were in highly seasonal climates. Climates with less seasonality, where temporal contrasts in water availability and primary productivity (i.e. soil water uptake) are not as marked as in highly seasonal tropical settings, are particularly in need of study. The exchange between soil-matrix and preferential flow path waters may be more frequent at low-seasonality sites [i.e., they show greater wetness interconnectivity; Phillips, 2010]. Therefore, we hypothesize that the degree of ecohydrological separation would be less for ecosystems where rates of precipitation input and primary productivity are more in-phase.

Here we test for evidence of ecohydrological separation using similar species of mahogany trees (*Swietenia spp.*) at two low-seasonality but contrasting sites in northeastern and southwestern Puerto Rico, having significant differences in rainfall amount as well as atmospheric evaporative demand (i.e. potential evapotranspiration, PET). The site in the northeastern part of the island (Luquillo, hereafter LUQ) is a mesic-hydric ecosystem with ample rainfall throughout the year; the site in the southwest (Susua, hereafter SUS) represents a xeric ecosystem with about a fifth of the rainfall amount received in LUQ. Despite these contrasts in overall moisture regime, each site has little seasonal variation in terms of temperature and day length so that within-site hydrologic (e.g. precipitation, soil moisture) and primary productivity variability are in-phase. The mesic-hydric and xeric sites remain relatively wet and dry, respectively, on intra- and inter-annual timescales (see Figure 2.1). Thus, the sites provide an opportunity to test for the ecohydrological separation hypothesis under conditions where hydrology and primary productivity are in-phase, and where there is a significant contrast in rainfall amount and PET between sites. We anticipated the results would also provide information on the degree of wetness interconnectivity (exchange between matrix water and preferential flow water) at the sites.

We also explore the partitioning of water sources as an integrated signal in the xylem. Heretofore, much of the work in stable isotope tropical ecohydrology has centered on source water partitioning approaches that examine relationships between leaf phenology, differences in

rooting patterns, and root activity (Meinzer *et al*. 1999) among other plant and environmental variables (Jackson *et al*. 1995; Stratton *et al*. 2000; Andrade *et al*. 2005; Gutierrez-Soto *et al*. 2008; Rosatto *et al*. 2012; Bertrand *et al*. 2014). Stable isotope methods used in partitioning source contributions to xylem water fall under two main categories: process-based mixing (PBM) models and simple linear mixing (SLM) models (see Ogle *et al*. 2014). PBM models (e.g. *RAPID* by Ogle *et al*. 2004; Ogle *et al*. 2014) integrate stable isotope data and a biophysical model (e.g. root water uptake) into a Bayesian framework. PBM models are useful if the goals are to arrive at greater predictive ability of how changes in space and time affect root water uptake and an improved mechanistic understanding of ecosystem behavior. Traditional SLM models are useful in estimating two or three water sources (e.g. Thorburn and Walker 1993; Brunel *et al*. 1995). Relatively recent SLM models can deal with multiple sources via an iterative mass balance approach (e.g. *IsoSource* by Phillips and Gregg 2003) or when used in a Bayesian inverse modeling framework (e.g. *MixSIR* by Moore and Semmens 2008; *SIAR* by Parnell *et al*. 2010). There have been few plant source water partitioning studies using SLM models in a Bayesian framework, however, (e.g. Leng *et al*. 2013; Barbeta *et al*. 2015), and in this paper we examine the usefulness of this approach.

Specifically, we address the following questions:

1. Do analyses of stable isotopes in stream water, groundwater, bulk soil water, and plant xylem water for the contrasting wet- and dry-climate sites show evidence of ecohydrological separation?
2. What can we learn from a simple linear mixing model, implemented in a Bayesian inference framework, regarding the sources of water for the sampled mahogany trees?

We utilized the natural abundances of hydrogen (^{2}H or deuterium, D) and oxygen (^{18}O) stable isotopes in plant xylem water, and derived line-conditioned excess (lc-excess*) (Landwehr and Coplen 2006) to test the ecohydrological separation at the two sites. The lc-excess* can help to

differentiate water samples that have undergone evaporation under non-equilibrium conditions (Dansgaard 1964) from those that have maintained the isotopic characteristics of regional precipitation. By using the lc-excess* to differentiate between evaporated (shallow soil water, standing water) and non-evaporated (precipitation, stream and groundwater) sources, we can test the ecohydrological separation. Finally, we compare estimates of the potential sources of xylem water by exploring the utility of a simple linear mixing model, implemented within a Bayesian framework (*SIAR*, Parnell *et al*. 2010).

2.3 Materials and Methods

2.3.1 Study area

The Luquillo Mountains in northeastern Puerto Rico rise steeply from the coast to over 1000 m in elevation over a distance of 15 to 20 km. They are characterized by steep slopes, rugged peaks, and highly dissected valleys (Pike *et al*., 2010). The rapid increase in elevation corresponds to major changes in climate, soil type, as well as structure and species composition of the vegetation (Scatena and Lugo, 1995). The site in the Luquillo Mountains (LUQ) chosen for this study was Rio Chiquito near Sabana (18°19'N, 65°43'W) at an elevation of approximately 160 to 207 m above sea level (Table 2.1). The site is underlain by volcaniclastic rocks (tuffaceous sandstones and indurated siltstones) that have weathered into a predominantly clayey substrate. Soils at this site are Typic Haplohumults of the Humatas Series with a solum thickness between 56 and 130 cm (USDA NRCS, 2002) that is underlain by saprolite down to 20–60 m depth (Buss et al., 2013). The uppermost 20 cm of the soil is highly permeable but the soil below is rather poorly drained. As a result, most stormflow travels laterally through macropores in the topsoil (Schellekens *et al*., 2004). The LUQ site is part of the Tabonuco (*Dacryodes excelsa*) forest type (Wadsworth, 1951), a forest community found at elevations <600 m, with an average canopy height of 20–25 m. While no definitive survey on rooting depth exists for *Swietenia* spp. in Puerto Rico, Lugo *et al*. (2003) reported that mahogany trees at LUQ are less resistant to wind stress, possibly due to their relatively shallow rooting pattern. A soil survey by the USDA NRCS (2002) reported medium-sized and fine roots (tree species not identified) down to a depth of almost 1 m at our site in LUQ. Most roots, however, were reported to be in the top 0.24-0.40 m (Lenart *et al*. 2010). The semi-deciduous hardwood species

Swietenia macrophylla x *S. mahagoni* – a hybrid between small- and big-leaf mahoganies – was introduced in Luquillo more than 50 years ago (Lugo, 1992) and remains abundant in some parts of the Tabonuco forest including the present study site. The climate is maritime tropical (type A2m in the Köppen classification) with a mean annual rainfall (1988–2002) of ca. 3700 mm (Heartsill-Scalley *et al*., 2007) distributed over 267 rain days (Schellekens *et al*., 2000) while air temperatures vary seasonally between 22 and 25^0C. The site is exposed to the NE trade winds and receives relatively higher rainfall in the months of May, June, and October (> 300 mm each) than at other times of the year while January through April typically have relatively low rainfall (< 200 mm $month^{-1}$) (Heartsill-Scalley *et al*., 2007). Potential evapotranspiration (PET) according to the method of Hargreaves & Allen (2003) is ca. 1450 mm y^{-1} (Beck *et al*., 2013).

Situated in the southwestern part of the island and on the leeward side of the Cordillera Central, Susua (SUS) has a much drier climate than Luquillo. The study site is located on the southern extreme of the Susua Forest Reserve, along the banks and upper slopes of the Rio Loco (18°04'N, 66°54'W) at an elevation of 132–172 m (Table 2.1). Mean annual rainfall is estimated to be 1200 mm (Medina *et al*., 1994) and air temperature varies seasonally between 25 and 29^0C. Like LUQ, January through April typically have lower rainfall than the rest of the year. Annual PET according to the Hargreaves method is estimated at ca. 1650 mm. The landscape is underlain by serpentinite that has weathered into the clayey, ferruginous, shallow Typic Hapludox of the Rosario Series – well-drained, moderate to rapidly permeable soils on side slopes and stable ridges with no aquic conditions for most of the year (USDA NRCS, 2002). The plantation species *Swietenia mahagoni* (small-leaf mahogany) was introduced in SUS more than 50 years ago (Lugo, 1992) and remains abundant in the area. Like the hybrid mahogany at LUQ, small-leaf mahogany in SUS is facultatively deciduous – leaf shedding may be deferred or reduced to a rapid leaf replacement when sufficient soil moisture persists during the drier months (Burton, 2007). Unlike the hybrid mahogany at LUQ, small-leaf mahogany trees at SUS show more resistance to wind stress, possibly due to a deeper rooting pattern (Lugo *et al*. 2003).

2.3.2 Ecohydrological seasonality

A prime motivation for our study was testing the ecohydrological separation hypothesis in a setting where plant ecology (i.e. primary productivity) and site hydrology (i.e. moisture input) are in-phase, and where hydrological seasonality (in terms of precipitation inputs and streamflow outputs) is lower than at previously studied sites. To demonstrate that our Puerto Rico sites meet these conditions we performed a time-series analysis of rainfall (as a metric of hydrological conditions) and gross primary productivity GPP (as a metric of ecosystem performance) for the period January 2005 to June 2013.

We calculated GPP by first estimating the above-ground net primary productivity (ANPP) using the empirical relationship between ANPP and evapotranspiration of Webb *et al*. (1978). Since direct measures of below-ground net primary productivity (BNPP) are mostly lacking for tropical forests, we used the lower and upper bound estimates of Clark *et al*. (2001) [BNPP = 0.2-1.2(ANPP)] to calculate BNPP, and therefore obtain a first estimate of total NPP (i.e. ANPP + BNPP). We tested the validity of this approach by comparing our calculated total NPP to reported values in the literature for our study sites: Wang *et al*. (2003) for LUQ and Murphy *et al*. (1995) for SUS. We then calculated GPP (GPP = total NPP + respiration) by using reported values in the literature for the relationship between respiration and total NPP (Wang *et al*. 2003). Comparing our calculated GPP to simulated and observed values at our sites enabled us to test for the robustness of this approach.

To support our interpretation of the rainfall and GPP time-series analysis, we employed an additional approach whereby we estimated the actual evapotranspiration as a function of a site's aridity index (i.e. PET/P *sensu* Budyko, 1974). PET was calculated based on temperature and day-length (Hamon 1963), and setting the fraction of day that is day-time to 0.5. Actual evapotranspiration (AET) was calculated as the difference between annual precipitation and streamflow (Jones *et al*. 2012). Streamflow data from Rio Mameyes (USGS ID 50065500) and Rio Cerrillos (USGS 50114000) were used for LUQ and SUS, respectively. Budyko (1974) and many others since (e.g. Potter *et al*., 2005; Gerrits *et al*., 2009) have shown that catchments where monthly potential evaporation (including transpiration) and precipitation rates are in-phase plot closer to or above the Budyko curve than sites that are out of phase. The Budyko curve

approach, therefore, was applied to test whether the LUQ and SUS sites are indeed “in phase” or “out of phase”.

2.3.3 Environmental waters and plant water uptake

Rainfall amounts in LUQ were measured at the nearby (482 m) Bisley watershed meteorological station, situated ~ 275 m above the soil- and vegetation sampling sites. Rainfall and stream water samples were collected in the Mameyes watershed as part of the long-term stable isotope monitoring program by the United States Geological Survey (USGS) following the collection methodology outlined by Scholl *et al*. (2009). Groundwater stable isotope data from a network of wells (depths 70-100 cm) (see McDowell *et al*. 1992) sampled at stream bank and upslope positions in the nearby Bisley watershed in LUQ were also used. At the SUS site, rainfall data from the closest weather station (30 km) in the municipality of Ponce were used, while groundwater isotope estimates for this site were derived from the simulations of Jasechko *et al*. (2014).

Local meteoric water lines (LMWLs) for the LUQ site were plotted to compare with the stable isotopic distributions in rainfall, xylem water, soil water, stream water and groundwater in a dual isotope space. At SUS, the LMWL was derived from near-monthly rainfall isotopic values in the Guanica Dry Forest (Govender *et al*., 2013), 14 km from the sampling site.

Samples of precipitation, from January 2008 to March 2013 were analyzed for δD and $\delta^{18}O$ in the USGS Reston Stable Isotope Laboratory in Virginia, USA using either isotope ratio mass spectrometry (IRMS) or cavity ring-down spectroscopy (CRDS) (data in Scholl *et al*. 2014). Samples of xylem water, bulk soil water, and stream water were analyzed for δD and $\delta^{18}O$ at the Stable Isotope Ratio Facility for Environmental Research (SIRFER) at the University of Utah, USA, using cryogenic vacuum distillation and isotope ratio infrared spectroscopy (IRIS) on a Picarro CRDS. No spectral interference was observed when using the IRIS technique. To address any concerns about potential errors when using the IRIS technique instead of the traditional

IRMS technique (West *et al*. 2010), we randomly selected samples for comparison of the two methods. The randomly selected samples were compared to a CO_2 equilibration method on the IRMS. Results of the comparison showed that the values generated from both techniques were not significantly different (values ranged from 0.2–0.6‰ $\delta^{18}O$) for both plant xylem water and bulk soil water samples, with an inter-technique correspondence close to unity.

We use conventional notation for isotope composition (Coplen 2011) where $\delta^{18}O$ or $\delta^{2}H = [(R_{sample}/R_{SMOW})-1]$, with R as the ratio of $^{18}O/^{16}O$ or $^{2}H/^{1}H$ in the sample or in Standard Mean Ocean Water: SMOW. Laboratory precision (1SD) for the Picarro CRDS at SIRFER was no greater than 1.1 and 0.2‰ for δD and $\delta^{18}O$, respectively, and no greater than 1 and 0.1‰ at the USGS Reston Stable Isotope Laboratory.

To understand the depth of soil water-uptake patterns, xylem water in mahogany trees and bulk soil water were collected during a relatively "wet" (9–13 July 2012) and a relatively "dry" (11–15 February 2013) sampling period. Samples of stream water were also taken at this time to examine to what extent it differed isotopically from bulk soil water and xylem water. Xylem water samples were taken from the part of twigs with mature bark that were closest to the main branch (following Dawson, 1993) to minimize the effect of evaporative enrichment by water loss through unsuberized stems. Xylem water was analyzed for $\delta^{18}O$ and $\delta^{2}H$. We calculated the classic deuterium-excess (*d*-excess) parameter values (Dansgaard, 1964) and report these for soils, for the comparison to previous evaporation studies (e.g. Simonin *et al*., 2013):

$$d\text{-excess} = \delta^{2}H - 8\,(\delta^{18}O) \qquad (2.1)$$

In addition, to test for ecohydrological separation, we calculated the line-conditioned excess (lc-excess*) of soil water, xylem water, and groundwater (Landwehr and Coplen, 2006):

$$lc\text{-}excess^{*} = [\delta^{2}H - a\,\delta^{18}O - b] / S \quad (2.2)$$

where *a* and *b* are the slope and y-intercept, respectively, of the LMWL, and *S* is one standard deviation measurement uncertainty for both $\delta^{18}O$ and $\delta^{2}H$. Equation (2.2) was used to quantify the degree of "offset" of environmental waters from rainfall. That is, a negative offset that is greater than the standard deviation of the LMWL suggests that water has undergone some evaporative isotopic enrichment.

Soil cores were extracted at a distance of approximately twice the average diameter at breast height (DBH) from each tree [0.62±0.32 m at LUQ vs. 0.41±0.29 m at SUS (mean±1SD)]. Cores were taken down to depths of 30 and 60 cm during the July 2012 (wet conditions) and February 2013 (dry conditions) sampling campaigns, respectively. Cores were subdivided into 10-cm depth intervals for subsequent water stable isotope analysis. *d*-excess values at each depth in the soil profile were then calculated for both sampling periods. For LUQ we calculated the so-called characteristic length L_C for Stage 1 evaporation (i.e. the "constant rate period", Or *et al*., 2013) to see how the patterns of *d*-excess values with soil depth compared with L_C. L_C was calculated over a range of apparent soil water evaporation rates e_0 of sites considered representative of conditions prevailing in the forest at LUQ (0.14-0.19 mm d^{-1}, Roche 1982; Jordan and Heuveldop 1981):

$$L_C = \frac{L_G}{1+\frac{e_0}{K_{eff}}} \quad (2.3)$$

where K_{eff} (mm d^{-1}) is effective soil hydraulic conductivity and L_G (mm d^{-1}) is the gravity characteristic length (following Or *et al*., 2013):

$$L_G = \frac{1}{\alpha(n-1)}\left(\frac{2n-1}{n}\right)^{\left(\frac{2n-1}{n}\right)}\left(\frac{n-1}{n}\right)^{\frac{1-n}{n}} \quad (2.4)$$

where α and *n* are the van Genuchten model parameters for the silty clay soils in LUQ. We state a caveat that the e_0 estimates used here are based on micro-lysimeters (Jordan and Heuveldop 1981) and evaporation pans placed beneath the rain forest canopy (Roche 1982) , and therefore driven by atmospheric parameters, notably temperature, wind speed, relative humidity, and solar radiation. In contrast, the derivation of Equation (2.3) is driven not by atmospheric parameters but by porous media properties (Lehmann *et al*. 2008). Calculating L_C, therefore, was done to serve as a learning tool and to derive potential insights on soil water evaporation as indicated by the obtained patterns of *d*-excess values with soil depth.

Finally, to determine the sources of water uptake by the mahogany trees at different landscape positions, we employed an SLM Bayesian model approach. Ridge-top trees in LUQ were situated 95 m away from the stream valley on a slope of 12%; while ridge-top trees in SUS were situated 243 m away from the stream valley on a slope of 16%. We used the SIAR (stable-isotope analysis in R) Bayesian mixing model statistical package (Parnell *et al*. 2010) to explore the structure (and plausible meaning) of the data in probability space (i.e. in p-space). SIAR is widely used in food web and animal foraging studies, and was used here to determine the relative importance of various sources of water that may contribute to xylem water using Markov Chain Monte Carlo (MCMC) methods. We classified four potential sources of xylem water when running the Bayesian model: (1) soil water at 0-10 cm ("shallow soil water"); (2) soil water at ≥20 cm ("deep soil water"); (3) "rain"; and (4) "groundwater". We recognize that the distinguished depths are not strictly "shallow" and "deep" *per se*, but the terms are used here only to designate the two soil water end-members that can be resolved by SIAR vis-à-vis our sampled soil depths. The trophic enrichment factor (TEF) and concentration dependence of the original model were set to 0. The model was run with 500,000 iterations (discarding the first 50,000) and a source water's most likely contribution (i.e. the mean of the posterior distribution of the MCMC simulation) to xylem water was obtained for all trees at a site.

2.4 Results

2.4.1 Ecohydrologic phasing: in-phase vs. out-of-phase

Figures 2.1a and 2.1b show rainfall amount (mm), estimated GPP (g m^{-2} y^{-1}), and rainfall $\delta^{18}O$ (where available) for the LUQ and SUS sites, respectively. At LUQ, our calculated total annual GPP ranged from a minimum of 5400 g m^{-2} y^{-1} in 2011 to a maximum of 5600 g m^{-2} y^{-1} in 2012. Between 2005 and 2012, the mean (±SD) calculated annual GPP was 5500 (± 44) g m^{-2} y^{-1}, well within the range of simulated (Wang *et al*. 2003) and observed (LTER-LUQ) GPP estimates at 5000 and 6000 g m^{-2} y^{-1}, respectively. Over the same period, rainfall amount and rainfall $\delta^{18}O$ (median, interquartile range) at LUQ were 3696 (1369) mm and -1.83 (1.8) ‰, respectively. Volume-weighted average rainfall $\delta^{18}O$ and $\delta^{2}H$ were -2.5 and -8.6 ‰, respectively. At SUS, our calculated total annual GPP ranged from a minimum of 3000 g m^{-2} y^{-1} in 2008 to a maximum of 3100 g m^{-2} y^{-1} in 2010. Between 2005 and 2012, calculated mean annual GPP was 3105 (± 7) g m^{-2} y^{-1}. The absence of information on observed or simulated GPP estimates for the forest at SUS did not allow us to directly compare the present GPP estimates. However, at 564 (± 8) g m^{-2} y^{-1}, our total NPP estimates agreed closely with the NPP of ~550 g m^{-2} y^{-1} derived for this forest type by Murphy *et al*. (1995). Over the same period, rainfall amount (median, interquartile range) at SUS was 916 (386) mm. Between 2008 and 2012, the amount-weighted average rainfall $\delta^{18}O$ and $\delta^{2}H$ were -3.5 and -17.4 ‰, respectively (Govender *et al*. 2013).

Using the time-series from Figures 2.1a and 2.1b, we calculated the respective spectral density patterns (Baldocchi *et al*., 2001) for rainfall, GPP, and rainfall isotopic composition to examine whether any periodic structure existed in the data and to identify the frequencies associated with any such periodicity. For LUQ, Figure 2.1c demonstrates that both GPP and rainfall isotopic composition have a periodicity (i.e. occurrence of dominant peaks) of ~12 months. There are also underlying alternative periodic components (i.e. smaller peaks) recurring about every ~7 and ~6 months for GPP and rainfall isotopic composition, respectively. Using Fisher's Kappa statistic to test the null hypothesis that the time series is drawn from a normal distribution, against the alternative hypothesis that the time series has some periodic component, we rejected the null hypothesis and confirmed the periodic components of GPP and rainfall isotopic composition in the case of LUQ (Fisher's Kappa = 16.23, $P<0.0001$).

Rainfall amount, on the other hand, showed no apparent dominant peaks or identifiable spectral pattern with this method, (Fisher's Kappa = 5.30, P = 0.20). Nevertheless, LUQ rainfall has the annual pattern of the Caribbean region, with a winter dry season (Dec-Apr), an early wet season (Apr-May), a mid-summer drier period (Jun-Jul) and a late wet season (Aug-Nov) (García-Martinó *et al*., 1996; Comarazamy and Gonzalez, 2011). The variability in timing and magnitude of these "seasons", suggests that a wet/dry bimodal pattern in rainfall may not become apparent as a signal with the same frequency (García-Martinó *et al*., 1996). A more recent effort to identify any periodic components in rainfall at LUQ (Van Beusekom *et al*., 2015), however, confirmed earlier research findings that rainfall in Puerto Rico generally has a periodic component with a recurrence interval between 4–12 months. This range corresponds reasonably well with that observed in the GPP and rainfall isotopic composition signals (Fig. 2.1a).

At SUS, Fig. 2.1d shows a generally similar pattern to that found for LUQ, except for a more pronounced absence of any dominant peaks in rainfall amount, and low-amplitude, smaller peaks in GPP and rainfall isotopic composition signals. Nevertheless, the results of the spectral density analyses for both sites support the observation that rainfall amount and GPP have periodic components of a few months to 1 year.

Finally, to demonstrate the temporal correspondence between rainfall amount and GPP, using the same data-sets we calculated the mean monthly values of the two variables. Figures 2.1e and 2.1f show that long-term mean monthly rainfall amount correlates positively with long-term mean monthly GPP (Pearson's $r = 0.20$ for LUQ, $r = 0.22$ for SUS; $P<0.05$ using two-tailed test). On the other hand, rainfall amount was negatively correlated with rainfall isotopic composition ($r = -0.38$ for LUQ, $r = -0.44$ for SUS; $P<0.05$ using two-tailed test).

On an annual timescale, Figure 2.2 shows the calculated actual evapotranspiration as a function of site aridity index (i.e. the ratio of potential evapotranspiration to precipitation, PET/P). Pertinently, the range of PET/P-values for SUS is much wider (1.68) than that for LUQ (0.09). On the other hand, the range of the ratio of actual evapotranspiration to precipitation (AET/P) at

SUS is narrower (0.09) than that for LUQ (0.13). Calculating the long-term average AET/P deviation from the general Budyko curve shows that LUQ has a slightly negative deviation of -0.60 (±0.28) (mean ± SD), which is statistically different (two-tailed t-test $P<0.05$) from SUS's slightly positive deviation of 0.10 (± 0.32) from the Budyko prediction. Taken altogether, the calculated AET/P at both sites are in excellent agreement with the Budyko curve's prediction ($r^2 = 0.98$, $P<0.0001$), suggesting that rain inputs and plant physiological behavior are "in phase".

2.4.2 Ecohydrological separation: line-conditioned excess

Stable isotope values of all water samples plotted in dual isotope space for the two study sites are shown in Figures 3a-d. The slope and intercept of the LMWL at LUQ ($\delta D = 8.59\ \delta^{18}O + 13.14$) are different from the LMWL at SUS ($\delta D = 7.79\ \delta^{18}D + 10.85$); the SUS intercept (10.85) is closer to that of the GMWL (($\delta D = 8\delta^{18}D + 10$) while the LUQ intercept (13.14) reflects the generally higher *d*-excess in precipitation samples there (Scholl *et al*. 2014). At LUQ, while bulk soil and plant xylem water were isotopically distinct from stream water, groundwater, and rainfall (LMWL), this separation, as shown by the lc-excess*, was more evident during the wet period (inset Figure 2.3a) than during the dry period (inset Figure 2.3b). Table 2.2 shows the key statistical information derived from the data in Figure 2.3. Differences in soil and xylem water lc-excess* at LUQ were not statistically significant in either moisture period ($P>0.05$ using two-tailed *t*-test). These soil and plant xylem water lc-excess* patterns at LUQ indicate that the variability of soil water isotopic composition – down to depths of 30 and 60 cm during the wet and the dry period, respectively – can explain a fair degree of the observed variability in xylem water composition. The difference in groundwater lc-excess* at LUQ, however, was statistically significant between the two periods with contrasting moisture status ($P<0.0001$ using two-tailed *t*-test). Also, the lc-excess* values of soil water and xylem water were statistically different from the lc-excess* of groundwater during both periods ($P<0.0001$ using non-parametric Steel-Dwass Method).

Like at LUQ, bulk soil and plant xylem water isotopic composition was also distinct from that of groundwater and rainfall at SUS during the wet period (inset Fig. 2.3c) and the dry period (inset

Fig. 2.3d). Differences in soil water lc-excess* at SUS were statistically significant ($P<0.00001$ using two-tailed *t*-test) between the two moisture periods. Xylem water lc-excess* values, on the other hand, were not significantly different between the two periods. Unlike at LUQ, the soil and plant xylem water lc-excess* patterns observed at SUS suggest that the isotopic variability of soil water may not explain the variability in xylem water. Like at LUQ, the lc-excess* values of soil water and xylem water at SUS were statistically different from the lc-excess* of groundwater during both the wet and the dry period ($P<0.0001$ using non-parametric Steel-Dwass Method).

Depth profiles of soil water *d*-excess values during the wet and dry periods are shown in Figure 2.4 while Table 2.3 lists the corresponding key statistical information. At LUQ (Fig. 2.4a), *d*-excess values of soil water between 10 and 30 cm depth were closer to the LMWL during the dry period than during the wet period. Differences in soil water *d*-excess between the wet and dry periods were statistically significant at depths of 10 cm and 20 cm. Conversely, the difference at 30 cm depth was not statistically significant between the two moisture periods. However, the inferred magnitudes of evaporation between 10 and 30 cm depth during the wet period were not statistically different. During the dry period, a pairwise comparison of soil water *d*-excess values between 10 and 50 cm showed that only the *d*-excess values at 20 and 50 cm depth were statistically different from each other ($P<0.0001$, non-parametric Steel-Dwass method). At 60 cm, the mean *d*-excess was highest and closest to the LMWL, while it differed statistically from values derived for all depths between 10 and 50 cm. The inset in Figure 2.4a shows the modeled characteristic length (L_C) for Stage 1 evaporation (Equation 3) which suggests an L_C of ~180 cm for the low soil water evaporation rates considered applicable at LUQ (0.14-0.19 mm d^{-1}). Higher evaporation rates (~0.71 mm d^{-1}), however, would be required to explain the depth of soil water evaporation, as inferred from observed soil water *d*-excess below the LMWL value, which persisted down to 50 cm (Fig. 2.4a).

Figure 2.4b shows that soil water *d*-excess patterns at SUS were different from those found for LUQ. During the wet period, soil water *d*-excess values were more positive than during the dry period. Differences in soil water *d*-excess between wet and dry periods were statistically significant at a depth of 10 cm only, but not at 20 cm and 30 cm. Similarly, the magnitude of soil

water evaporation inferred from *d*-excess between 20 and 30 cm depth during the two moisture periods was not statistically different. During the dry period, comparison of differences in soil water *d*-excess between 10 and 60 cm showed that the *d*-excess values at 10 and 60 cm were statistically significant from those at 50 and 30 cm depth only ($P<0.05$, Tukey-Kramer HSD).

2.4.3 Source water partitioning: Bayesian simple linear mixing (SLM) model

Potential sources of xylem water were determined using a Bayesian mixing model approach. Figures 5 and 6 show the results for LUQ and SUS, respectively, for both wet and dry periods and all landscape positions, while Table 2.4 lists the corresponding key statistical information. Also shown are the respective probability density plots for each end-member, superimposed on the plots of their relative contributions to xylem water. At LUQ, groundwater contribution to xylem water in ridge-top trees decreased from (mean ±1SD) 26±12% during the wet period to 14±12% during the dry period, while "deep" soil water contribution increased from 27±13% to 53±19%, respectively. Groundwater contribution to xylem water in valley-bottom (i.e. riparian) trees increased from 25±15% during the wet period to 28±14% during the dry period, while rain water contribution decreased from 42±18% to 21±13%, respectively. Trees on slopes also showed an increase in groundwater contribution from 21±13% to 29±15%. At SUS, groundwater contribution to ridge-top trees increased from 23±12% (wet period) to 35±9% (dry period). Overall differences in source water proportions for ridge-top and valley-bottom trees at LUQ were statistically significant ($P<0.05$) between wet and dry periods. Source water proportion differences, however, were not significant ($P>0.05$) for all landscape positions at SUS, nor for the trees on the slope at LUQ between wet and dry periods.

2.5 Discussion

Stable isotope ratios of water from trees, soils, streams, wells, and rainfall were used to test for ecohydrological separation (plants using soil matrix water rather than rapidly percolating water that contributes to groundwater recharge and streamflow). Our two sites in Puerto Rico had contrasting moisture dynamics: a tropical wet forest at Luquillo (LUQ) and a tropical dry forest at Susua (SUS). Both these sites have lower seasonality (i.e. precipitation input is more 'in

phase' with primary productivity) than previously studied sites for which there is evidence of ecohydrological separation between preferential flow and soil matrix water (see Evaristo *et al*., 2015). We originally hypothesized that the plant water use patterns that would indicate ecohydrological separation as reported by Brooks *et al*. (2010) and Goldsmith *et al*. (2012) might not be equally evident at our sites where rainfall and gross primary productivity are more in-phase, because exchange between soil-matrix and preferential flow path waters may be more frequent (*sensu* Phillips, 2010). We found instead a clear separation between water forming plant transpiration and water forming groundwater recharge and/or streamflow at both our sites. We also showed how mahogany trees at our two contrasting sites may have partitioned the sources of water by demonstrating the utility of a simple linear mixing model (SLM), implemented within a Bayesian framework. In the following we will discuss the processes that may lead to evaporative isotopic enrichment of soil water; examine the state-of-the-research regarding the ecohydrological separation hypothesis; and, explore the utility of a simple linear mixing model, implemented in a Bayesian framework, in understanding source water partitioning for mahogany trees at different landscape positions and moisture periods.

2.5.1 Evaporative isotopic enrichment of soil water

Soil water isotope concentrations at SUS generally reflected more evaporation than those at LUQ, with greater apparent soil water evaporation during the dry period than during the wet period. We found the opposite pattern at LUQ where apparent soil water evaporation appeared to be greater during the wet period than during the dry period. Direct measurement of evaporation rates from the forest floor soil and litter (*Es*) at LUQ are not available but annual totals observed in old-growth lowland equatorial rain forests in French Guyana (Roche, 1982) and Amazonian Venezuela (Jordan and Heuveldop, 1981) as well as in subtropical evergreen forest in South China (Liu *et al*., 2015) ranged between 36 and 68 mm only (0.14–0.19 mm d^{-1}). Actual values of *Es* in the studied mahogany stand at LUQ may well be somewhat higher, however, given the site's location in the trade-wind belt and the occasional passage of canopy-opening hurricanes. Conversely, (very) high wet-canopy evaporation rates (*Ew*) during and shortly after rainfall have been reported for the Tabonuco forest close to where we conducted our study. Whilst estimates of *Ew* for the Bisley forest vary depending on the methodology used (Schellekens *et al*., 2000;

Holwerda *et al*., 2006, 2012) the best estimates converge around a value of ~0.6 mm h^{-1} (Holwerda *et al*., 2012). Such evaporation rates are well in excess of levels sustained by net radiant energy in the area (Schellekens *et al*., 2000; Holwerda *et al*., 2012). Instead, the observed high rates of *Ew* are thought to be maintained by a negative downward sensible heat flux from the overlying (warmer) air towards the (cooler) wetted canopy. In addition, evaporative exchange between the canopy and the atmosphere appears to be facilitated by the complex topography of the area which may lead to enhanced turbulence and thus greater aerodynamic conductance (Holwerda *et al*., 2012). We considered whether the well documented high rates of *Ew* at LUQ would lead to throughfall with evaporated isotopic signatures. If true, such isotopically enriched throughfall would infiltrate into the soil, filling parts of the soil profile that are accessible by the roots. This might then explain the observed evaporated signal in the xylem water even with minimal soil evaporation rates. A corollary, however, is that parcels of the same evaporated throughfall input should be detectable in groundwater and stream baseflow. Our LUQ groundwater (e.g. Figure 2.3), stream, and long-term stream isotope data in eastern Puerto Rico (Scholl *et al*., 2014) do not support the interpretation of a considerable contribution from throughfall with an evaporated isotopic signature. An alternative but as yet unproven explanation would be that most of the high Ew occurs during low-intensity rain events of long duration (cf. Schellekens *et al*. 1999). The associated (and enriched) throughfall would be absorbed by the soil matrix and taken up by the trees. Conversely, high-intensity rain events of short duration would be less prone to enrichment by wet-canopy evaporation but would tend to contribute to preferential flow rather than being absorbed by the matrix (cf. Schellekens *et al.* 2004). Event-based sampling for stable isotopes analysis of throughfall associated with the two types of rainstorms (cf. Te Linde *et al.* 2001) would be required to demonstrate the existence of such a mechanism.

The range of soil water evaporation rates typically found for old-growth lowland rain forests (0.14–0.19 mm d^{-1}) that we used initially to calculate the characteristic length L_C (Stage I evaporation) was also too low (i.e. calculated L_C too large) to explain the extent of evaporative enrichment inferred from the *d*-excess parameters for soil water. The inset in Figure 2.5a shows that higher evaporation rates (0.70-0.72 mm d^{-1}) would be required to explain the *d*-excess

derived depth of soil water evaporation. Indeed, as stated earlier, it is not impossible that actual rates of soil evaporation in the studied mahogany plantation may have been somewhat higher than these initially low assumed values as the LUQ stand is likely to be better ventilated than the dense equatorial forests for which the cited rates were derived (cf. Roberts *et al.*, 2005). Furthermore, the characteristic length L_C is derived from models that are "porous media centric" rather than 'atmospherically centered'. That is, these soil-based models are informed parsimoniously by two parameters derived from the properties of the soil: the van Genuchten model parameters *n* and α. An explanation is therefore needed for the observed vertical extent of soil water with an evaporated isotopic signature —i.e. down to 50 cm. Interestingly, very little variation in soil water *d*-excess was observed between 10 cm and 50 cm (Figure 2.5a), suggesting that evaporative isotopic enrichment either did not systematically decrease with depth or that evaporation was restricted to the top 10 cm and transported vertically with depth. Another possibility is the mixing of rainfall having different isotopic signatures would lead to a relatively constant *d*-excess with depth. The *d*-excess values of rainfall prior to sampling, however, closely tracked the weighted rainfall *d*-excess, suggesting that mixing may not be as important a factor as evaporative enrichment. The last possibility we want to discuss is that pathways may exist for transport of water vapor from deeper pore spaces to the surface during capillary-driven Stage 1 evaporation (or similarly, during drainage) and *vice versa* during vapor-diffusion-driven Stage 2 evaporation (see Or *et al*. (2013) for discussion). One plausible way for vapor transport to persist with depth is via a subsurface architecture of soil macropores due to soil cracks, root channels, and animal burrows (as seen at LUQ by Stallard and Murphy (2012) and Larsen *et al*. (2012)) where air moves in and out of the soil system. Indeed, Silver *et al*. (1999) found that Tabonuco forest soils, where our samples were collected, remained well-aerated close to ambient O_2 concentrations of 21% down to a depth of 35 cm, which was their maximum sampling depth. Medium-size and fine roots have also been observed at our site in LUQ down to a depth of 97 cm (USDA NRCS, 2002). Further work on rooting depths, oxygen dynamics, and vapor transport in soils may shed some light on this topic in the future.

In addition to evaporation, root water uptake also leads to soil drying. How soil drying, as a direct result of root water uptake, affects liquid-vapor fluxes within the soil profile, however, is

not well understood, nor are the effects of evaporation and root water uptake taking place in parallel with drainage (e.g. after a rainfall event) during redistribution of water within the rooting zone. Several recent studies have questioned the reliability of commonly used soil water extraction methods for isotopic analysis (Meissner *et al*. 2014; Oerter *et al*. 2014). These studies provided evidence that soil physico--chemical characteristics may play a role in isotopic fractionation, particularly with respect to $\delta^{18}O$, such that $\delta^{18}O$ in xylem water may not necessarily reflect the $\delta^{18}O$ of soil water (e.g. Geris *et al*., 2015). On the other hand, an earlier study by Ellsworth and Williams (2007) provided evidence to the contrary in that $\delta^{18}O$ in xylem water did reflect $\delta^{18}O$ in soil water. Clearly, more studies are needed to resolve the apparent issues with soil water sampling and laboratory techniques for water extraction and isotope analysis. Techniques for *in-situ,* high-frequency measurements of liquid and vapor isotopes in the unsaturated zone (Volkmann and Weiler, 2013; Gaj *et al*. 2016; Sprenger *et al*., 2015) hold great potential for exploring many of the research questions that remain unanswered with respect to ecohydrological separation (Bowen, 2015).

2.5.2 Ecohydrological separation research techniques: New approaches

We know, based on stable isotopes, that the water that drains through the soil profile (preferential flow water) and replenishes groundwater and streamflow is isotopically different from the residual topsoil water (soil matrix water) that roots take up for transpiration. There is now widespread, global-in-scale evidence for ecohydrological separation. The meta-analysis of Evaristo *et al*. (2015) adapted the lc-excess* method of Landwehr and Coplen (2006) while Good *et al*. (2015) used an approach that required ecohydrological separation in order to close the global water-isotope budget. These lines of evidence notwithstanding, we still lack a complete process-based understanding behind the apparent separation between topsoil water and xylem water on the one hand, and groundwater recharge and stream water on the other.

While cryogenic vacuum distillation (and now many other forms of complete water extraction) identify ‘tightly bound water’, clues have already been given regarding the role of mycorrhizal fungi in facilitating extraction of water held under tensions much greater than the hydrological

community might expect (as reviewed by Auge (2001); Auge *et al*., (2015)) and the many papers thereafter (e.g. Allen (2007); Barzana *et al*. (2012)). Lodge (1996) reported that 98% of all trees at LUQ have roots that form symbiotic relationships with mycrorrhizal fungi to facilitate nutrient uptake from the soil. Recently, big-leaf mahogany (*Swietenia macrophylla*) was also reported to have mycorrhizal fungi associations, with diversity that was twice greater in mature trees than in seedlings (Rodríguez-Morelos *et al*., 2014). An even more intriguing observation is that many mycorrhizal-associated plants appear to have a mechanism for extracting water below the wilting point of non-mycorrhizal-associated species (Bethlenfalvay *et al*., 1988; Franson *et al*., 1991). However, current extraction techniques prevent us from interrogating the water the plants are actually extracting for isotope analysis, both in time and space. This is a key issue for progress.

At present, we can only sample either the most mobile waters via suction lysimeters or effectively "all the water" via cryogenic vacuum distillation (-10 to -15 MPa) or hydraulic squeezing (~41 MPa). Even more problematic is the range of spatial scales at which these current techniques are able to extract water. The range of pore sizes and subsurface architecture amenable to our extraction techniques (10^{-5}<range<10^{-2} m) is orders of magnitude greater than the scales that may be relevant to water uptake by roots (10^{-5}<diameter<10^{-3} m) and/or fungal hyphae (10^{-6}<diameter<10^{-5} m) (Smith *et al*., 2010). Moreover, the destructive nature of sampling related to these extraction techniques eliminates the opportunity to account for effects on soil properties by soil microfauna and microflora (Hallett *et al*., 2013) and *vice versa* (Schwartz *et al*., 2016; Kravchenko *et al*., 2013). Given the spatio-temporal incongruence between our soil water extraction techniques and plant (root/mycorrhizal) water uptake mechanisms, we need to develop fundamentally new extraction approaches that are able to interrogate water sources and root water uptake mechanisms at matching scales.

2.5.3 Ecohydrological separation and groundwater use?

Ecohydrological separation – defined as plants using water of a character different to mobile water found in soils, groundwater and streams – in no way suggests that plants do not use groundwater. There is recognition of the role of groundwater as a water source for plants when

and where phreatic water is accessible (see review by Fan 2015). Our Bayesian mixing model results show that groundwater contribution to dry period xylem water of valley-bottom (i.e. riparian) trees could comprise as much as 38±10% and 28±14% at the xeric (SUS) and mesic-hydric (LUQ) sites, respectively. Source water partitioning to riparian trees, between soil and phreatic water, is known to be influenced by moisture input fluctuations and local, or tree-level, conditions such as floodplain surface elevation and gravel layer elevation in the subsurface (Singer *et al*., 2014). These insights notwithstanding, in landscape positions (e.g. ridge-tops) at which source water partitioning results show groundwater contribution –we underline that mixing model results are dependent on the chosen end members. One plausible explanation for our mixing model-inferred groundwater use by trees on ridge tops is that deep soil water , saprolite water (Oshun *et al*. 2015) or perched groundwater within the hillslope may be isotopically the same as deeper groundwater. Synthesis of water stable isotope data may need to be cognizant of such a caveat when surveying groundwater use patterns by vegetation from regional to global scales. Nevertheless, the role of landscape position in routing and redistribution of soil water (Du *et al*., 2015) across space and time scales will need to be considered in future studies.

2.6 Conclusion

In this work we provided another line of evidence for ecohydrological separation (i.e. trees using a different water source from groundwater and streams) in two contrasting ecosystems of the less seasonal tropics in Puerto Rico. These results suggest that ecohydrological separation might be related less to temporal phase differences between hydrology (i.e. precipitation inputs) and ecology (i.e. primary productivity and water uptake by the vegetation) than with the fundamental processes that drive soil drying – e.g. soil water evaporation, root water uptake, and drainage. The interplay between the water that replenishes streamflow (preferential flow), and the water that is retained in the soil matrix for root water uptake, remains poorly understood. Future work should be focused at assessing the relative importance of these processes in both space and time; and on developing new experimental designs and methods for isotopic analysis of soil water and plant tissue. Event-based sampling for stable isotopes analysis of throughfall associated with different storm types, for example, may also prove instructive in the future. Lastly, we

partitioned the sources of water by using a Bayesian mixing model. This showed that groundwater contribution to xylem water was greater for valley-bottom (i.e. riparian trees) than for ridge-top trees, and at the xeric site than at the mesic-hydric site.

2.7 Transition Statement

This chapter provided a vital link to the following chapter, which established ecohydrological separation as a widespread phenomenon. It may be useful to note that heretofore, ecohydrological separation was demonstrated only in settings with high seasonality, particularly, in Oregon (USA) and Veracruz (Mexico). Indeed, the original proposition (Phillips, 2010) for the controls on ecohydrological separation was predicated on the temporal phasing between hydrologic input and primary productivity. This work in Puerto Rico provided evidence that ecohydrological separation was more fundamental than the latter original interpretation. The evidence, insights, and conclusions drawn from this chapter laid the foundation for the global-in-scale investigation that would follow and is presented in the following chapter.

2.8 Dedication

This work is dedicated to Frederick N. Scatena III (1954-2013), whose inspiration, guidance, support, and knowledge of the Luquillo Mountains made this work possible.

2.9 Acknowledgements

Funding for this work was provided by the National Science Foundation Luquillo Critical Zone Observatory (NSF EAR-0722476). J.E thanks the personnel of the US Forest Service Sabana Field and El Verde Field stations in Luquillo, the US Forest Service in Susua, and two graduate students (Kaizad Patel and Chennery Fife) from the University of Pennsylvania for their assistance and support in the field, as well as Brent Helliker and David Vann, University of Pennsylvania, for fruitful discussions during sampling design and execution. J.E. also thanks the Stable Isotope Ratio Facility for Environmental Research (SIRFER) at the University of Utah for careful handling and analyses of our samples, as well as Jim

Ehleringer, Todd Dawson, and the Stable Isotope Biogeochemistry & Ecology (Iso-Camp) 2012 summer course instructors for the intellectual guidance surrounding the implementation of this work. We all thank Anna Coles, Chris Gabrielli, Willemijn Appels, Dyan Pratt, and Kim Janzen for very helpful and insightful comments on an early draft of this manuscript. Finally, the three anonymous reviewers are thanked for helpful criticism and feedback. Any use of trade, firm or product names is for descriptive purposes only and does not imply endorsement by the U.S. Government.

2.10 Author contributions

J.E designed the study, collected the samples, and conducted all data analysis except for Bayesian modeling which was performed by K.P.C. M.A.S. provided the isotope data on rainfall and stream water isotopes at the Luquillo site. J.E. wrote paper. J.J.M., M.A.S, and L.A.B. edited and commented on the manuscript and contributed to the text in later iterations.

2.11 References

1. Andrade J., Meinzer F., Goldstein G., Schnitzer S. 2005. Water uptake and transport in lianas and co-occurring trees of a seasonally dry tropical forest. *Trees-Structure and Function* **19** : 282-9. DOI: 10.1007/s00468-004-0388-x.

2. Auge R.M. 2001. Water relations, drought and vesicular-arbuscular mycorrhizal symbiosis. *Mycorrhiza* **11** : 3-42. DOI: 10.1007/s005720100097.

3. Auge R.M., Toler H.D., Saxton A.M. 2015. Arbuscular mycorrhizal symbiosis alters stomatal conductance of host plants more under drought than under amply watered conditions: a meta-analysis. *Mycorrhiza* **25** : 13-24. DOI: 10.1007/s00572-014-0585-4.

4. Baldocchi D., Falge E., Wilson K. 2001. A spectral analysis of biosphere-atmosphere trace gas flux densities and meteorological variables across hour to multi-year time scales. *Agricultural and Forest Meteorology* **107** : 1-27. DOI: 10.1016/S0168-1923(00)00228-8.

5. Barbeta A., Mejia-Chang M., Ogaya R., Voltas J., Dawson T.E., Penuelas J. 2015. The combined effects of a long-term experimental drought and an extreme drought on the use of plant-water sources in a Mediterranean forest. *Global Change Biology* **21** : 1213-25. DOI: 10.1111/gcb.12785.

6. Barzana G., Aroca R., Antonio Paz J., Chaumont F., Carmen Martinez-Ballesta M., Carvajal M., Manuel Ruiz-Lozano J. 2012. Arbuscular mycorrhizal symbiosis increases relative apoplastic water flow in roots of the host plant under both well-watered and drought stress conditions. *Annals of Botany* **109** : 1009-17. DOI: 10.1093/aob/mcs007.

7. Beck H.E., Bruijnzeel L.A., van Dijk A.I.J.M., McVicar T.R., Scatena F.N., Schellekens J. 2013. The impact of forest regeneration on streamflow in 12 mesoscale humid tropical catchments. *Hydrology and Earth System Sciences* **17** : 2613-35. DOI: 10.5194/hess-17-2613-2013.

8. Bertrand G., Masini J., Goldscheider N., Meeks J., Lavastre V., Celle-Jeanton H., Gobat J., Hunkeler D. 2014. Determination of spatiotemporal variability of tree water uptake using stable isotopes (d 18O, d 2H) in an alluvial system supplied by a high- altitude watershed, Pfyn forest, Switzerland. *Ecohydrology* **7** : 319-33. DOI: 10.1002/eco.1347.

9. Bethlenfalvay G.J., Thomas R.S., Dakessian S., Brown M.S., Ames R.N. 1988. *Mycorrhizae in stressed environments: effects on plant growth, endophyte development, soil stability and soil water.*; 1029.

10. Bonan G.B., Levis S., Kergoat L., Oleson K.W. 2002. Landscapes as patches of plant functional types: An integrating concept for climate and ecosystem models. *Global Biogeochemical Cycles* **16** : 5-1.

11. Bowen G. 2015. HYDROLOGY The diversified economics of soil water. *Nature* **525** : 43-4.

12. Brooks J.R., Barnard H.R., Coulombe R., McDonnell J.J. 2010. Ecohydrologic separation of water between trees and streams in a Mediterranean climate. *Nature Geoscience* **3** : 100-4. DOI: 10.1038/NGEO722.

13. Brunel J.P., Walker G.R., Kennettsmith A.K. 1995. Field Validation of Isotopic Procedures for Determining Sources of Water used by Plants in a Semiarid Environment. *Journal of Hydrology* **167** : 351-68. DOI: 10.1016/0022-1694(94)02575-V.

14. Budyko M. I. 1974. Climate and Life, Academic, Orlando, Fla.

15. Burton F.J. 2007. Vegetation Classification for the Cayman Islands. In: Burton, F.J. 2007. Threatened Plants of the Cayman Islands. Kew Publishers, London.

16. Buss H.L., Brantley S.L., Scatena F.N., Bazilievskaya E.A., Blum A., Schulz M., Jimenez R., White A.F., Rother G., Cole D. 2013. Probing the deep critical zone beneath the Luquillo Experimental Forest, Puerto Rico. *Earth Surface Processes and Landforms* **38** : 1170-86. DOI: 10.1002/esp.3409.

17. Clark D.A., Brown S., Kicklighter D.W., Chambers J.Q., Thomlinson J.R., Ni J., Holland E.A. 2001. Net primary production in tropical forests: An evaluation and synthesis of existing field data. *Ecological Applications* **11** : 371-84.

18. Comarazamy D.E., González J.E. 2011. Regional long-term climate change (1950-2000) in the midtropical Atlantic and its impacts on the hydrological cycle of Puerto Rico. *Journal of Geophysical Research: Atmospheres***116**. DOI: 10.1029/2010JD015414.

19. Coplen T.B. 2011. Guidelines and recommended terms for expression of stable-isotope-ratio and gas-ratio measurement results. *Rapid Communications in Mass Spectrometry* **25** : 2538-60. DOI: 10.1002/rcm.5129.

20. Dansgaard W. 1964. Stable Isotopes in Precipitation. *Tellus* **16** : 436-68.

21. Dawson T.E. 1993. Hydraulic lift and water use by plants: implications for water balance, performance and plant-plant interactions. *Oecologia* **95** : 565-74.

22. D'Odorico P., Laio F., Porporato A., Ridolfi L., Rinaldo A., Rodriguez-Iturbe I. 2010. Ecohydrology of terrestrial ecosystems. *Bioscience* **60** : 898-907.

23. Du Z., Riveros-Iregui D.A., Jones R.T., McDermott T.R., Dore J.E., McGlynn B.L., Emanuel R.E., Li X. 2015. Landscape position influences microbial composition and function via

redistribution of soil water across a watershed. *Appl Environ Microbiol* 81:8457–8468. doi:10.1128/AEM.02643-15.

24. Ehleringer J.R., Dawson T.E. 1992. Water uptake by plants: perspectives from stable isotope composition. *Plant, Cell & Environment* **15** : 1073-82.

25. Ellsworth P.Z., Williams D.G. 2007. Hydrogen isotope fractionation during water uptake by woody xerophytes. *Plant and Soil* **291** : 93-107. DOI: 10.1007/s11104-006-9177-1.

26. Evaristo J., Jasechko S., McDonnell J.J. 2015. Global separation of plant transpiration from groundwater and streamflow. *Nature* **525** : 91,+. DOI: 10.1038/nature14983.

27. Fan Y. 2015. Groundwater in the Earth's critical zone: Relevance to large-scale patterns and processes. *Water Resources Research* **51** : 3052-69.

28. Franson R.L., Brown M.S., Bethlenfalvay G.J. 1991. The Glycine-Glomus-Bradyrhizobium Symbiosis .11. Nodule Gas-Exchange and Efficiency as a Function of Soil and Root Water Status in Mycorrhizal Soybean. *Physiologia Plantarum* **83** : 476-82. DOI: 10.1034/j.1399-3054.1991.830322.x.

29. Gaj M., Beyer M., Koeniger P., Wanke H., Hamutoko J., Himmelsbach T. 2016. In-situ unsaturated zone stable water isotope (^{2}H and ^{18}O) measurements in semi-arid environments using tunable off-axis integrated cavity output spectroscopy, Hydrol. Earth Syst. Sci. **12** : 6115-6149. DOI: 10.5194/hess-20-715-2016

30. García-Martinó A.R., Warner G.S., Scatena F.N., Civco D.L. 1996. Rainfall, runoff and elevation relationships in the Luquillo Mountains of Puerto Rico. *Caribbean Journal of Science* **32** : 413-24.

31. Geris J., Tetzlaff D., McDonnell J.J., Anderson J., Paton G., Soulsby C. 2015. Ecohydrological separation in wet, low energy northern environments? A preliminary assessment using different soil water extraction techniques. *Hydrological Processes* **29** : 5139-5152. DOI: 10.1002/hyp.10603.

32. Gerrits A.M.J., Savenije H.H.G., Veling E.J.M., Pfister L. 2009. Analytical derivation of the Budyko curve based on rainfall characteristics and a simple evaporation model. *Water Resources Research* **45**. DOI: 10.1029/2008WR007308.

33. Goldsmith G.R., Muñoz-Villers L.E., Holwerda F., Mcdonnell J.J., Asbjornsen H., Dawson T.E. 2012. Stable isotopes reveal linkages among ecohydrological processes in a seasonally dry tropical montane cloud forest. *Ecohydrology* **5** : 779-90.

34. Good S.P., Noone D., Bowen G. 2015. Hydrologic connectivity constrains partitioning of global terrestrial water fluxes. *Science* **349** : 175-7. DOI: 10.1126/science.aaa5931.

35. Gouet-Kaplan M., Arye G., Berkowitz B. 2012. Interplay between resident and infiltrating water: Estimates from transient water flow and solute transport. *Journal of Hydrology* **458-459** : 40-50.

36. Govender Y., Cuevas E., Sternberg L.D.S., Jury M.R. 2013. Temporal variation in stable isotopic composition of rainfall and groundwater in a tropical dry forest in the northeastern Caribbean. *Earth Interactions* **17** : 1-20.

37. Green M.B., Laursen B.K., Campbell J.L., McGuire K.J., Kelsey E. P. 2015. Stable water isotopes suggest sub-canopy water recycling in a northern forested catchment. Hydrol. Process., **29**: 5193–5202. doi: 10.1002/hyp.10706.

38. Gutierrez-Soto M.V., Ewel J.J. 2008. Water use in four model tropical plant associations established in the lowlands of Costa Rica. *Revista de biologia tropical* **56** : 1947-57.

39. Hallett P.D., Karim K.H., Bengough A.G., Otten W. 2013. Biophysics of the Vadose Zone: From Reality to Model Systems and Back Again. *Vadose Zone Journal* **12**. DOI: 10.2136/vzj2013.05.0090.

40. Hamon WR. 1963. Computation of direct runoff amounts from storm rainfall. International Association of Scientific Hydrological Publications **63**: 52–62.

41. Hargreaves G., Allen R. 2003. History and evaluation of Hargreaves evapotranspiration equation. *Journal of Irrigation and Drainage Engineering-Asce* **129** : 53-63. DOI: 10.1061/(ASCE)0733-9437(2003)129:1(53).

42. Heartsill-Scalley T., Scatena F.N., Estrada C., McDowell W.H., Lugo A.E. 2007. Disturbance and long-term patterns of rainfall and throughfall nutrient fluxes in a subtropical wet forest in Puerto Rico. *Journal of Hydrology* **333**: 472-85.

43. Helmer E.H., Ramos O., López T. del M., Quinones M., Diaz W. 2002. Mapping the forest type and land cover of Puerto Rico, a component of the Caribbean Biodiversity Hotspot. *Caribbean Journal of Science*. 38: 165–183.

44. Holwerda F., Bruijnzeel L.A., Scatena F.N., Vugts H.F., Meesters A.G.C.A. 2012. Wet canopy evaporation from a Puerto Rican lower montane rain forest: The importance of realistically estimated aerodynamic conductance.*Journal of Hydrology* **414** : 1-15. DOI: 10.1016/j.jhydrol.2011.07.033.

45. Holwerda F., Scatena F.N., Bruijnzeel L.A. 2006. Throughfall in a Puerto Rican lower montane rain forest: A comparison of sampling strategies. *Journal of Hydrology* **327** : 592-602. DOI: 10.1016/j.jhydrol.2005.12.014.

46. Jackson P., Cavelier J., Goldstein G., Meinzer F., Holbrook N. 1995. Partitioning of Water-Resources among Plants of a Lowland Tropical Forest. *Oecologia* **101** : 197-203. DOI: 10.1007/BF00317284.

47. Jasechko S., Birks S.J., Gleeson T., Wada Y., Fawcett P.J., Sharp Z.D., McDonnell J.J., Welker J.M. 2014. The pronounced seasonality of global groundwater recharge. *Water Resources Research* **50** : 8845-67. DOI: 10.1002/2014WR015809.

48. Jasechko S., Taylor R.G. 2015. Intensive rainfall recharges tropical groundwaters. *Environmental Research Letters* **12** : 24015-. doi: 10.1088/1748-9326/10/12/124015.

49. Jones J.A., Creed I.F., Hatcher K.L., Warren R.J., Adams M.B., Benson M.H., Boose E., Brown W.A., Campbell J.L., Covich A., Clow D.W., Dahm C.N., Elder K., Ford C.R., Grimm N.B., Henshaw D.L., Larson K.L., Miles E.S., Miles K.M., Sebestyen S.D., Spargo A.T., Stone A.B., Vose J.M., Williams M.W. 2012. Ecosystem Processes and Human Influences Regulate Streamflow Response to Climate Change at Long-Term Ecological Research Sites.*Bioscience* **62** : 390-404. DOI: 10.1525/bio.2012.62.4.10.

50. Jordan C.F.,Heuveldop J. 1981.The water budget of an Amazonian rain forest. Acta Amazonica **11** : 87-92.

51. Kravchenko A., Chun H.-., Mazer M., Wang W., Rose J.B., Smucker A., Rivers M. 2013. Relationships between intra-aggregate pore structures and distributions of Escherichia coli within soil macro-aggregates. *Applied Soil Ecology* **63** : 134-42. DOI: 10.1016/j.apsoil.2012.10.001.

52. Landwehr J., Coplen T. 2006. in Isotopes in Environmental Studies 132–135 (IAEA-CN-118/56, International Atomic Energy Agency)

53. Larsen M.C., Liu, Z., Zou, X. 2012. Effects of earthworms on slopewash, surface runoff, and fine-litter transport on a humid tropical forested hillslope, Luquillo Experimental Forest, Puerto Rico, ch. G in Murphy, S.F., and Stallard, R.F., eds., Water quality and landscape processes of four watersheds in eastern Puerto Rico: U.S. Geological Survey Professional Paper 1789, p. 179–198.

54. Lee J.-., Oliveira R.S., Dawson T.E., Fung I. 2005. Root functioning modifies seasonal climate. *Proceedings of the National Academy of Sciences of the United States of America* **102** : 17576-81.

55. Lehmann P., Assouline S., Or D. 2008. Characteristic lengths affecting evaporative drying of porous media. *Physical Review E* **77** : 056309. DOI: 10.1103/PhysRevE.77.056309.

56. Lenart M.T., Falk D.A., Scatena F.N., Osterkamp W.R. 2010. Estimating soil turnover rate from tree uprooting during hurricanes in Puerto Rico. *Forest Ecology and Management* **259** : 1076-84. DOI: 10.1016/j.foreco.2009.12.014.

57. Leng X., Cui J., Zhang S., Zhang W., Liu Y., Liu S., An S. 2013. Differential water uptake among plant species in humid alpine meadows. *Journal of Vegetation Science* **24** : 138-47. DOI: 10.1111/j.1654-1103.2012.01439.x.

58. Leng X., Cui J., Zhang S., Zhang W., Liu Y., Liu S., An S. 2013. Differential water uptake among plant species in humid alpine meadows. *Journal of Vegetation Science* **24** : 138-47. DOI: 10.1111/j.1654-1103.2012.01439.x.

59. Liu X., Li Y., Chen X., Zhou G., Cheng J., Zhang D., Meng Z., Zhang Q. 2015. Partitioning evapotranspiration in an intact forested watershed in southern China. *Ecohydrology* **8**, 1037-1047 DOI: 10.1002/3eco.1561

60. Lodge D.J. 1996. Microorganisms. In: Reagan, D.P.; Waide, R.B. The food web of a tropical rain forest. Chicago, IL: University of Chicago Press: **53**–108.

61. Lugo A.E., Figueroa-Colon J.C., Alayon M. 2003. Big-Leaf Mahogany: Genetics, Ecology and Management. Ecological Studies 159. New York, NY: Springer Verlag.

62. Lugo A.E. 1992. The search for carbon sinks in the tropics. *Water, air, and soil pollution* **64** : 3-9.

63. McDonnell J.J. 2014. The two water worlds hypothesis: ecohydrological separation of water between streams and trees? *WIREs Water* **1** : 323–329.

64. McDowell W., Bowden W., Asbury C. 1992. Riparian Nitrogen Dynamics in 2-Geomorphologically Distinct Tropical Rain-Forest Watersheds - Subsurface Solute Patterns. *Biogeochemistry* **18** : 53-75. DOI: 10.1007/BF00002703.

65. Medina E., Cuevas E., Figueroa J., Lugo A.E. 1994. Mineral content of leaves from trees growing on serpentine soils under contrasting rainfall regimes in Puerto Rico. *Plant and Soil* **158** : 13-21.

66. Meinzer F., Andrade J., Goldstein G., Holbrook N., Cavelier J., Wright S. 1999. Partitioning of soil water among canopy trees in a seasonally dry tropical forest. *Oecologia* **121** : 293-301. DOI: 10.1007/s004420050931.

67. Meissner M., Koehler M., Schwendenmann L., Hoelscher D., Dyckmans J. 2014. Soil water uptake by trees using water stable isotopes (delta H-2 and delta O-18)-a method test regarding soil moisture, texture and carbonate. *Plant and Soil* **376** : 327-35. DOI: 10.1007/s11104-013-1970-z.

68. Moore J.W., Semmens B.X. 2008. Incorporating uncertainty and prior information into stable isotope mixing models. *Ecology Letters* **11** : 470-80. DOI: 10.1111/j.1461-0248.2008.01163.x.

69. Murphy P.G., Lugo A.E., Murphy A.J., Nepstad D.C. 1995. The dry forests of Puerto Rico's south coast. In: Lugo, A.E., Lowe, C. (Eds.), Tropical Forests: Management and Ecology. Springer, New York, pp. 178–209.

70. Oerter E., Finstad K., Schaefer J., Goldsmith G.R., Dawson T., Amundson R. 2014. Oxygen isotope fractionation effects in soil water via interaction with cations (Mg, Ca, K, Na) adsorbed to phyllosilicate clay minerals. *Journal of Hydrology* **515** : 1-9. DOI: 10.1016/j.jhydrol.2014.04.029.

71. Ogle K., Wolpert R., Reynolds J. 2004. Reconstructing plant root area and water uptake profiles. *Ecology* **85** : 1967-78. DOI: 10.1890/03-0346.

72. Ogle K., Tucker C., Cable J.M. 2014. Beyond simple linear mixing models: process-based isotope partitioning of ecological processes. *Ecological Applications* **24** : 181-95. DOI: 10.1890/1051-0761-24.1.181.

73. Or D., Lehmann P., Shahraeeni E., Shokri N. 2013. Advances in soil evaporation physics-A review. *Vadose Zone Journal* **12**.

74. Oshun J., Dietrich W.E., Dawson T.E., Fung I. 2015. Dynamic, structured heterogeneity of water isotopes inside hillslopes, Water Resour. Res., **51** : doi:10.1002/ 2015WR017485.

75. Parnell A.C., Inger R., Bearhop S., Jackson A.L. 2010. Source Partitioning Using Stable Isotopes: Coping with Too Much Variation. *Plos One* **5** : e9672. DOI: 10.1371/journal.pone.0009672.

76. Phillips D.L., Gregg J.W. 2003. Source partitioning using stable isotopes: coping with too many sources. *Oecologia* **136** : 261-9. DOI: 10.1007/s00442-003-1218-3.

77. Phillips F.M. 2010. Hydrology: Soil-water bypass. *Nature Geoscience* **3** : 77-8.

78. Pike A.S., Scatena F.N., Wohl E.E. 2010. Lithological and fluvial controls on the geomorphology of tropical montane stream channels in Puerto Rico. *Earth Surface Processes and Landforms* **35** : 1402-17.

79. Potter N.J., Zhang L., Milly P.C.D., McMahon T.A., Jakeman A.J. 2005. Effects of rainfall seasonality and soil moisture capacity on mean annual water balance for Australian catchments. *Water Resources Research* **41** : 1-11. DOI: 10.1029/2004WR003697.

80. Roberts J.M., Gash J.H.C., Tani M., Bruijnzeel L.A. 2005. Controls on evaporation in lowland tropical rainforest. Pp. 287-313 in M. Bonell & L.A. Bruijnzeel (editors), *Forests, Water and People in the Humid Tropics*. Cambridge University Press.

81. Roche M.-. 1982. (Actual evapotranspiration of the Amazonian forest in French Guyana). *Cahiers ORSTOM, Serie Hydrologie* **19** : 37-44.

82. Rodriguez-Morelos V.H., Soto-Estrada A., Perez-Moreno J., Franco-Ramirez A., Diaz-Rivera P. 2014. Arbuscular mycorrhizal fungi associated with the rhizosphere of seedlings and mature trees of Swietenia macrophylla (Magnoliophyta: Meliaceae) in Los Tuxtlas, Veracruz, Mexico. *Revista Chilena De Historia Natural* **87** : 9. DOI: 10.1186/s40693-014-0009-z.

83. Rossatto D.R., de Carvalho Ramos Silva L., Villalobos-Vega R., Sternberg L.D.S.L., Franco A.C. 2012. Depth of water uptake in woody plants relates to groundwater level and vegetation structure along a topographic gradient in a neotropical savanna. *Environmental and experimental botany* **77** : 259-66. DOI: 10.1016/j.envexpbot.2011.11.025.

84. Scatena F.N., Lugo A.E. 1995. Geomorphology, disturbance, and the soil and vegetation of two subtropical wet steepland watersheds of Puerto Rico. *Geomorphology* **13** : 199-213.

85. Schellekens J., Scatena F.N., Bruijnzeel L.A., Wickel A.J. 1999. Modelling rainfall interception by a lowland tropical rain forest in Eastern Puerto Rico. *Journal of Hydrology* **225** : 168-184.

86. Schellekens J., Bruijnzeel L.A., Scatena F.N., Bink N.J., Holwerda F. 2000. Evaporation from a tropical rain forest, Luquillo Experimental Forest, eastern Puerto Rico. *Water Resources Research* **36** : 2183-96.

87. Schellekens J., Scatena F., Bruijnzeel L., van Dijk A., Groen M., van Hogezand R. 2004. Stormflow generation in a small rainforest catchment in the luquillo experimental forest, Puerto Rico. *Hydrological Processes* **18** : 505-30. DOI: 10.1002/hyp.1335.

88. Scholl M.A., Torres-Sanchez A., Rosario-Torres M. 2014. Stable isotope (d18O and d2H) values for precipitation, stream water and groundwater in Puerto Rico, U.S. Geol. Surv. Open File Rep., 2014-1011, 25 p., in press.

89. Scholl M.A., Shanley J.B., Zegarra J.P., Coplen T.B. 2009. The stable isotope amount effect: New insights from NEXRAD echo tops, Luquillo Mountains, Puerto Rico. *Water Resources Research* **45**. DOI: 10.1029/2008WR007515.

90. Schwartz N., Carminati A., Javaux M. 2016. The impact of mucilage on root water uptake—A numerical study. *Water Resources Research* : n/a,n/a. DOI: 10.1002/2015WR018150.

91. Silver W.L., Lugo A.E., Keller M. 1999. Soil oxygen availability and biogeochemistry along rainfall and topographic gradients in upland wet tropical forest soils. *Biogeochemistry* **44** : 301-28.

92. Simonin K.A., Link P., Rempe D., Miller S., Oshun J., Bode C., Dietrich W.E., Fung I., Dawson T.E. 2013. Vegetation induced changes in the stable isotope composition of near surface humidity. *Ecohydrology* .

93. Singer M.B., Sargeant C.I., Piegay H., Riquier J., Wilson R.J.S., Evans C.M. 2014. Floodplain ecohydrology: Climatic, anthropogenic, and local physical controls on partitioning of water sources to riparian trees. *Water Resources Research* **50** : 4490-513. DOI: 10.1002/2014WR015581.

94. Smith S.E., Facelli E., Pope S., Smith F.A. 2010. Plant performance in stressful environments: interpreting new and established knowledge of the roles of arbuscular mycorrhizas. *Plant and Soil* **326** : 3-20. DOI: 10.1007/s11104-009-9981-5.

95. Sprenger M., Herbstritt B., Weiler M. 2015. Established methods and new opportunities for pore water stable isotope analysis. *Hydrol. Process*., **29**: 5174–5192. DOI: 10.1002/hyp.10643.

96. Stallard R.F., Murphy S.F. 2012. Water quality and mass transport in four watersheds in eastern Puerto Rico, in Water Quality and Landscape Processes of Four Watersheds in Eastern Puerto Rico, edited by S. F. Murphy and R. F. Stallard, pp. 113–152, U.S. Geological Survey Professional Paper 1789.

97. Stratton L., Goldstein G., Meinzer F. 2000. Temporal and spatial partitioning of water resources among eight woody species in a Hawaiian dry forest. *Oecologia* **124** : 309-17. DOI: 10.1007/s004420000384.

98. Te Linde A.H., Bruijnzeel L.A., Groen J.M., Scatena F.N., Meijer H.A.J. 2001. Stable isotopes in rainfall and fog in the Luquillo Mountains, eastern Puerto Rico: a preliminary study. Pp. 181-184 in R.S. Schemenauer & H. Puxbaum (Editors), *Second International Conference on Fog and Fog Collection*, IDRC, Ottawa, Canada.

99. Thorburn P.J., Walker G.R. 1993. The source of water transpired by *Eucalyptus camaldulensis*: soil, groundwater, or streams? Pages 511–527 *in* J. R. Ehleringer, A. E. Hall, and G. D. Farquhar, editors. Stable isotopes and plant carbon–water relations. Academic Press, San Diego, California, USA.

100. Troch P.A., Martinez G.F., Pauwels V.R.N., Durcik M., Sivapalan M., Harman C., Brooks P.D., Gupta H., Huxman T. 2009. Climate and vegetation water use efficiency at catchment scales. *Hydrological Processes* **23** : 2409-14.

101. USDA-NCSS. 2002. Soil Survey of Caribbean National Forest and Luquillo Experimental Forest, Commonwealth of Puerto Rico. National Resources Conservation Service. Washington D.C.

102. Van Beusekom A.E., Gonzalez G., Rivera M.M. 2015. Short-Term Precipitation and Temperature Trends along an Elevation Gradient in Northeastern Puerto Rico. *Earth Interactions* **19** : UNSP 3. DOI: 10.1175/EI-D-14-0023.1.

103. Vivoni E.R., Rinehart A.J., Mendez-Barroso L.A., Aragon C.A., Bisht G., Cardenas M.B., Engle E., Forman B.A., Frisbee M.D., Gutierrez-Jurado H.A., Hong S., Mahmood T.H., Tai K., Wyckoff R.L. 2008. Vegetation controls on soil moisture distribution in the Valles Caldera, New Mexico, during the North American monsoon. *Ecohydrology* **1** : 225-38. DOI: 10.1002/eco.11.

104. Volkmann T.H.M., Weiler M. 2014. Continual in situ monitoring of pore water stable isotopes in the subsurface. *Hydrology and Earth System Sciences* **18** : 1819-33. DOI: 10.5194/hess-18-1819-2014.

105. Wadsworth F.H. 1951. Forest management in the Luquillo Mountains, part I. The setting. Caribbean Forester. **12**: 93–114.

106. Wang H., Hall C.A.S., Scatena F.N., Fetcher N., Wu W. 2003. Modeling the spatial and temporal variability in climate and primary productivity across the Luquillo Mountains, Puerto Rico. *Forest Ecology and Management* **179**: 69-94. DOI: 10.1016/S0378-1127(02)00489-9.

107. Webb W., Szarek S., Lauenroth W., Kinerson R., Smith M. 1978. Primary Productivity and Water-use in Native Forest, Grassland, and Desert Ecosystems. *Ecology* **59** : 1239-47. DOI: 10.2307/1938237.

108. West A.G., Goldsmith G.R., Brooks P.D., Dawson T.E. 2010. Discrepancies between isotope ratio infrared spectroscopy and isotope ratio mass spectrometry for the stable isotope analysis of plant and soil waters. *Rapid Communications in Mass Spectrometry* **24** : 1948-54.

109. Zimmermann U., Münnich K.O., Roether W., Kreutz W., Schubach K., Siegel O. 1966. Tracers determine movement of soil moisture and evapotranspiration. *Science* **152** : 346-7.

Table 2.1. Summary of site characteristics

Site Name[1]	Elevation (masl)	MAP[2] (mm y^{-1})	Mean Annual RH[2] (%)	Lifezone and Geology[3]	Topography [4]	Land use	Mahogany species[5]
LUQ	160-207	3700	86.4	wet ; volcanic sedimentary	R, S, V	protected forest	big-leaf (*S. macrophylla*)
SUS	132-172	1200	65.5	dry; serpentine	R, V	protected forest	small-leaf (*S. mahagoni*)

[1]LUQ=Luquillo; SUS=Susua

[2]MAP=mean annual precipitation; RH=relative humidity; Sources: Luquillo Critical Zone Observatory website for LUQ, Weather Underground for SUS between 2004 and 2012

[3]Puerto Rico falls within the subtropical belt of the Holdridge Life Zone System (Helmer *et al.* 2002)

[4]R, S, V mean ridge, slope, and valley, respectively

[5]Hybrid (*S. macrophylla x S. mahagoni*) also present in LUQ

Table 2.2. Stable isotope ratios and lc-excess* of soil, xylem water, and groundwater (mean (1 ±SD)).

Site	Moisture Period	Bulk soil water			N	Plant xylem water			N	Groundwater			N
		δ^2H	$\delta^{18}O$	lc-excess*		δ^2H	$\delta^{18}O$	lc-excess*		δ^2H	$\delta^{18}O$	lc-excess*	
LUQ	Wet	-4 (8.3)	-1.1 (1.2)	-4.2 (1.8)	54	-17 (7.8)	-2.3 (1.2)	-6.5 (2.9)	18	-7.4 (2.8)	-2.7 (0.36)	1.1 (0.84)	37
	Dry	-6 (6.7)	-1.8 (0.89)	-4.7 (1.9)	94	-13 (8.6)	-2.6 (1.1)	-5.2 (2.8)	18	-3.1 (3.6)	-2.3 (0.42)	-0.7 (0.54)	12
SUS	Wet	5.76 (11)	0.64 (1.7)	-5.1 (3.3)	33	-8.5 (4.8)	-1 (0.68)	-6.3 (1.8)	12	-8.1 (5.2)	-2.4 (0.58)	0.26 (1.1)	150
	Dry	-14 (13)	-1.6 (2.2)	-8.1 (2.6)	65	-19 (5.5)	-2.2 (0.66)	-8.2 (2.8)	12	-6.4 (3.2)	-2.2 (0.39)	-0.9 (1.0)	120

Table 2.3. Stable isotope ratios, *d*-excess of soil water per depth and moisture period, mean (1 ±SD).

Site	Moisture Period	Depth (cm)	δ^2H	$\delta^{18}O$	*d*-excess	N
LUQ	Wet	10	-4 (9.5)	-1 (1.4)	4.4 (3.1)	18
		20	-2.6 (8.4)	-0.9 (1.3)	4.4 (3.1)	18
		30	-5.4 (6.6)	-1.4 (0.92)	5.8 (3.0)	18
	Dry	10	-1 (6.2)	-1 (0.95)	7.2 (3.7)	18
		20	-7.1 (5.0)	-2 (0.62)	9 (1.7)	18
		30	-11 (7.1)	-2.4 (0.62)	8.1 (3.8)	17
		40	-6.6 (5.8)	-1.8 (0.55)	7.6 (3.7)	15
		50	-4 (6.8)	-1.2 (0.82)	5.8 (2.2)	17
		60	-7.6 (5.4)	-2.5 (0.47)	12.3 (1.5)	9
SUS	Wet	10	8.17 (7.0)	0.73 (1.4)	2.44 (4.7)	12
		20	3.1 (16)	0.44 (2.2)	-0.6 (6.8)	12
		30	6.1 (8.6)	0.79 (1.2)	-0.1 (6.3)	9
	Dry	10	-1.8 (5.7)	0.43 (1.2)	-5.4 (4.2)	12
		20	-16 (13.2)	-1.8 (2.2)	-1.6 (5.4)	12
		30	-18 (13.8)	-2.4 (2.0)	0.92 (2.6)	12
		40	-17 (9.8)	-1.9 (1.9)	-1.5 (5.9)	12
		50	-21 (14)	-2.9 (2.4)	2 (5.8)	12
		60	-5.5 (4.1)	0.24 (1.3)	-7.5 (6.5)	5

Table 2.4. Bayesian mixing model results, mean (1 ±SD).

Remarks: Water source proportion differences in Ridge-top and Valley-bottom (i.e. riparian) trees at LUQ are statistically significant ($P<0.05$) between wet and dry periods. However, it is not the case for all landscape positions at SUS and for the slope position at LUQ ($P>0.05$) between wet and dry periods.

Site	Wet period											
	Ridge				Slope				Valley			
	Ground water	Deep soil	Shallow soil	Rain	Ground water	Deep soil	Shallow soil	Rain	Ground water	Deep soil	Shallow soil	Rain
LUQ	0.26 (0.12)	0.27 (0.13)	0.19 (0.11)	0.28 (0.10)	0.21 (0.13)	0.23 (0.14)	0.27 (0.14)	0.28 (0.14)	0.25 (0.15)	0.20 (0.13)	0.13 (0.10)	0.42 (0.18)
SUS	0.23 (0.10)	0.32 (0.12)	0.30 (0.11)	0.15 (0.10)	-	-	-	-	0.31 (0.11)	0.28 (0.09)	0.20 (0.11)	0.22 (0.11)
	Dry period											
LUQ	0.14 (0.12)	0.53 (0.19)	0.24 (0.15)	0.08 (0.08)	0.29 (0.15)	0.25 (0.14)	0.24 (0.14)	0.22 (0.14)	0.28 (0.14)	0.30 (0.15)	0.21 (0.13)	0.21 (0.13)
SUS	0.35 (0.09)	0.25 (0.11)	0.19 (0.10)	0.21 (0.10)	-	-	-	-	0.38 (0.10)	0.24 (0.12)	0.24 (0.12)	0.14 (0.09)

Figure 2.1 Demonstrating "in phase" correspondence between hydrology (precipitation) and ecology (primary productivity). (A) and **(B)** Monthly GPP, rainfall amount, and rainfall isotope between January 2005 and June 2013 in LUQ and SUS, respectively. **(C)** and **(D)** Power Spectral Density analysis of GPP, rainfall amount, and rainfall isotope in LUQ and SUS, respectively. **(E)** and **(F)** Long-term, monthly means (error bars are standard error) of GPP, rainfall amount, and rainfall isotope over the same 2005-2013 period.

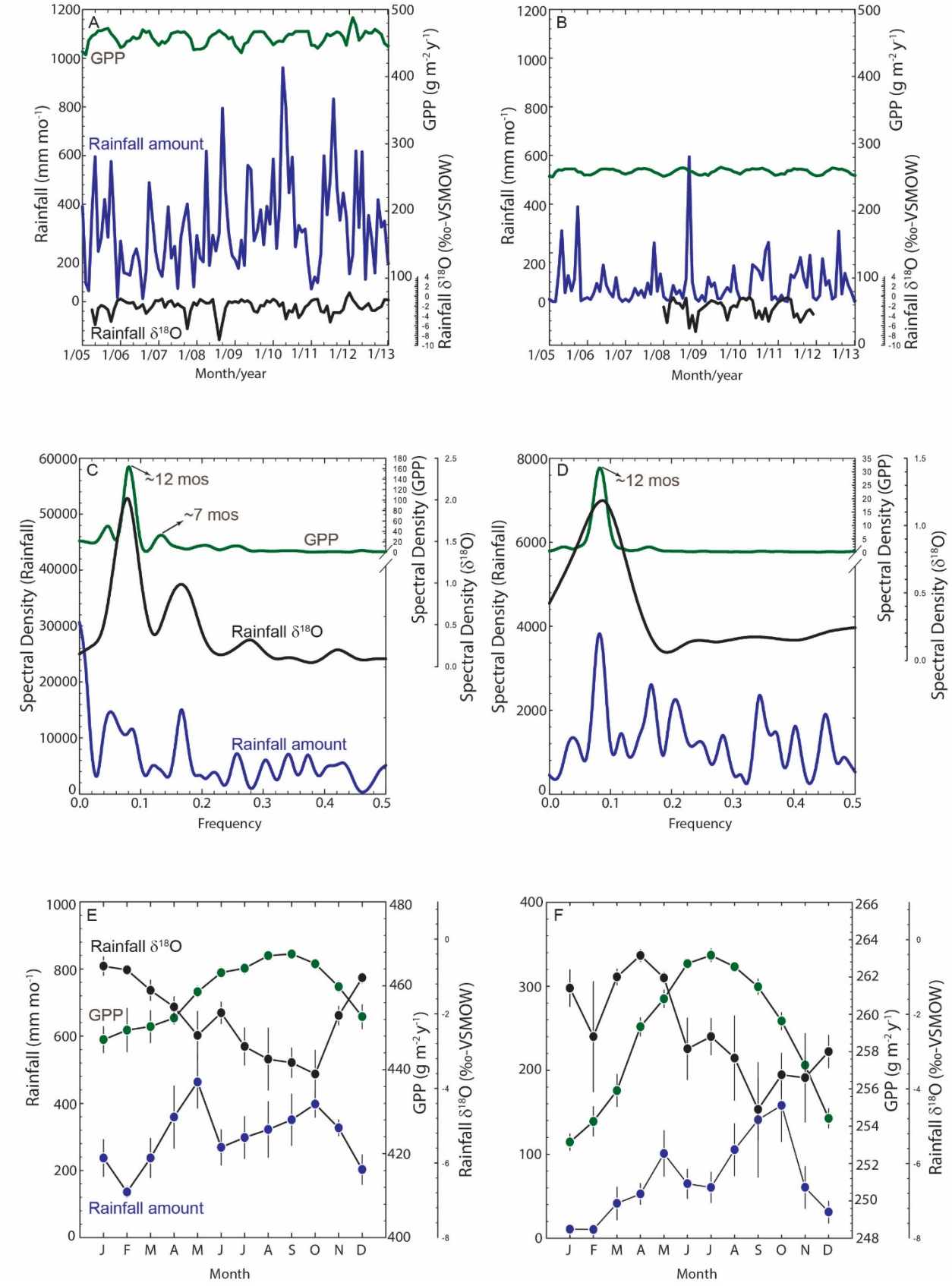
A
GPP
Rainfall amount
Rainfall δ18O
Rainfall (mm mo-1)
GPP (g m-2 y-1)
Rainfall δ18O (‰-VSMOW)
1/05 1/06 1/07 1/08 1/09 1/10 1/11 1/12 1/13
Month/year
B
C
~12 mos
~7 mos
GPP
Rainfall δ18O
Rainfall amount
Spectral Density (Rainfall)
Spectral Density (GPP)
Spectral Density (δ18O)
Frequency
D
E
Rainfall δ18O
GPP
Rainfall amount
J F M A M J J A S O N D
Month
F

Figure 2.2. Inter-annual ecohydrologic variability and the Budyko curve. AET/P vs. PET/P calculated between 2005 and 2013. AET = actual evapotranspiration; PET = potential evapotranspiration; P = precipitation. PET was calculated after Hamon (1963). Data sources: Luquillo Critical Zone Observatory website for LUQ; Weather Underground for SUS; USGS stations 50065500 and 50114000, respectively.

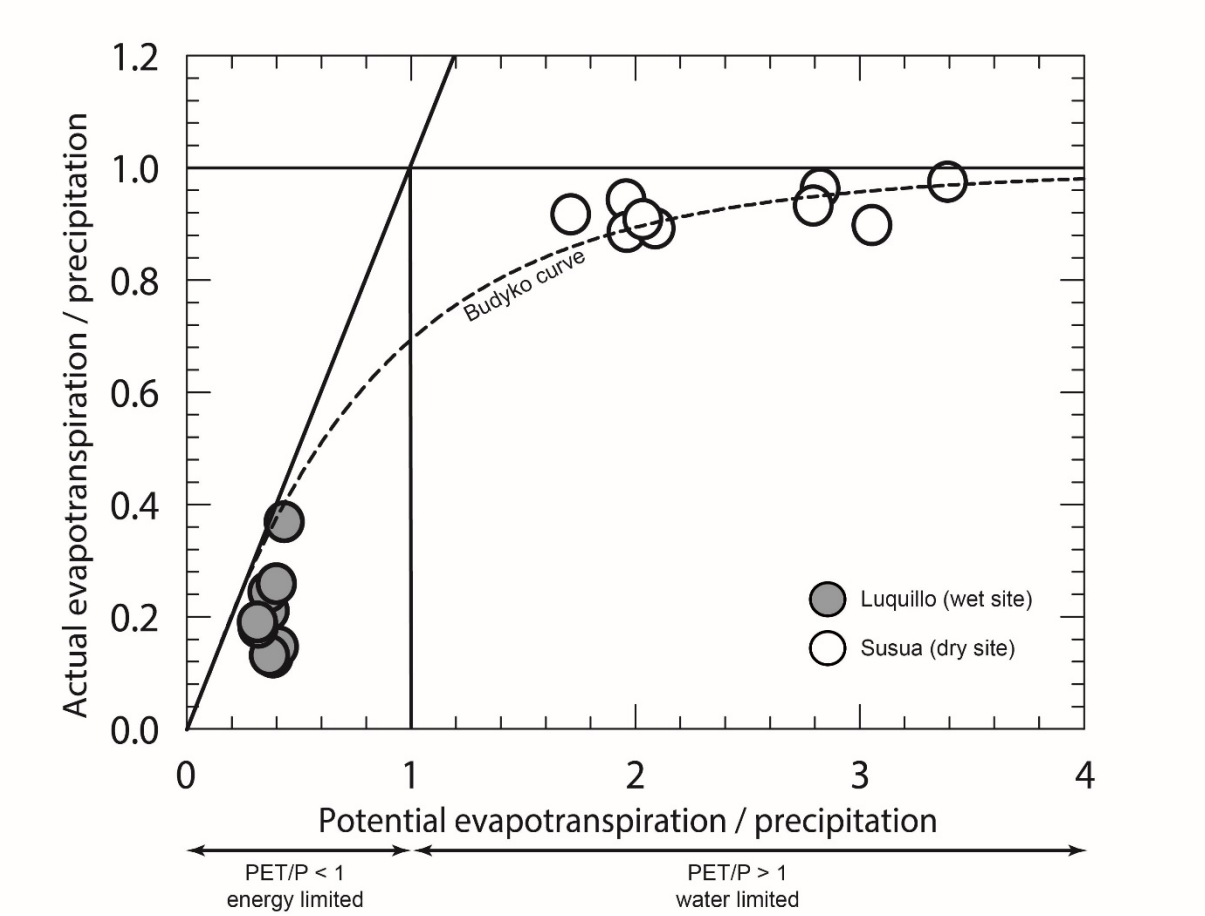

Figure 2.3. Dual isotope plot. (A) and **(B)** Stable isotopes of water from xylem (N=18), bulk soil (N=54 "wet period", 9–13 July 2012; N=94 "dry period", 11–15 February 2013), stream (N=166), and groundwater wells (N=37 wet period; N=12 dry period) at LUQ. **(C)** and **(D)** Stable isotopes of water from xylem (N=12 wet period; N=11 dry period), bulk soil (N=33 wet period; N=65 dry period), and groundwater (N=31 wet period; N=16 dry period) at SUS. LUQ LMWL: $\delta D=8.59\delta^{18}O+13.14$; SUS LMWL: $\delta D=7.79\delta^{18}O+10.85$ (Govender *et al*., 2013). Insets show respective line-conditioned excess (lc-excess*) values (using Equation 2). All samples were taken during the rainless periods within the dates indicated. Values of groundwater and rainfall represent long-term averages of each site's respective "wet" and "dry" periods. The extents of the boxes show the 25th and 75th percentiles; whiskers show the extents of outliers.

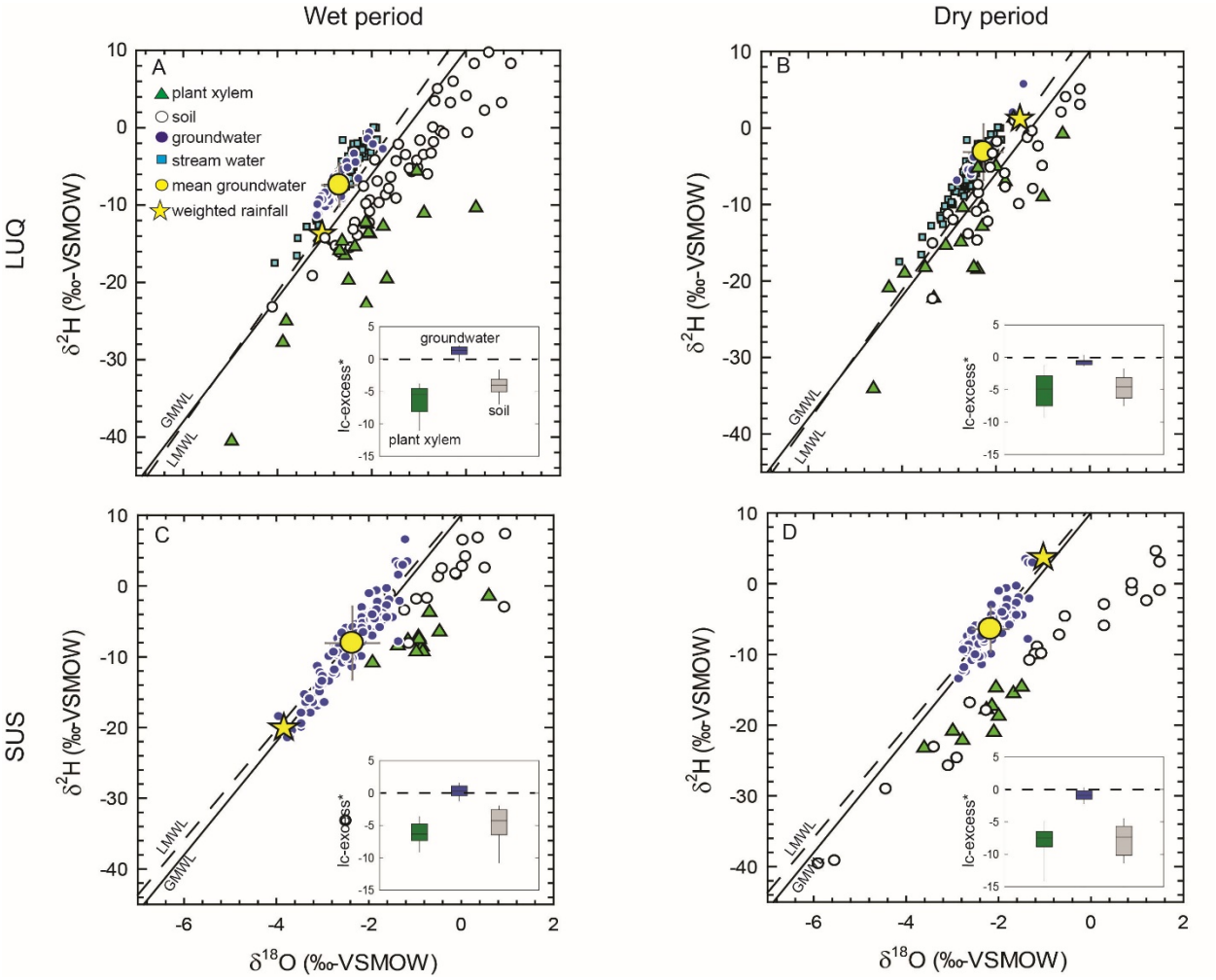

Figure 2.4. Soil water *d*-excess. Soil water and LMWL d-excess in LUQ **(A)** and SUS **(B)** during wet (dark gray circles) and dry (light gray circles) periods; error bars are 1SD; **statistically significant (α=0.05); N.S. Not Significant. LMWL d-excess was calculated using long-term annual VWA values δ^2H and $\delta^{18}O$. Inset in (A) shows the calculated evaporation rate e0 and characteristic length L_C in LUQ using van Genuchten model parameters (after Or et al., 2013). Depth sample sizes are: 10-cm N=18, 20-cm N=18, 30-cm N=18 during wet period in LUQ; 10-cm N=18, 20-cm N=18, 30-cm N=17, 40-cm N=15, 50-cm N=15, 60-cm N=9 during dry period in LUQ; 10-cm N=9, 20-cm N=12, 30-cm N=12 during wet period in SUS; 10-cm N=12, 20-cm N=12, 30-cm N=12, 40-cm N=12, 50-cm N=12, 60-cm N=5 during dry period in SUS.

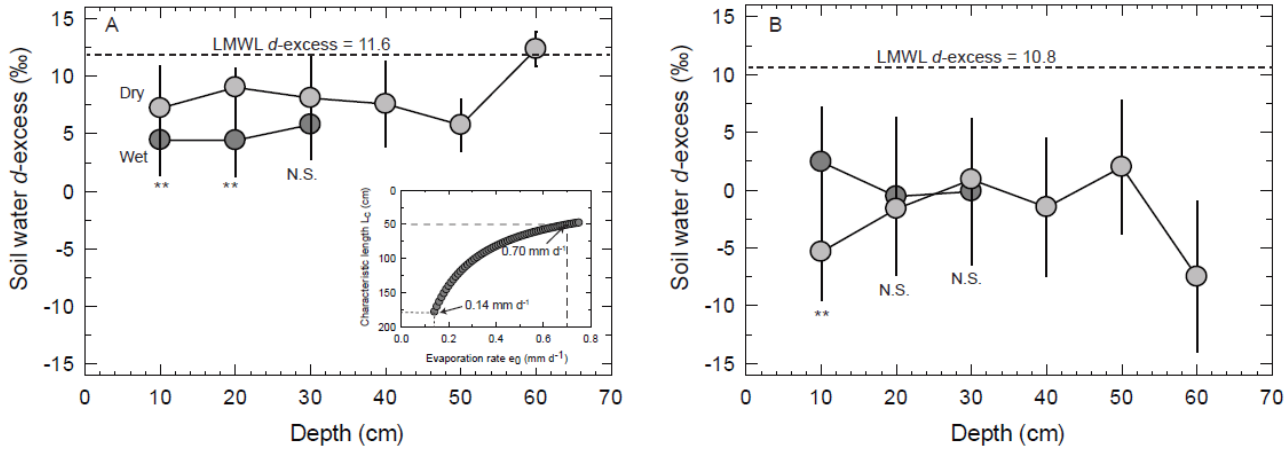

Figure 2.5. Source water partitioning using Bayesian mixing model (results shown for LUQ). Top-left illustration shows distance from ridgetop to stream divide and slope steepness (in percent slope). Also shown are the respective probability density plots of each putative source water superimposed on plots of relative contribution to xylem water.

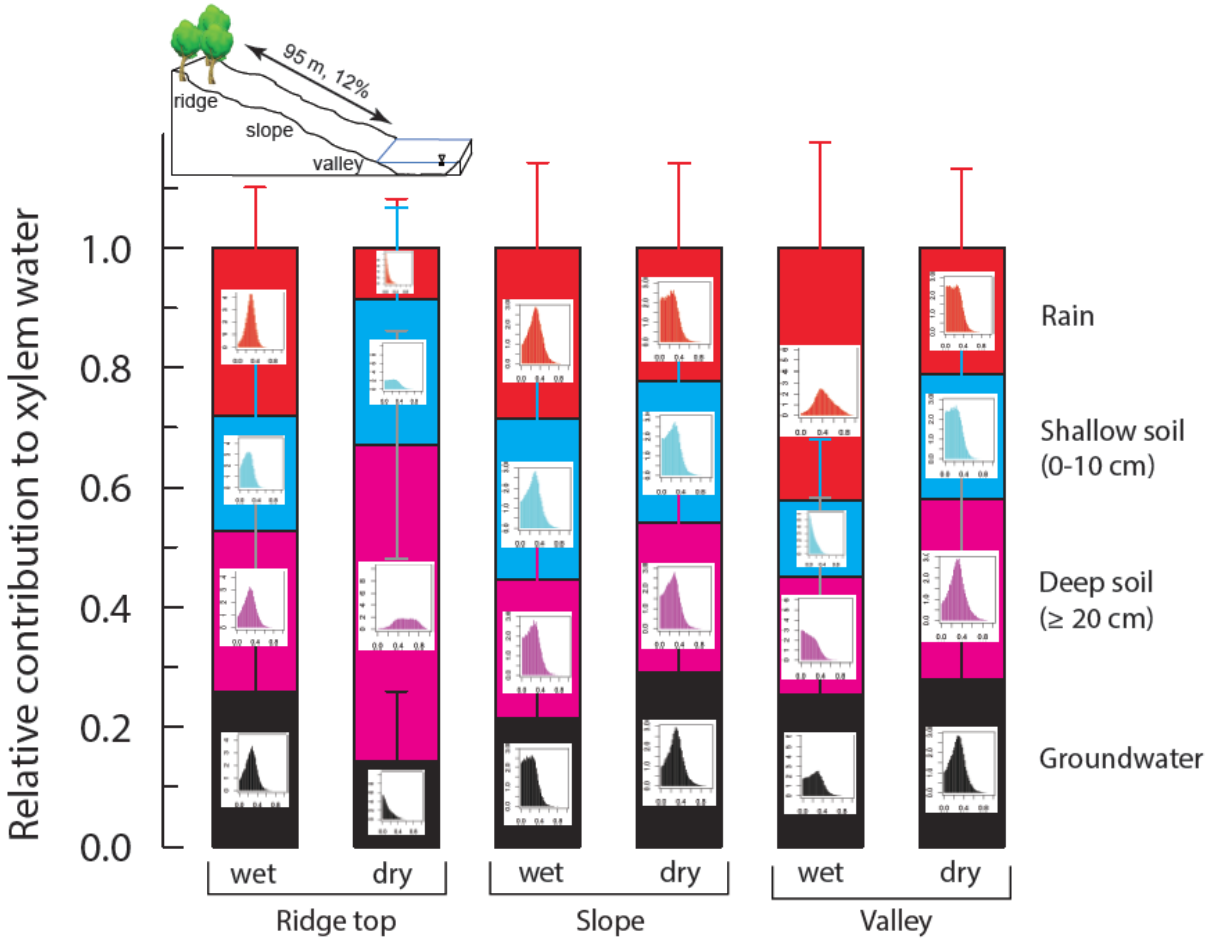

Figure 2.6. Source water partitioning using Bayesian mixing model (results shown for SUS). Top-left illustration shows distance from ridgetop to stream divide and slope steepness (in percent slope). Also shown are the respective probability density plots of each putative source water superimposed on plots of relative contribution to xylem water.

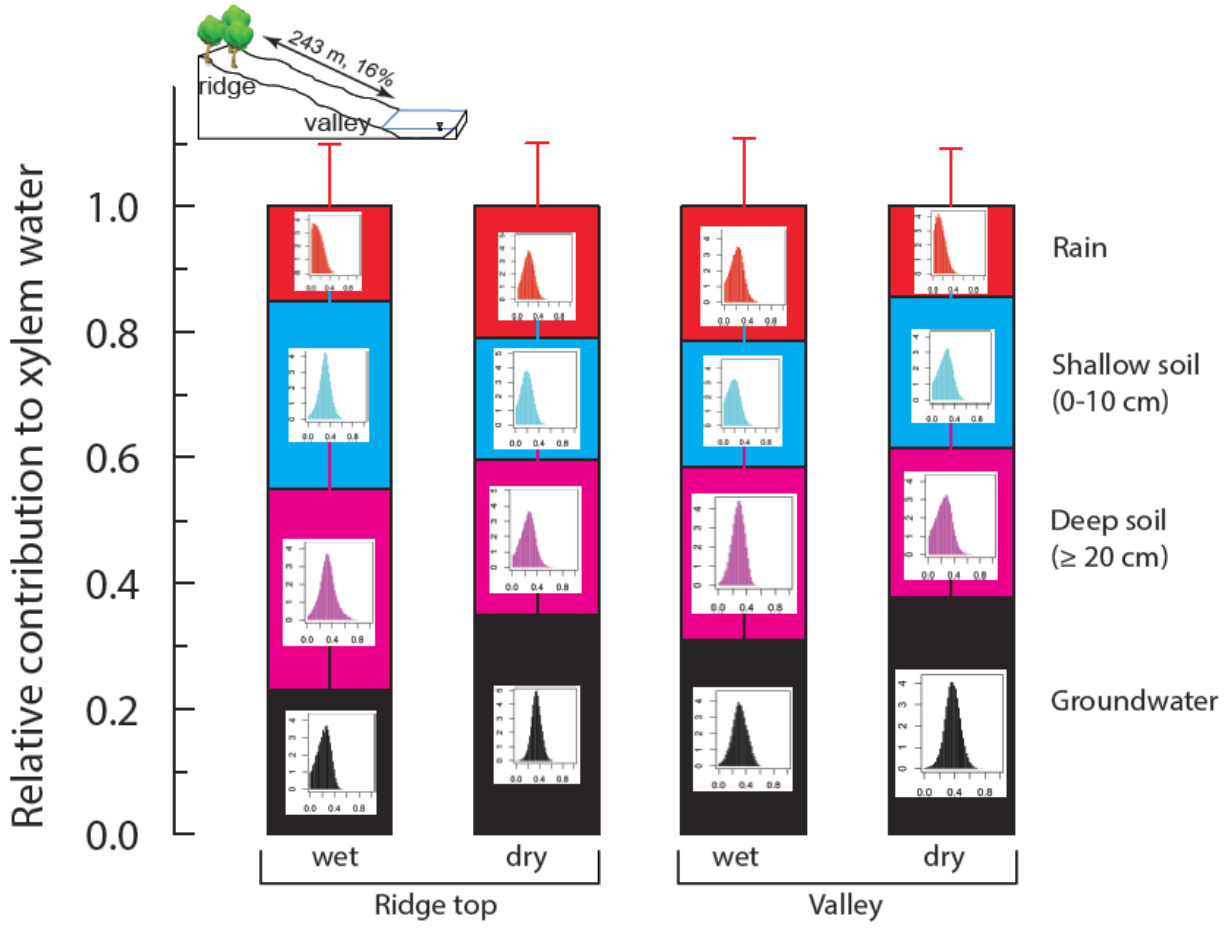

CHAPTER 3

GLOBAL SEPARATION OF PLANT TRANSPIRATION FROM GROUNDWATER AND STREAMFLOW

Status: Published

Citation: Evaristo, J., S. Jasechko, and J. J. McDonnell (2015), Global separation of plant transpiration from groundwater and streamflow, *Nature, 525*, 91-94.

3.1 Abstract

Current land surface models assume that plant transpiration, groundwater and streamflow are all sourced and mediated by the same well mixed reservoir—the soil. Recent work in Oregon[1] and Mexico[2] has shown evidence of ecohydrological separation, whereby different subsurface compartmentalized pools of water supply either plant transpiration fluxes or the combined fluxes of groundwater and streamflow. However, these findings have not yet been widely tested. Here we use hydrogen and oxygen isotopic data from 47 globally-distributed sites to show that ecohydrological separation is widespread across different biomes. Precipitation, stream water and groundwater from each site plot approximately along the $\delta^2H/\delta^{18}O$ slope of local precipitation inputs. Soil and plant xylem waters extracted from the 47 studies all plot below the local stream water and groundwater on the meteoric water line, suggesting that plants use soil water that does not itself contribute to groundwater recharge or streamflow. Our results further show that at 80% of the sites, the precipitation that supplies groundwater recharge and stream flow is different from the water that supply parts of soil water recharge and plant transpiration. The ubiquity of subsurface water compartmentalization found here and the segregation of storm types relative to hydrological and ecological fluxes may be used to improve numerical simulations of runoff generation, streamwater transit time and evaporation-transpiration partitioning. Future land surface model parameterizations should be closely examined for how vegetation, groundwater recharge and streamflow are assumed to be coupled.

3.2 Main Text

Fresh water fluxes via plant transpiration (45,000[3] to 62,000 km^3/year[4]), streamflow (37,000 to 40,000 km^3/year[5]) and groundwater recharge (12,000 to 16,200 km^3 per year[6]) are central components of the terrestrial hydrosphere. Understanding the sources of water and processes that govern each component is of fundamental importance for predicting the effects of global change on water security and ecosystem services[7]. One of the most useful tools for quantifying water cycle components and the linkages between plant ecology and physical hydrology is stable isotope tracing[8]. Global isotopic databases developed over the past 60 years[9] have enabled continental-scale assessments of transpiration/evaporation ratios[4] and recycling of rainfall back into the atmosphere[10].

While global datasets of precipitation[9], streamflow[9] and groundwater[11] are now available for analysis, measurements of plant xylem waters (i.e., water moving within plants) remain dispersed throughout the primary, specialist literature. Synthesizing global groundwater, streamflow and plant xylem water isotopic data is important because recent watershed-based case studies have shown evidence of ecohydrological separation[1,2] —meaning that the water that supplies plant transpiration is isolated from the water that recharges groundwater and replenishes streamflow. These two recent field studies both showed that plant transpiration is supplied by waters within unsaturated soils but that local streamflow and groundwater were supplied by mobile water (linked to infiltrating precipitation) that moves through the soil seemingly unmixed with the waters that are retained in the soil.

Compartmentalization of a poorly mobile plant transpiration water pool versus a highly mobile stream/groundwater pool, if widespread, would challenge existing land surface model parameterizations that assume that plants and streams draw from a singular, well-mixed subsurface water reservoir[12]. Such widespread ecohydrologic separation if true, would also have important implications for isotope-based assessments of evaporation/transpiration ratios reliant on well-mixed systems[4]. Here we apply a new global ecohydrological isotope database to test the

ecohydrological compartmentalization hypothesis: that the isotopic composition of waters that supply plant transpiration differs from waters that supply groundwater and streamflow. The global ecohydrological isotope database consists of $^{18}O/^{16}O$ and $^{2}H/^{1}H$ ratios of plant xylem water (n = 1460), soil water (n = 1830), stream water (n = 336), groundwater (n = 2749) and precipitation (n = 488) at 47 globally-distributed locations (Table 3.1, Figure 3.1).

Our approach is predicated on the knowledge that precipitation $\delta^{2}H$ and $\delta^{18}O$ values co-vary along a regression with a $\delta^{2}H/\delta^{18}O$ slope of eight (i.e. the global meteoric water line, GMWL)[13]. The physical process of evaporation occurs under disequilibrium and produces a strong kinetic isotope effect that yields $\delta^{2}H/\delta^{18}O$ slopes of less than eight[14] and results in a situation where water samples that have undergone some evaporation plot "below" the regression of precipitation isotopic data. We use this well-known difference between the meteoric water line and the local evaporation line as a key marker for ecohydrological compartmentalization (refs 1, 2).

Figures 2.1a-d show isotopic data for groundwater, stream water, plant xylem water and soil water, respectively, from our compiled database. Globally, headwater streams and groundwater plot approximately along the GMWL. These patterns suggest that stream water and groundwater follow the local precipitation input signal[15]. Plant xylem and soil waters extracted from the 47 studies plot below the regression of global meteoric waters, a result of the strong kinetic isotope effect via the process of evaporation[14].

To quantify the similarities or differences between waters used by plants and waters contributing to groundwater and streamflow, we use a site-by-site comparison based on a precipitation offset[16]:

$$\text{Precipitation offset} = [\delta^{2}H - a \cdot \delta^{18}O - b] / S \qquad (3.1)$$

where a and b are slope and y-intercept, respectively, calculated from monthly measurements of $\delta^{18}O$ and $\delta^{2}H$ of local precipitation at each study site, and S is one standard deviation

measurement uncertainty for both $\delta^{18}O$ and $\delta^{2}H$. The precipitation offset describes the difference in the isotopic composition of environmental waters from that of local precipitation, which has by definition, a precipitation offset of zero. The precipitation offset is able to distinguish hydrological processes that occur under chemical equilibrium (e.g. the condensation of vapour[13]) from hydrological processes that occur under disequilibrium (e.g. evaporation[17]). Plant transpiration does not impact the precipitation offset, whereas the evaporation of meteoric water near the land surface results in precipitation offset values of less than zero. By comparing the local precipitation offsets of our four water types (i.e. soil water, plant xylem water, stream water and groundwater) we can use the stable isotopes to distinguish evaporated waters from non-evaporated waters and to test whether streamflow, groundwater and plant transpiration are supplied by one well-mixed subsurface water reservoir, or more than one water reservoir (water that is retained in the soil vs water that recharges groundwater and discharges in streams).

Figure 3.2 shows that plant xylem water offsets (median, interquartile range, $p<0.0001$ using nonparametric Steel-Dwass Method) (−5.6, 4.7) and soil water offsets (−6.2, 4.4) are significantly different from the offset of groundwater (−1.8, 3.2) and stream water (0.22, 3.7) in all five biomes represented by the 47 sites in our database. Of our 47 sites, 40 sites have groundwater precipitation offsets that are statistically distinct ($p<0.05$ using two-tailed homoscedastic/heteroscedastic tests, as applicable) from both soil water and plant xylem water precipitation offsets. Our analysis is suggestive of widespread occurrence of ecohydrological separation, i.e. poor and incomplete mixing of subsurface water, with one reservoir of water sustaining plant transpiration, and another reservoir contributing to groundwater recharge and streamflow. On a site by site basis, groundwater and streamwater have a precipitation offset that is on average 5.4 and 4.8 higher (i.e. closer to zero) than soil and plant xylem waters. The greatest differences between the precipitation offsets of streamwater/groundwater and plant-xylem/soil water are found in the tropical and Mediterranean biomes (7.7 and 5.4, respectively), with smaller differences observed in the arid, temperate grassland, and temperate forest biomes (3.6, 2.4, and 1.6 on average, respectively).

Recent work has shown that different storm types contribute disproportionately to groundwater recharge (e.g. refs 11, 18). Some studies have shown that more intense storms dominate groundwater recharge[18], others present evidence to the contrary[19]. While our analyses do not allow us to associate storm intensity with either plant transpiration or groundwater recharge fluxes, we can nevertheless trace the isotopic composition of the precipitation from which plant xylem water originated. We calculated the intersection points of local plant xylem evaporation lines (EL) with local meteoric water lines (LMWL), i.e. plant xylem δ source value (see Figure 3.3 and Methods):

$$\delta^2\text{H intercept} = \delta^2\text{H} - m \cdot \delta^{18}\text{O} \quad (3.2)$$

$$\delta^{18}\text{O intercept} = [\delta^2\text{H intercept} - b] / a \quad (3.3)$$

where *m*, *a*, and *b* are slope of evaporation line, LMWL-intercept, and LMWL-slope, respectively.

Results of this analysis show that at 80% of the sites (see Table 3.2, 37 of 46) where plant xylem water δ source values may be calculated, groundwater isotope values (median, interquartile range, $p<0.05$ using nonparametric Wilcoxon Method) (-52, 63 ‰ δ^2H,) are statistically different from plant xylem water δ source values (-82, 83 ‰ δ^2H). This suggests that in many cases, ecologically and hydrologically important precipitation is segregated in both space and time even before the fate of these waters become further segregated in the subsurface for plant transpiration or for groundwater recharge and streamflow (see Methods and Figures 2.4 and 2.6).

We also use Equations (3.2) and (3.3) to trace the isotopic composition of precipitation from which soil water originated, i.e. soil water δ source value. We find that at 83% of the sites (Table 3.2, 29 of 35) where soil water isotopic data are available, soil water δ source values (-104, 96 ‰ δ^2H) are statistically different from groundwater isotope values. The significant difference between soil water δ source and groundwater isotope values suggests that some forms of precipitation recharging the subsurface may be more important than others to plant transpiration fluxes. We assess the uncertainties in parameter *m* (Equation 3.2) and find overall average

uncertainties of 1.07 ‰ for $\delta^{18}O$ and 5.54 ‰ for $\delta^{2}H$ (2σ). These are slightly less than but somewhat comparable to the prediction uncertainties in precipitation isotope values (1.17 ‰ for $\delta^{18}O$ and 9.4 ‰ for $\delta^{2}H$; ref. 20).

Plants regulate water fluxes from the subsurface to the atmosphere[4]. Our discovery that ecohydrological separation is widespread throughout the terrestrial water cycle has major implications for isotope-based estimates of runoff sources[12], streamwater residence times[21] and evaporation/transpiration partitioning[4]. Recent estimates[4] of catchment-scale transpiration/evapotranspiration ratios (T/ET) have followed an assumption of well-mixed water stores within the critical zone consistent with most land surface parameterizations[12]; our findings here of widespread ecohydrological separation fundamentally challenge the well-mixed reservoir assumption of catchment-based evapotranspiration partitioning[4,22,23] and most land surface models[12]. Our work would suggest that downstream water isotope compositions are biased to precipitation and groundwater source contributions and do not reflect the composition of water seen in soil. This in turn casts doubt on the estimates of transpiration/evapotranspiration made in other studies if based-solely on isotope data, meaning that evapotranspiration partitioning based on downstream water isotope compositions may not represent an integrated catchment-wide isotopic signature as widely applied . Notwithstanding these issues, the general finding that transpiration comprises the greatest fraction of terrestrial evapotranspiration is reinforced by multiple lines of evidence shown in ref. [4] in addition to land surface models [terrestrial T/ET of 59% to 80%[23,24]], atmospheric vapor isotope measurements [European T/ET of 62%[26]], global syntheses of stand-level transpiration measurements [terrestrial T/ET of ~61%[5]] and some but not all general circulation models (see refs [27, 28]). While transpiration is, indeed, the largest component of terrestrial evapotranspiration[4], the results in this current work show that the mechanisms by which such partitioning takes place, and links to other components of the water cycle[29], are still very poorly understood. These combined findings point the way to critical new research that is needed to understand the ecophysiological basis of ecohydrological separation across biomes. Lastly, our results also suggest that existing land surface model parameterizations of plant physiological processes and runoff[30] (i.e. stream flow) can be more realistic through incorporation of ecohydrological separation.

3.3 Methods

3.3.1 Data compilation and treatment

We performed a keyword-based search in published literature for stable water isotopes in ecology and hydrology. Since ecohydrological separation[31] is based on the offset of a water sample from the local meteoric water line [i.e. *precipitation offset*[16], Equation (2.1) in Main Text], we included only dual isotope findings and excluded papers that utilized either δ^2H or δ^{18}O isotopes only. Stable isotope values from the 47 papers were then extracted in one of two ways: [1] where data were reported in tabular form, we compiled the data directly into the database; [2] where plant xylem and soil water isotope data were not reported in tabular form, we used a graphical user interface to extract data points from figures in the original paper. We then calculated the *precipitation offset* values based on Equation (2.1) in the Main Text. The measurement uncertainty *S* in Equation (2.1) was calculated as:

$$S = [(\delta^2\text{H analytical error})^2 + (\delta^{18}\text{O analytical error})^2]^{0.5} \qquad (3.4)$$

Reported analytical errors for δ^2H and δ^{18}O are 1‰ and 0.2‰ on average, respectively.

We extracted groundwater isotope data for 45 of 47 sites either from the compiled papers (n = 24) or from a comprehensive global groundwater database (n = 21) of S. Jasechko. Of the 21 groundwater datasets compiled using the latter database, 16, 2, 1, and 2 datasets are within 200-, 300-, 400-, and 500-km radius of actual study sites. The motivation for the choice of radii within which groundwater data were extracted was so that we could build groundwater datasets for most of the 47 sites in our database. To test whether or not the choice of radii imposed a scale-dependent variation (i.e. bias) in isotopic trends, we performed a sensitivity analysis by calculating the precipitation offset values of groundwater at distances 25, 50 and 100 km. We found that precipitation offset values of groundwater did not differ statistically in space. That is, precipitation offset of groundwater at 25-km radius (-3.5 ±2.2, n = 688) of study sites was not statistically different from precipitation offset at 50 km (-2.5 ±2.4, n = 1605), 100 km (-2.4 ±2.4, n = 3295), 200 km (-2.7 ±2.2, n = 6598), 300 km (-2.5 ±4.5, n = 12000), 400 km (-2.8 ±4.6, n = 18239), and 500 km (-2.8 ±4.8, n = 24000). This scale-invariant behavior of groundwater precipitation offset supported our choice of radii in building the datasets for 45 of 47 sites in our

database. It also reinforced one of the key messages in this work in that groundwater isotopes generally fall along the local meteoric water line.

To show that plant transpiration water and groundwater recharge are related to different storm types, we traced the precipitation δ source value of plant xylem water by calculating the intersection points of local evaporation lines (LEL) with local meteoric water lines (LMWL) [Equations (3.2) and (3.3); see Figure 3.3]. On a site-by-site basis, we compared the calculated precipitation δ source value of plant xylem water and soil water with the mean groundwater δ value (see Table 3.2).

Comparing plant xylem water δ source values with mean groundwater δ values requires intuitively that both should be situated as close to each other as possible at a site. The distance of groundwater wells to actual study sites in our database, however, varies from 0 to almost 500 km. To test whether our approach of comparing both isotope composition values was statistically robust, we ran a sensitivity analysis by comparing plant xylem water δ source values with only the closest groundwater well to a given site. Increasing the radii between actual study sites and site of groundwater measurements were then used as a critical evaluation metric for the approach (see Figure 3.5). Our results showed that for five increasing radii ranges between actual xylem water study site and groundwater well site, the differences [median (interquartile ranges), absolute δ^2H ‰] between plant xylem water δ and groundwater δ values [24 (29), n = 7; 30 (30), n = 8; 31 (42), n = 7; 21 (22), n = 9; 23 (40), n = 11) are not statistically different from each other ($p>0.90$, Tukey-Kramer HSD). This suggests that our approach in comparing plant xylem water δ source values (i.e. xylem EL intercept with LMWL) and mean groundwater value at a site is valid. We underline that this does not imply that groundwater isotope values are invariant in space, but rather that the mean difference between plant xylem water δ source values and mean groundwater values is invariant in space (statistically not different) as shown in Figure 3.5.

We make a distinction between the two phenomena: “segregation” of storm types and “ecohydrological separation”. The former is related to source precipitation analysis [Equations (2.2) and (2.3)]; the latter to the fate of these waters either as groundwater or for plant transpiration [Equation (2.1)]. Segregation of storm types and ecohydrological separation *in space* is ubiquitous in the global dataset. We are unable to test for both phenomena *in time* due to limitations in the available information in the compiled source papers. That is, if a source paper

has data for at least two time points (usually contrasting moisture time points) then we can use such information to explore temporal contrasts (38 of 47 sites). For the 38 sites that satisfy this criterion, both storm type segregation and ecohydrological separation exist in 30 and 32 of 38 sites, respectively ($p<0.05$ using nonparametric Wilcoxon Method).

We recognize that non-weighted plant xylem water isotope values would be biased toward values where transpiration rates are low. To test the robustness of the precipitation offset parameter, we also calculate the transpiration-amount-weighted isotopic composition of plant xylem water ($\delta_{xyl(weighted)}$) using compiled long-term, global, biome-level transpiration rate estimates[3]:

$$\delta_{xyl(weighted)} = \frac{\sum_{i=1}^{n} \delta_{xyl(i)} T_i}{\sum_{i=1}^{n} T_i} \quad (3.5)$$

where, $\delta_{xyl(i)}$ represents the isotopic composition of xylem water during sampling month *i* and T_i represents the amount of transpiration during month *i*. As illustrated in Figure 3.2, both transpiration-amount-weighted and non-weighted plant xylem precipitation offsets are statistically different from zero, and supports our primary conclusion that plant transpiration water chemistries are different from groundwater and streamflow at 40 of 47 locations. We employ no amount weighting on groundwater isotope values, supported by observations that showed little change in groundwater isotopic composition on timescales of years and decades[32,33].

To trace the fate of water after precipitation (i.e. either as groundwater recharge or plant water uptake), we quantified the precipitation offset from the LMWL [Equation (2.1)]. We confirmed ecohydrological separation at a study site if plant xylem water and soil water isotopic composition fall below the regression of δ^2H and $\delta^{18}O$ values in local precipitation on the. LMWL.

Conventional notation for isotope composition is used where $\delta = (R_{sample}/R_{standard} - 1) \times 1000$ ‰, where R is the ratio of $^{18}O/^{16}O$ ($\delta^{18}O$) or $^{2}H/^{1}H$ ($\delta^{2}H$) in the sample, or in the international standard: (Vienna-Standard Mean Ocean Water, V-SMOW).

3.3.2 Statistical analysis

Parametric requirements of normality and equal variances, particularly for aggregate precipitation offset values, are not satisfied via attempts to transform the data. Testing whether group means are located similarly across groups is performed using nonparametric tests, which use functions of the response ranks (or rank scores). A Kruskal-Wallis/Steel-Dwass Method is performed to test whether or not the precipitation offset values of the water types – groundwater, stream water, plant xylem water, and soil water -- differ statistically with each other. We perform a similar nonparametric test (Dunn All Pairs for Joint Ranks Method) by computing ranks on all the data. The results are the same as the pairwise method Kruskal-Wallis/Steel-Dwass test. To test whether each water type is statistically different from zero (i.e. the precipitation offset value of local precipitation), the Dunn Method for Joint Ranking is performed. The test shows that plant xylem water and soil water are statistically different from zero, while groundwater and stream water are not statistically different from zero. This test result supports the interpretation that groundwater and stream water fall along the $\delta^2H/\delta^{18}O$ slopes of local meteoric water lines, while plant xylem water and soil water fall "below" the slopes of this linear regression. The same method is also used to test for statistical significance of precipitation offset values of each water type across biomes. These nonparametric tests are based on ranks and control for the overall alpha level ($\alpha = 0.05$). The Dunn Method, which reports p-values after a Bonferroni adjustment, is used to correct for multiple testing problem that may arise from an inflated Type I error rate. Where parametric requirements are met, particularly for intra-site tests on water types, Student's t/Tukey-Kramer HSD tests are performed as applicable. Uncertainty estimation, particularly for Equations (2.2) and (2.3) parameters, is performed via Jackknifing approach[34].

3.3.3 A mechanism for Ecohydrological Separation

Partial mixing of "new" (incoming) and "old" (resident) water in the subsurface is rarely considered in conceptual models[35,36]. Our key finding that groundwater/stream water and soil/plant uptake water are fundamentally (physically and temporally) separated supports the dynamic partial mixing model of ref (37). In fact, it was the contrasting conclusions drawn by ref (1) compared to those of refs (38) and (39) regarding the mixing mechanisms that led ref (37) to

propose the use of the following dimensionless mixing coefficient$C_{M,i}$, controlled mainly by soil moisture content:

$$C_{M,i} = \frac{1}{2} - \frac{1}{2} erf\left(\frac{\frac{S_U}{S_{U_{max}}} - \mu C_{M,i}}{\sigma C_{M,i}\sqrt{2}}\right) \quad (3.6)$$

where S_U, $S_{U_{max}}$ are actual storage and storage capacity within the root zone, respectively; and, $\mu C_{M,i}$, and $\sigma C_{M,i}$ are location and shape parameters, respectively. Equation (2.6) above is applied to tracer (e.g. stable water isotopes) balance equations, which may then enable functional comparisons amongst other alternative diagnostic models (e.g. the more widely used complete mixing model).

Our *precipitation offset* parameter analysis [Equation (2.1) in Main Text] is used to modify Equation (2.6) by substituting the precipitation offset value of soil water for the term $\frac{S_U}{S_{U_{max}}}$:

$$C_{M,i} = \frac{1}{2} - \frac{1}{2} erf\left(\frac{|P_x| - \mu C_{M,i}}{\sigma C_{M,i}\sqrt{2}}\right) \quad (3.7)$$

where $|P_x|$ is the absolute value of precipitation offset parameter. This results in a dimensionless mixing coefficient $C_{M,i}$ value that decreases as precipitation offset $|P_x|$ value increases. When $C_{M,i}$ is applied in tracer mass balance equations [as outlined in ref (37)], mixing between "new" and "old" water increases as soil moisture decreases; or, conversely, separation between "new", "fast flowing" waters and "old", "matrix" waters increases with higher antecedent soil moisture. The persistence of "old" water within the soil matrix and reduced participation in dispersive and diffusive exchange with preferential flow path water lead to continued exposure to evaporation [via Stage 1 (capillary action) and Stage 2 (vapor diffusion) evaporation) For details regarding evaporation from porous media, please see review by ref (40).

Our conceptual formulation as outlined in Equation (2.7) is supported by the results of our precipitation offset analysis. Our analysis provides a site-by-site (see Table 3.3 below) and

biome-level (see Table 3.4) quantification of the magnitude of separation – and by extension, mixing – between groundwater recharge and stream discharge, and the water that recharges the soil matrix and is being taken up by plants for transpiration. Table 3.4 shows that in soils of the arid biome, the precipitation offset value is highest (i.e. closer to zero); conversely, in soils of the humid tropics where antecedent soil wetness is high, the precipitation offset value is lower. Calculating the dimensionless mixing coefficient $C_{M,i}$ using the precipitation offset values in Table 3.4 and plugging these values into Equation (2.7) support the observation that in the dry soils of the arid biome, mixing between "new", "fast flowing" waters and "old", "matrix" waters increases. The opposite is true for the other extreme in humid tropical soils where antecedent soil wetness is high. In general, since plants in our compiled database use soil water, these precipitation offset trends in soils are therefore consistent with plant xylem water data. That is, the magnitude of ecohydrological separation – plants using evaporated soil water that is isotopically distinct from groundwater recharge and stream discharge – increases with antecedent soil wetness. The relationship between soil wetness and dimensionless mixing coefficient $C_{M,i}$ is discussed in detail and tested with actual, long-term catchment-level data in ref (37). We, however, state a caveat that the use of the precipitation offset parameter in Equation (2.7) may be considered as a coarse (first-order) approximation given the nonlinear relationship between evaporative loss and the precipitation offset parameter.

While ref (1) was the first to develop the ecohydrological separation concept and was relatively successful at proposing a mechanistic explanation for the observed results, other works have shown that such mechanism may not universally explain the observed ecohydrological separation. For example, ref (2) also found ecohydrological separation in a seasonally dry cloud forest in Mexico, they argued that the mechanism proposed by ref (1) was not likely to explain the observed isotopic separation in their study. Plant xylem water values in ref (1) are more enriched than most of the soil water values, which was the opposite to that observed and reported by ref (2). If the "first-in-last-out" mechanism proposed by ref (1) was correct, then the measured plant xylem values should have matched those of (or at least be bounded by) their measured soil water values. Their data suggests that this was not the case. In contrast, ref (2) observed their plant xylem water to lie completely in between precipitation and bulk soil water values. The aggregate result from our global dataset lends support more to the interpretation of ref (2) than to ref (1).

3.3.4 Water extraction techniques

As underlined in the central message of this work, plant xylem water and soil water isotopes plot "off" the local meteoric water lines (LMWL), supporting the widespread occurrence of ecohydrological separation on a global scale. This finding is true across the different techniques used to extract water out of soil and plant stem samples in our dataset. Ref (1) argued that plant transpiration is supplied by "tightly bound" waters within unsaturated soils. This interpretation was inferred from the laboratory technique employed to extract water out of a soil sample (i.e. cryogenic vacuum distillation) that uses suction pressures orders of magnitude greater than those used in other field techniques (e.g. suction lysimetry). Potential nuances in the fidelity of water extraction from soil samples using existing laboratory techniques have recently been explored[41,42,43]. These findings suggest that soil physico-chemical characteristics may play a role in isotopic fractionation, specifically with respect to $\delta^{18}O$. We explored the relationship between water extraction techniques and plant xylem water/soil water $\delta^{18}O$ in our dataset. Figure 3.7 shows the plant xylem water/soil water $\delta^{18}O$ values using liquid-vapor equilibration technique from cryogenic vacuum distillation and azeotropic distillation. While there is statistically significant differences ($p<0.0001$, nonparametric Dunn Method for Joint Ranking) between both cryogenic vacuum ($n = 2640$) and azeotropic distillation ($n = 441$), and liquid-vapor equilibration methods ($n = 204$), there is no significant difference in plant xylem water $\delta^{18}O$ between the two more widely used techniques, cryogenic vacuum and azeotropic distillation ($p = 0.35$, nonparametric Dunn Method for Joint Ranking). Despite these differences in $\delta^{18}O$ of plant xylem water and soil water with respect to water extraction techniques, both water types plot "off" the LMWL in dual isotope space. This suggests that ecohydrological separation exists beyond any differences in soil water $\delta^{18}O$ related to different water extraction techniques.

3.3.5 Global map of plant xylem water $\delta^{2}H$ and $\delta^{18}O$

For the first time in the literature, we also provide not only a global map of plant xylem $\delta^{2}H$ and $\delta^{18}O$, but also their relationship to respective local meteoric water lines as integrated in the *precipitation offset* parameter – a fundamental descriptor of ecohydrological separation (see

Figure 3.8). Our compilation of global plant xylem δ^2H and $\delta^{18}O$ may complement other existing large-scale isotopic datasets in precipitation[44] and streams[45], in pursuing future research questions related to plant-water relations from continental to global scales.

3.4 Transition Statement

This chapter has established that ecohydrological separation is a widespread phenomenon, transcending large-scale differences in physiographic settings including species, seasonality and biome. Implicit in the global-in-scale demonstration of ecohydrological separation, however, is the outstanding question on the degree of groundwater use by vegetation. Notwithstanding the more than three decades of using water stable isotopes as a tool in ecohydrological investigations, a global synthesis of published literature specifically quantifying groundwater use by vegetation was wanting. This chapter, therefore, provided an impetus for the following chapter, which sought to quantify the magnitude of groundwater use by vegetation at the scale of the globe.

3.5 Acknowledgements

J.E. thanks the Saskatchewan Innovation and Opportunity Scholarship, Global Institute for Water Security, and School of Environment and Sustainability (University of Saskatchewan) for financial support.

3.6 Author Contributions

J.J.M. conceived the idea to test the ecohydrological compartmentalization hypothesis with global data. J.E., S.J., and J.J.M. brainstormed on how to do this. J.E. designed the approach, compiled the data set, and conducted the statistical analyses. J.E. wrote the first paper draft. S.J. and J.J.M. edited and commented on the manuscript and contributed to the text in later iterations.

3.7 Brief Communications Arising

An error in Equations 2.2 and 2.3 was corrected and published as a Brief Communications Arising Comment [Citation: Javaux, M., Rothfuss, Y., Vanderborght, J., Vereecken, H. & Brüggemann, N. Isotopic composition of plant water sources. *Nature* **536**, doi:10.1038/nature18946 (2016)]. An appropriate Reply was initiated and published [Citation: Evaristo, J., Jasechko, S., & McDonnell, J.J. *Reply to* Isotopic composition of plant water sources. *Nature* **536**, doi:10.1038/nature18947 (2016)]. The Comment authors found that rainfall segregation could be observed at only 74% of the sites, and not 80% as we originally reported.

3.8 References

1. Brooks, J. R., Barnard, H. R., Coulombe, R. & McDonnell, J. J. Ecohydrologic separation of water between trees and streams in a Mediterranean climate. *Nature Geoscience* **3**, 100-104 (2010).
2. Goldsmith, G. R. *et al*. Stable isotopes reveal linkages among ecohydrological processes in a seasonally dry tropical montane cloud forest. *Ecohydrology* **5**, 779-790 (2012).
3. Schlesinger, W. H. & Jasechko, S. Transpiration in the global water cycle. *Agric. For. Meteorol.* **189**, 115-117 (2014).
4. Jasechko, S. *et al*. Terrestrial water fluxes dominated by transpiration. *Nature* **496**, 347-350 (2013).
5. Dai, A. & Trenberth, K. E. Estimates of freshwater discharge from continents: Latitudinal and seasonal variations. *J. Hydrometeorol.* **3**, 660-687 (2002).
6. Oki, T. & Kanae, S. Global hydrological cycles and world water resources. *Science* **313**, 1068-1072 (2006).
7. Wada, Y., Van Beek, L. P. H., Wanders, N. & Bierkens, M. F. P. Human water consumption intensifies hydrological drought worldwide. *Environ. Res. Lett.* **8** (2013).
8. Yakir, D. & Wang, X. -. Fluxes of CO2 and water between terrestrial vegetation and the atmosphere estimated from isotope measurements. *Nature* **380**, 515-517 (1996).

9. IAEA/WMO, 2014. www.iaea.org/water/ International Atomic Energy Agency's Water Resources Programme

10. Levin, N. E., Zipser, E. J. & Cerling, T. E. Isotopic composition of waters from Ethiopia and Kenya: Insights into moisture sources for eastern Africa. *Journal of Geophysical Research D: Atmospheres* **114** (2009).

11. Jasechko, S. *et al*. The pronounced seasonality of global groundwater recharge. *Water Resour. Res.* **50**, 8845-8867 (2014).

12. Birkel, C., Tetzlaff, D., Dunn, S. M. & Soulsby, C. Towards a simple dynamic process conceptualization in rainfall-runoff models using multi-criteria calibration and tracers in temperate, upland catchments. *Hydrol. Process.* **24**, 260-275 (2010).

13. Friedman, I. Deuterium content of natural waters and other substances. *Geochim. Cosmochim. Acta* **4**, 89-103 (1953).

14. Craig, H. Isotopic variations in meteoric waters. *Science* **133**, 1702-1703 (1961).

15. Dutton, A. R. Groundwater Isotopic Evidence for Paleorecharge in U.S. High Plains Aquifers. *Quatern. Res.* **43**, 221-231 (1995).

16. Landwehr, J., and Coplen, T. Line-conditioned excess: A new method for characterizing stable hydrogen and oxygen isotope ratios in hydrologic systems: Isotopes in Environmental Studies. International Atomic Energy Agency, Monaco, p.132–135 (2006).

17. Dansgaard W. Stable isotopes in precipitation. Tellus **16**: 436–468 (1964).

18. Taylor, R. G. *et al*. Evidence of the dependence of groundwater resources on extreme rainfall in East Africa. *Nature Climate Change* **3**, 374-378 (2013).

19. Scholl, M. A. & Murphy, S. F. Precipitation isotopes link regional climate patterns to water supply in a tropical mountain forest, eastern Puerto Rico. *Water Resour. Res.* **50**, 4305-4322 (2014).

20. Good, S. P. *et al*. Patterns of local and nonlocal water resource use across the western US determined via stable isotope intercomparisons. *Water Resour. Res.* **50**, 8034-8049 (2014).

21. Syed, T. H., Famiglietti, J. S., Zlotnicki, V. & Rodell, M. Contemporary estimates of Pan-Arctic freshwater discharge from GRACE and reanalysis. *Geophys. Res. Lett.* **34** (2007).

22. Ferguson, P. R., Weinrauch, N., Wassenaar, L. I., Mayer, B., and Veizer, J. Isotope constraints on water, carbon, and heat fluxes from the northern Great Plains region of North America, *Global Biogeochem. Cycles* **21,** GB2023 (2007).

23. Gibson, J. J. & Edwards, T. W. D. Regional water balance trends and evaporation-transpiration partitioning from a stable isotope survey of lakes in northern Canada. *Global Biogeochem. Cycles* **16**, 1026 (2002).

24. Dirmeyer, P. A. *et al*. GSWP-2 - Multimodel anlysis and implications for our perception of the land surface. *Bull. Am. Meteorol. Soc.* **87**, 1381-+ (2006).

25. Wang-Erlandsson, L., van der Ent, R. J., Gordon, L. J. & Savenije, H. H. G. Contrasting roles of interception and transpiration in the hydrological cycle - Part 1: Temporal characteristics over land. *Earth System Dynamics* **5**, 441-469 (2014).

26. Aemisegger, F. *et al*. Deuterium excess as a proxy for continental moisture recycling and plant transpiration. *Atmospheric Chemistry and Physics* **14**, 4029-4054 (2014).

27. Sutanto, S. J. *et al*. HESS Opinions "A perspective on isotope versus non-isotope approaches to determine the contribution of transpiration to total evaporation". *Hydrology and Earth System Sciences* **18**, 2815-2827 (2014).

28. Lawrence, D. M., Thornton, P. E., Oleson, K. W. & Bonan, G. B. The partitioning of evapotranspiration into transpiration, soil evaporation, and canopy evaporation in a GCM: Impacts on land-atmosphere interaction. *J. Hydrometeorol.* **8**, 862-880 (2007).

29. Gouet-Kaplan, M., Tartakovsky, A. & Berkowitz, B. Simulation of the interplay between resident and infiltrating water in partially saturated porous media. *Water Resour. Res.* **45**, W05416 (2009).

30. Stöckli, R., Vidale, P. L., Boone, A. & Schär, C. Impact of scale and aggregation on the terrestrial water exchange: Integrating land surface models and rhône catchment observations. *J. Hydrometeorol.* **8**, 1002-1015 (2007).

31. McDonnell, J.J. The two water worlds hypothesis: Ecohydrological separation of water between streams and trees? *WIREs Water* (2014).

32. Darling, W. G., Bath, A. H. & Talbot, J. C. The O & H stable isotopic composition of fresh waters in the British Isles. 2. Surface waters and groundwater. *Hydrology and Earth System Sciences* **7**, 183-195 (2003).

33. Genty, D. *et al*. Rainfall and cave water isotopic relationships in two South-France sites. *Geochim. Cosmochim. Acta* **131**, 323-343 (2014).

34. Wu, C. Jackknife, Bootstrap and Other Resampling Methods in Regression-Analysis - Discussion. *Ann. Stat.* **14**, 1261-1295 (1986).

35. Van der Velde, Y., Torfs, P. J. J. F., van der Zee, S. E. A. T. M.,and Uijlenhoet, R.: Quantifying catchment-scale mixing and its effects on time-varying travel time distributions, *Water Resour. Res*., **48**, W06536 (2012).

36. Page, T., Beven, K. J., Freer, J., and Neal, C.: Modelling the chloride signal at Plynlimon, Wales, using a modified dynamic TOPMODEL incorporating conservative chemical mixing (with uncertainty), *Hydrol. Process.*, **21**, 292–307 (2007).

37. Hrachowitz, M., Savenije, H., Bogaard, T. A., Tetzlaff, D. & Soulsby, C. What can flux tracking teach us about water age distribution patterns and their temporal dynamics? *Hydrology and Earth System Sciences* **17**, 533-564 (2013).

38. Legout, C., Molenat, J., Aquilina, L., Gascuel-Odoux, C., Faucheux, M., Fauvel, Y., and Bariac, T.: Solute transfer in the unsaturated zone-groundwater continuum of a headwater catchment, *J. Hydrol*., **332**, 427–441 (2007).

39. Klaus, J., Zehe, E., Elsner, M., K¨ulls, C., and McDonnell, J. J.: Macropore flow of old water revisited: experimental insights from a tile-drained hillslope, *Hydrol. Earth Syst. Sci*., **17**, 103–118, (2013).

40. Or, D., Lehmann, P., Shahraeeni, E. & Shokri, N. Advances in soil evaporation physics-A review. *Vadose Zone Journal* **12** (2013).

41. Oerter, E. *et al*. Oxygen isotope fractionation effects in soil water via interaction with cations (Mg, Ca, K, Na) adsorbed to phyllosilicate clay minerals. *Journal of Hydrology* **515**, 1-9 (2014).

42. Meissner, M., Koehler, M., Schwendenmann, L., Hoelscher, D. & Dyckmans, J. Soil water uptake by trees using water stable isotopes (delta H-2 and delta O-18)-a method test regarding soil moisture, texture and carbonate. *Plant Soil* **376**, 327-335 (2014).

43. Orlowski, N., Frede, H., Brüggemann, N. & Breuer, L. Validation and application of a cryogenic vacuum extraction system for soil and plant water extraction for isotope analysis. *Journal of Sensors and Sensor Systems*, **2**: 179-193 (2013).

44. Bowen, G. J. & Wilkinson, B. Spatial distribution of delta O-18 in meteoric precipitation. *Geology* **30**, 315-318 (2002).

45. Kendall, C. & Coplen, T. B. Distribution of oxygen-18 and deuterium in river waters across the United States. *Hydrol. Process.* **15**, 1363-1393 (2001).

46. Boutton, T. W., Archer, S. R. & Midwood, A. J. Stable isotopes in ecosystem science: Structure, function and dynamics of a subtropical savanna. *Rapid Commun. Mass Spectrom.* **13**, 1263-1277 (1999).

47. McKeon, C. *et al*. Growth and water and nitrate uptake patterns of grazed and ungrazed desert shrubs growing over a nitrate contamination plume. *J. Arid Environ.* **64**, 1-21 (2006).

48. Snyder, K. A. & Williams, D. G. Water sources used by riparian trees varies among stream types on the San Pedro River, Arizona. *Agric. For. Meterol.* **105**, 227-240 (2000).

49. Williams, D. G. & Ehleringer, J. R. Intra- and interspecific variation for summer precipitation use in pinyon-juniper woodlands. *Ecol. Monogr.* **70**, 517-537 (2000).

50. Zhou Ya-Dan, Chen Shi-Ping, Song Wei-Min, Lu Qi & Lin Guang-Hui. Water-use strategies of two desert plants along a precipitation gradient in northwestern China. *Chinese Journal of Plant Ecology* **35**, 789-800 (2011).

51. Zhou Hai, Zheng Xin-Jun, Tang Li-Song & Li Yan. Differences and similarities between water sources of Tamarix ramosissima, Nitraria sibirica and Reaumuria soongorica in the southeastern Junggar Basin. *Chinese Journal of Plant Ecology* **37**, 665-673 (2013).

52. Zhu Lin, Xu Xing & Mao Gui-Lian. Water sources of shrubs grown in the northern Ningxia Plain of China characterized by shallow groundwater table. *Chinese Journal of Plant Ecology* **36**, 618-628 (2012).

53. Bijoor, N. S., McCarthy, H. R., Zhang, D. & Pataki, D. E. Water sources of urban trees in the Los Angeles metropolitan area. *Urban Ecosystems* **15**, 195-214 (2012).

54. February, E. C., West, A. G. & Newton, R. J. The relationship between rainfall, water source and growth for an endangered tree. *Austral Ecol.* **32**, 397-402 (2007).

55. Kurz-Besson, C. *et al*. Hydraulic lift in cork oak trees in a savannah-type Mediterranean ecosystem and its contribution to the local water balance. *Plant Soil* **282**, 361-378 (2006).

56. Swaffer, B. A., Holland, K. L., Doody, T. M., Li, C. & Hutson, J. Water use strategies of two co-occurring tree species in a semi-arid karst environment. *Hydrol. Process.* **28**, 2003-2017 (2014).

57. West, A. G. *et al*. Diverse functional responses to drought in a Mediterranean-type shrubland in South Africa. *New Phytol.* **195**, 396-407 (2012).

58. Ohte, N. *et al*. Water utilization of natural and planted trees in the semiarid desert of Inner Mongolia, China. *Ecol. Appl.* **13**, 337-351 (2003).

59. Sun, S., Huang, J., Han, X. & Lin, G. Comparisons in water relations of plants between newly formed riparian and non-riparian habitats along the bank of Three Gorges Reservoir, China. *Trees-Structure and Function* **22**, 717-728 (2008).

60. Berry, Z. C., Hughes, N. M. & Smith, W. K. Cloud immersion: an important water source for spruce and fir saplings in the southern Appalachian Mountains. *Oecologia* **174**, 319-326 (2014).

61. Jia, G., Yu, X., Deng, W., Liu, Y. & Li, Y. Determination of minimum extraction times for water of plants and soils used in isotopic analysis. *Journal of Food Agriculture & Environment* **10**, 1035-1040 (2012).

62. Rong, L., Chen, X., Chen, X., Wang, S. & Du, X. Isotopic analysis of water sources of mountainous plant uptake in a karst plateau of southwest China. *Hydrol. Process.* **25**, 3666-3675 (2011).

63. Tang, K. L. & Feng, X. H. The effect of soil hydrology on the oxygen and hydrogen isotopic compositions of plants' source water. *Earth Planet. Sci. Lett.* **185**, 355-367 (2001).

64. Wang, P., Song, X., Han, D., Zhang, Y. & Liu, X. A study of root water uptake of crops indicated by hydrogen and oxygen stable isotopes: A case in Shanxi Province, China. *Agric. Water Manage.* **97**, 475-482 (2010).

65. Wei, Y. F., Fang, J., Liu, S., Zhao, X. Y. & Li, S. G. Stable isotopic observation of water use sources of Pinus sylvestris var. mongolica in Horqin Sandy Land, China. *Trees-Structure and Function* **27**, 1249-1260 (2013).

66. Wei, L., Lockington, D. A., Poh, S., Gasparon, M. & Lovelock, C. E. Water use patterns of estuarine vegetation in a tidal creek system. *Oecologia* **172**, 485-494 (2013).

67. Zhang, W. *et al*. Using stable isotopes to determine the water sources in alpine ecosystems on the east Qinghai-Tibet plateau, China. *Hydrol. Process.* **24**, 3270-3280 (2010).

68. Anderegg, L. D. L., Anderegg, W. R. L., Abatzoglou, J., Hausladen, A. M. & Berry, J. A. Drought characteristics' role in widespread aspen forest mortality across Colorado, USA. *Global Change Biol.* **19**, 1526-1537 (2013).

69. Berkelhammer, M. *et al*. The nocturnal water cycle in an open-canopy forest. *Journal of Geophysical Research-Atmospheres* **118**, 10225-10242 (2013).

70. Bertrand, G. *et al*. Determination of spatiotemporal variability of tree water uptake using stable isotopes ($\delta^{18}O$, $\delta^{2}H$) in an alluvial system supplied by a high- altitude watershed, Pfyn forest, Switzerland. *Ecohydrology* **7**, 319-333 (2014).

71. Liu, Y. *et al*. Analyzing relationships among water uptake patterns, rootlet biomass distribution and soil water content profile in a subalpine shrubland using water isotopes. *Eur. J. Soil Biol.* **47**, 380-386 (2011).

72. Penna, D. *et al*. Tracing the water sources of trees and streams: isotopic analysis in a small pre-alpine catchment. *Four Decades of Progress in Monitoring and Modeling of Processes in the Soil-Plant-Atmosphere System: Applications and Challenges* **19**, 106-112 (2013).

73. Phillips, S. L. & Ehleringer, J. R. Limited uptake of summer precipitation by Bigtooth Maple (Acer-Grandidentatum Nutt) and Gambels Oak (Quercus-Gambelii Nutt). *Trees-Structure and Function* **9**, 214-219 (1995).

74. Rose, K. L., Graham, R. C. & Parker, D. R. Water source utilization by Pinus jeffreyi and Arctostaphylos patula on thin soils over bedrock. *Oecologia* **134**, 46-54 (2003).

75. Brunel, J. P., Walker, G. R. & Kennettsmith, A. K. Field Validation of Isotopic Procedures for Determining Sources of Water used by Plants in a Semiarid Environment. *Journal of Hydrology* **167**, 351-368 (1995).

76. Clinton, B. D., Vose, J. M., Vroblesky, D. A. & Harvey, G. J. Determination of the relative uptake of ground vs. surface water by Populus deltoides during phytoremediation. *Int. J. Phytoremediation* **6**, 239-252 (2004).

77. Eggemeyer, K. D. *et al*. Seasonal changes in depth of water uptake for encroaching trees Juniperus virginiana and Pinus ponderosa and two dominant C(4) grasses in a semiarid grassland. *Tree Physiol.* **29**, 157-169 (2009).

78. Holland, K. L., Tyerman, S. D., Mensforth, L. J. & Walker, G. R. Tree water sources over shallow, saline groundwater in the lower River Murray, south-eastern Australia: implications for groundwater recharge mechanisms. *Aust. J. Bot.* **54**, 193-205 (2006).

79. Kukowski, K. R., Schwinning, S. & Schwartz, B. F. Hydraulic responses to extreme drought conditions in three co-dominant tree species in shallow soil over bedrock. *Oecologia* **171**, 819-830 (2013).

80. McCole, A. A. & Stern, L. A. Seasonal water use patterns of Juniperus ashei on the Edwards Plateau, Texas, based on stable isotopes in water. *Journal of Hydrology* **342**, 238-248 (2007).

81. Mensforth, L. J., Thorburn, P. J., Tyerman, S. D. & Walker, G. R. Sources of water used by riparian Eucalyptus-Camaldulensis overlying highly saline groundwater. *Oecologia* **100**, 21-28 (1994).

82. Hartsough, P., Poulson, S. R., Biondi, F. & Estrada, I. G. Stable isotope characterization of the ecohydrological cycle at a tropical treeline site. *Arctic Antarctic and Alpine Research* **40**, 343-354 (2008).

83. Brunel, J. P., Walker, G. R., Dighton, J. C. & Monteny, B. Use of stable isotopes of water to determine the origin of water used by the vegetation and to partition evapotranspiration. A case study from HAPEX-Sahel. *Journal of Hydrology* **189**, 466-481 (1997).

84. February, E. C., Higgins, S. I., Newton, R. & West, A. G. Tree distribution on a steep environmental gradient in an arid savanna. *J. Biogeogr.* **34**, 270-278 (2007).

85. Garcin, Y. *et al*. Hydrogen isotope ratios of lacustrine sedimentary n-alkanes as proxies of tropical African hydrology: Insights from a calibration transect across Cameroon. *Geochim. Cosmochim. Acta* **79**, 106-126 (2012).

86. Deng, Y., Jiang, Z. & Qin, X. Water source partitioning among trees growing on carbonate rock in a subtropical region of Guangxi, China. *Environmental Earth Sciences* **66**, 635-640 (2012).

87. Evaristo, J., McDonnell, J. J., Scholl, M. A., Bruijnzeel, L. A. & Chun, K. P. Insights into plant water uptake from xylem-water isotope measurements in two tropical catchments with contrasting moisture conditions. *Hydrol. Process.* **30**, 3210-3227 (2016).

88. Nie, Y. *et al*. Seasonal water use patterns of woody species growing on the continuous dolostone outcrops and nearby thin soils in subtropical China. *Plant Soil* **341**, 399-412 (2011).

89. Rosado, B. H. P., De Mattos, E. A. & Sternberg, L. D. S. L. Are leaf physiological traits related to leaf water isotopic enrichment in restinga woody species? *An. Acad. Bras. Cienc.* **85**, 1035-1045 (2013).

90. Schwendenmann, L., Pendall, E., Sanchex-Bragado, R., Kunert, N. & Holsher, D. Tree water uptake in a tropical plantation varying in tree diversity: interspecific differences, seasonal shifts and complementarity. *Ecohydrology* (2014).

Table 3.1. Key information on 47 globally-distributed isotopic datasets.

Biome	Number of papers	RH (%)	MAT (°C)	MAP (mm y^{-1})	LMWL slope	Plant δ^2H	Soil δ^2H	Stream δ^2H	GW δ^2H
Arid	7	49 ± 8.5	13 ± 5.2	314 (89)	8.0 (0.3)	-66 (39)	-44 (51)	-73 (15)	-27 (50)
Mediterranean	6	58 ± 7.3	15 ± 4.0	331 (157)	7.1 (2.5)	-48 (19)	-43 (27)	-46 (24)	-31 (17)
Temperate forests	17	58 ± 8.5	8.9 ± 5.0	533 (692)	8.2 (0.8)	-79 (36)	-79 (23)	-91 (48)	-84 (41)
Temperate grasslands	7	56 ± 5.1	16 ± 3.8	478 (662)	7.1 (0.5)	-28 (18)	-28 (10)	-22 (14)	-30 (41)
Tropics	10	65 ± 11	23 ± 3.8	1350 (1340)	8.2 (0.3)	-34 (33)	-38 (64)	-7.4 (30)	-14 (10)

Abbreviations: RH (relative humidity), MAT (mean annual temperature), MAP (mean annual precipitation), LMWL (local meteoric water line), GW (groundwater). Values are mean ±1 SD, otherwise median (interquartile range).

Table 3.2. **Site-by-site source precipitation δ values for soil, plant xylem, and groundwater**. Plant xylem and soil water δ source precipitation values (median, interquartile range) are calculated using Equations (2.2) and (2.3) in Main Text. The last two columns on the right show whether or not the source precipitation values are statistically different amongst the three water compartments [** denotes statistically significant difference (alpha=0.05); N.S. means Not Significant]. Superscripts after site locations refer to the source paper (see references).

Site ID	Location	Plant xylem δ source (δ^2H)	Groundwater (δ^2H)	Soil water δ source (δ^2H)	Plant vs. Groundwater	Soil vs. Groundwater
1	Texas A, US[46]	-38 (27)	-25 (1.8)	-33 (27)	N.S.	**
2	Arizona A, US[47]	-131 (16)	-96 (22)	-91 (11)	**	N.S.
3	Arizona B, US[48]	-96 (43)	-56 (13)	-45 (53)	**	N.S.
4	Arizona-Utah, US[49]	-125 (30)	-81 (0.5)	-160 (24)	**	**
5	Northwest CN[50]	-91 (54)	-81 (17)	-30 (49)	N.S.	N.S.
6	Junggar Plain, CN[51]	-109 (9.9)	-49 (13)	-87 (40)	**	**
7	Ningxia Plain, CN[52]	-139 (26)	-76 (15)	-149 (21)	**	**
8	California A, US[53]	-86 (31)	-44 (5.5)	-57 (43)	**	**
9	Cape Town, ZA[54]	-58 (29)	-33 (20)	-	**	-
10	Evora, PT[55]	-46 (2.7)	-29 (2.3)	-51 (10)	**	**
11	Eyre Peninsula, AU[56]	-31 (10)	-24 (1)	-15 (6.4)	**	**
12	Mt. Natl Park, ZA[57]	-18 (13)	-18 (16)	-	N.S.	-
13	Ordos Plateau, CN[58]	-113 (33)	-63 (13)	-94 (34)	**	**
14	Hubei Province, CN[59]	-114 (34)	-66 (6.8)	-125 (50)	**	**
15	N. Carolina, US[60]	-52 (13)	-40 (4.1)	-56 (12)	**	**
16	Beijing, CN[61]	-90 (6.4)	-64 (23)	-102 (8.1)	**	**
17	Guizhou Prov, CN[62]	-152 (51)	-49 (7.2)	-145 (54)	**	**
18	New Hampshire, US[63]	-103 (29)	-52 (9.2)	-	**	-
19	Shanxi Prov, CN[64]	-98 (8.8)	-62 (4.8)	-108 (29)	**	**
20	Horqin, CN[65]	-147 (21)	-75 (8)	-141 (41)	**	**
21	Queensland, AU[66]	-18 (23)	-30 (3.3)	-	N.S.	-
22	Sichuan A, CN[67]	-120 (9.6)	-86 (12)	-131 (33)	**	**
23	Colorado A, US[68]	-214 (34)	-107 (17)	-190 (38)	**	**
24	Colorado B, US[69]	-156 (141)	-92 (13)	-	**	-
25	Sierre, CH[70]	-151 (39)	-106 (5.8)	-142 (56)	**	**
26	Oregon, US[1]	-130 (10)	-100 (53)	-132 (36)	**	**
27	Sichuan B, CN[71]	-127 (10)	-86 (12)	-124 (11)	**	**
28	Pre-Alpine, IT[72]	-	-56 (2.1)	-	-	-
29	Utah, US[73]	-128 (69)	-114 (23)		N.S.	-
30	California B, US[74]	-128 (21)	-92 (8.4)	-126 (49)	**	**
31	Victoria, AU[75]	-29 (32)	-35 (0.3)	-43 (22)	N.S.	N.S.
32	Texas B, US[76]	-64 (12)	-29 (2.6)	-	**	-
33	Nebraska, US[77]	-134 (42)	-73 (11)	-	N.S.	-
34	River Murray A, AU[78]	-14 (40)	-33 (7)	-29 (49)	N.S.	N.S.
35	Texas C, US[79]	-25 (18)	-17 (1.6)	-	**	-
36	Texas D, US[80]	-66 (37)	-26 (3.8)	-40 (29)	**	**
37	River Murray B, AU[81]	-42 (7.7)	-30 (3.3)	-36 (14)	**	**
38	West Central, MX[82]	-216 (43)	-71 (23)	-242 (105)	**	**
39	Niger[83]	-28 (4.9)	-41 (16)	-16 (25)	**	**
40	Limpopo, ZA[84]	-64 (19)	-19 (15)	-	**	-
41	Cameroon[85]	-45 (30)	-15 (2.7)	-	**	-
42	Guangxi A, CN[86]	-146 (26)	-49 (14)	-104 (119)	**	N.S.
43	Luquillo-Susua, PR[87]	-27 (19)	-8.8 (7.5)	-14 (26)	**	**
44	Veracruz, MX[2]	-67 (23)	-71 (23)	-126 (53)	N.S.	**
45	Guangxi B, CN[88]	-105 (45)	-49 (7.2)	-142 (113)	**	**
46	Rio de Janeiro, BR[89]	-32 (44)	-15 (2.7)	10.4 (23)	**	**
47	Sardinilla, PA[90]	-54 (22)	-15 (2.7)	-58 (29)	**	**

Table 3.3. **Site-by-site soil water precipitation offset values (**median, interquartile range**).**

Site ID	Precip offet$_{soil}$
1	-6.2 (1.1)
2	-0.2 (1.8)
3	-4.1 (1.6)
4	-7.4 (1.9)
5	-0.7 (4)
6	-5.6 (5.4)
7	-1.5 (0.6)
8	-7.5 (1.6)
10	-5.5 (3)
11	-3.6 (0.2)
13	-0.8 (1.2)
14	-4.5 (1)
15	-3 (0.9)
16	-1.4 (0.7)
17	-6 (1.1)
19	-4.5 (1.3)
20	1.78 (1.2)
22	-9.7 (1.2)
23	-6.5 (0.6)
25	-1.1 (1.1)
26	-5.6 (1)
27	-4.7 (0.6)
28	-6.4 (0.3)
30	-4 (2.4)
31	-5.4 (1)
34	-5.5 (1)
36	-4.1 (1.1)
37	-5 (1.3)
38	-3.9 (0.8)
39	-2.4 (2.5)
42	-12 (3.3)
43	-8.2 (0.9)
44	-10 (1.2)
45	-8.4 (1.4)
46	-9.9 (2.5)
47	-3.3 (0.8)

Table 3.4. **Biome-level soil water precipitation offset values** (median, interquartile range).

Biome_mod	Precip offet$_{soil}$
Arid	-3.7 (-4.6)
Mediterranean	-7 (3.6)
Temperate forests	-5.2 (2.4)
Temperate grasslands	-5.1 (1.1)
Tropics	-9.3 (2.2)

Figure 3.1. $\delta^{18}O$ and $\delta^{2}H$ values of groundwater, stream water, plant xylem water, and soil water at 47 globally-distributed sites [median (interquartile range) $\delta^{18}O$ and $\delta^{2}H$, respectively]**. a**, Groundwater [-7.7 (7.4), -51.5 (62.6), n = 2749]. **b,** Stream water [-6.2 (8.8), -37.1 (66.9), n = 336]. **c,** Plant xylem water [-5.5 (6.1), -50.6 (50.6), n = 1460]. **d,** Soil water [-7.5 (7.4), -63.9 (52.2), n = 1830]. Inset in **a** shows locations of 47 globally-distributed stable isotopic datasets. Histogram borders show partitioning of the dataset at 30 identical intervals or bins. The Global Meteoric Water Line (GMWL[13]) is also shown.

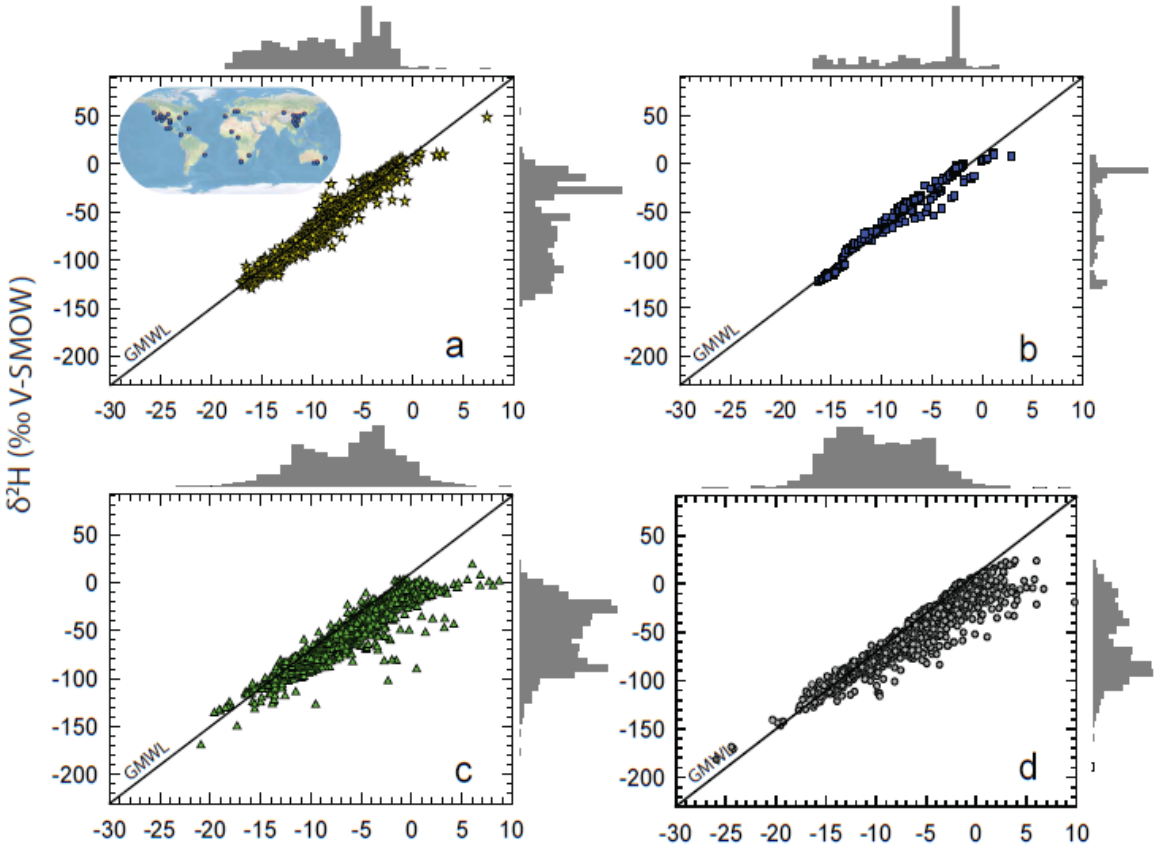

Figure 3.2. Precipitation offset values of groundwater, stream water, plant xylem water, and soil water for 47 sites grouped by biome. Extents of plant xylem (white) and soil (gray) water bars show 25th and 75th percentiles. All values of groundwater (squares) are shown for visualization of data density (i.e. darker regions) and dispersion (i.e. lighter regions). Mean values of stream water (circles) are also shown. Transpiration-amount-weighted values of plant xylem water (triangles) are also shown.

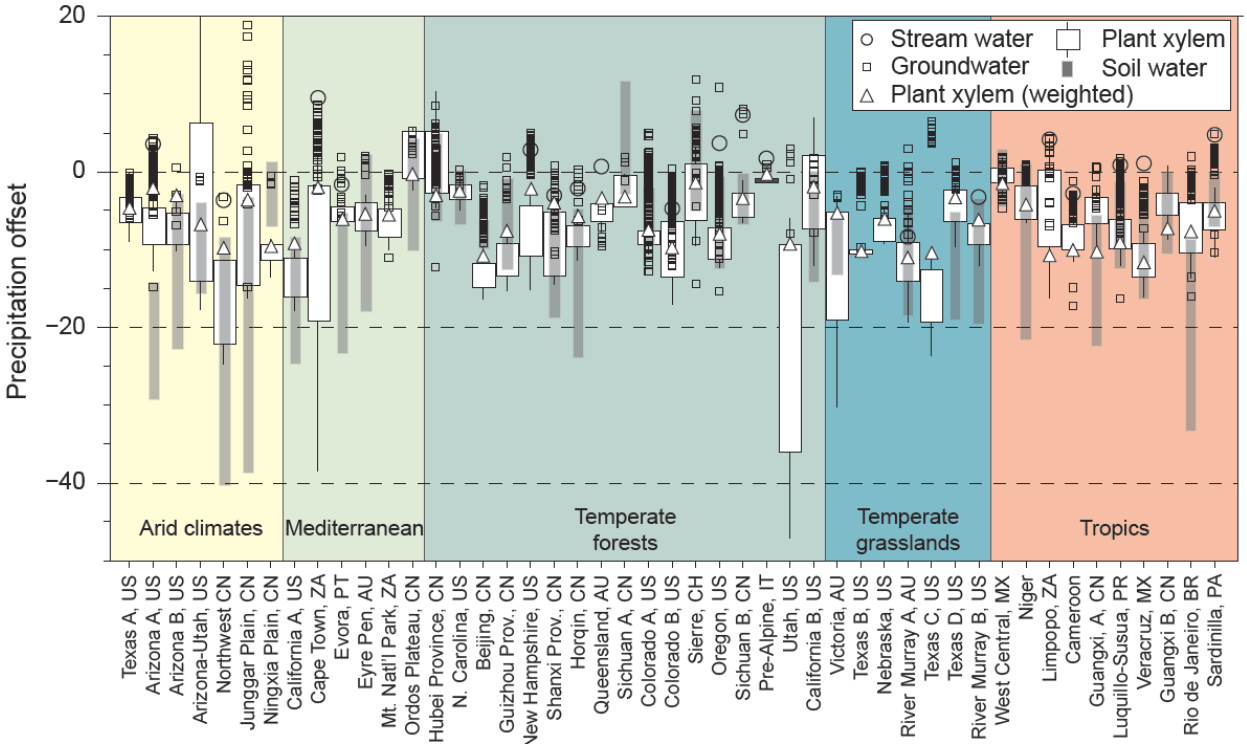

Figure 3.3. **Schematic representation for tracing the isotopic composition of source precipitation.** Plant xylem water isotopic values plot on a linear regression called the evaporation line (EL). The point in the local meteoric water line (LMWL) where plant xylem water EL intersects provide a good approximation of the mean isotopic value of plant xylem source precipitation. The same method is used in tracing the soil water δ source value.

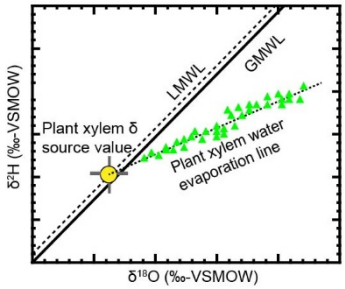

Figure 3.4. **Tracing the isotopic composition of plant xylem source precipitation versus mean groundwater value.** Plant xylem water (gray triangles) plotted in $\delta^{18}O$-$\delta^{2}H$ space. Shown are mean plant xylem source precipitation value (green triangle with error bars, ±1SD), mean groundwater value (blue circle with error bars, ±1SD), amount-weighted average precipitation (star), GMWL (solid black line), LMWL (dashed black line). Illustration of a case in Oregon, USA (ref 1) where mean groundwater isotope value is more positive than plant xylem source precipitation value. This is the case in 41 of 47 sites in the database.

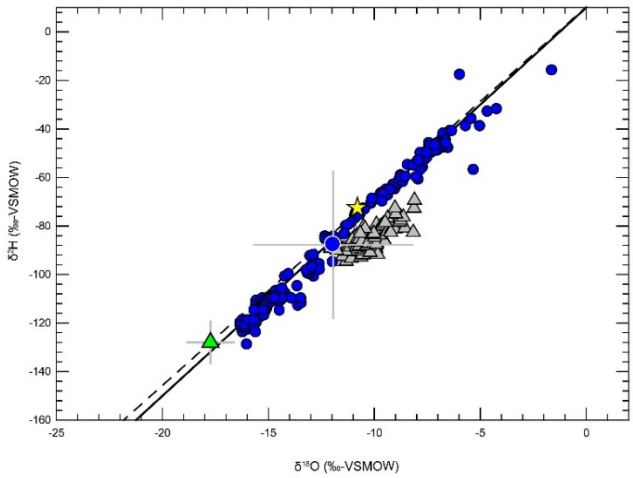

Figure 3.5. **Difference between precipitation δ-source precipitation values of plant xylem and mean groundwater value (abs ‰ δ^2H) plotted against increasing distance of groundwater locations from actual plant xylem study site.** Extents of boxes show 25th and 75th percentiles; whiskers show extents of outliers. Also shown are median (interquartile range) values for arbitrary distance ranges.

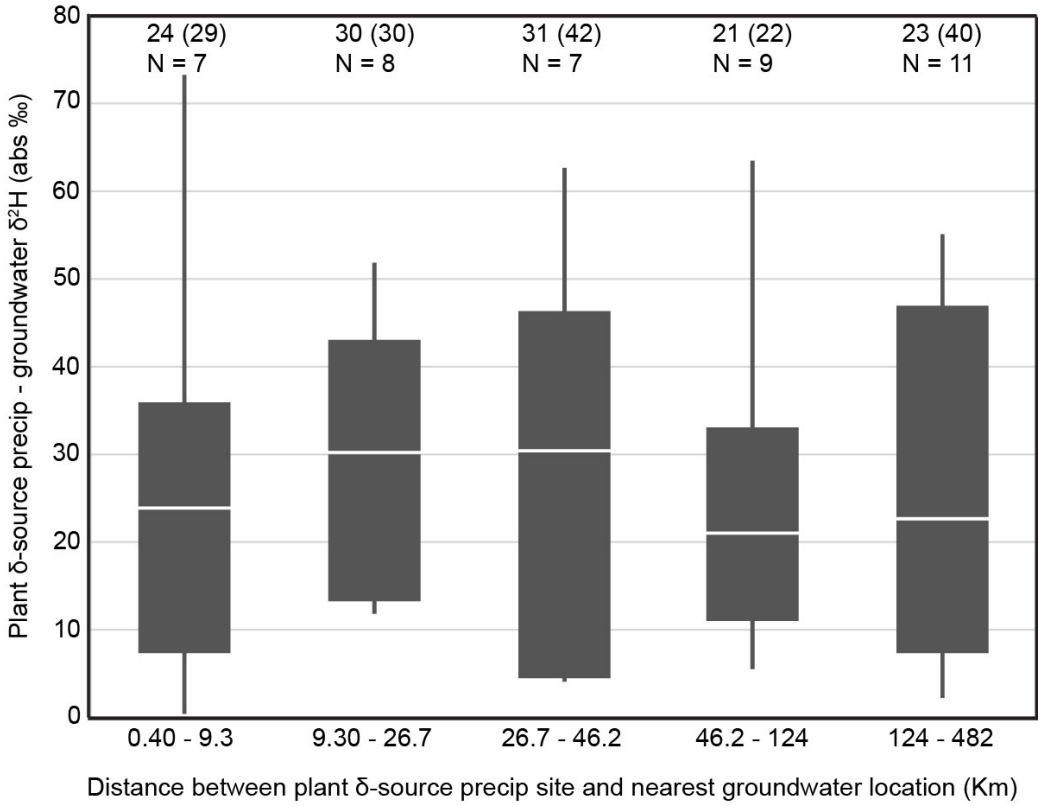

Figure 3.6. **Groundwater and plant xylem source precipitation.** $\delta^{18}O$-$\delta^{2}H$ plot of global plant xylem water (green triangles), soil water (gray circles), and groundwater (blue circles). Also shown are isotopic composition of source precipitation leading to groundwater recharge (blue circle with error bars, mean ±1SD) and precipitation leading to plant water uptake (green triangle with error bars, mean ±1SD). Inset shows linear regression of plant xylem water and soil water forming distinct evaporation lines (EL) whereby, at a site level, plant xylem water is completely bounded by soil water. Also shown are GMWL and LMWL in main plot and inset, respectively.

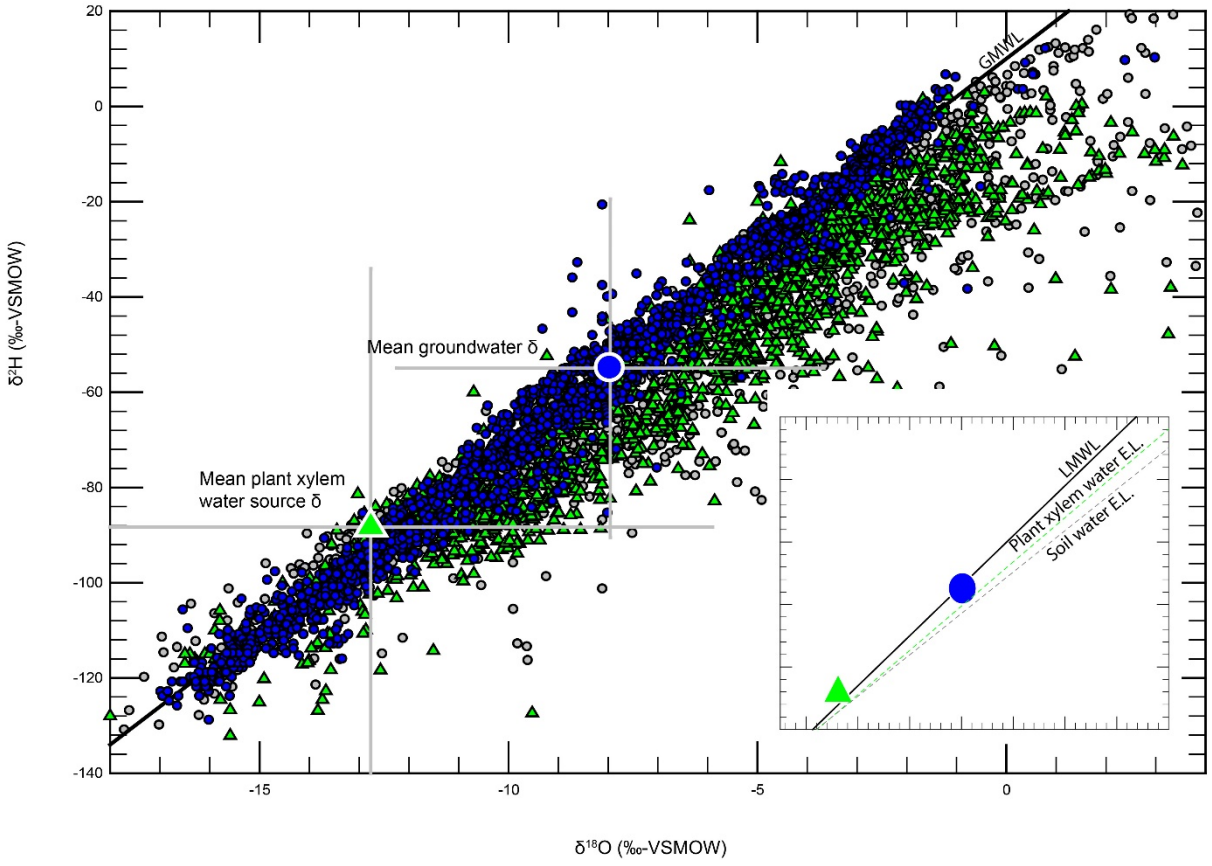

Figure 3.7. **Comparison of plant xylem (black boxes) and soil water (gray boxes) $\delta^{18}O$ based on water extraction techniques**. Extents of boxes show 25th and 75th percentiles, while whiskers show extents of outliers. Also shown are median (interquartile range) values for each water type and water extraction technique.

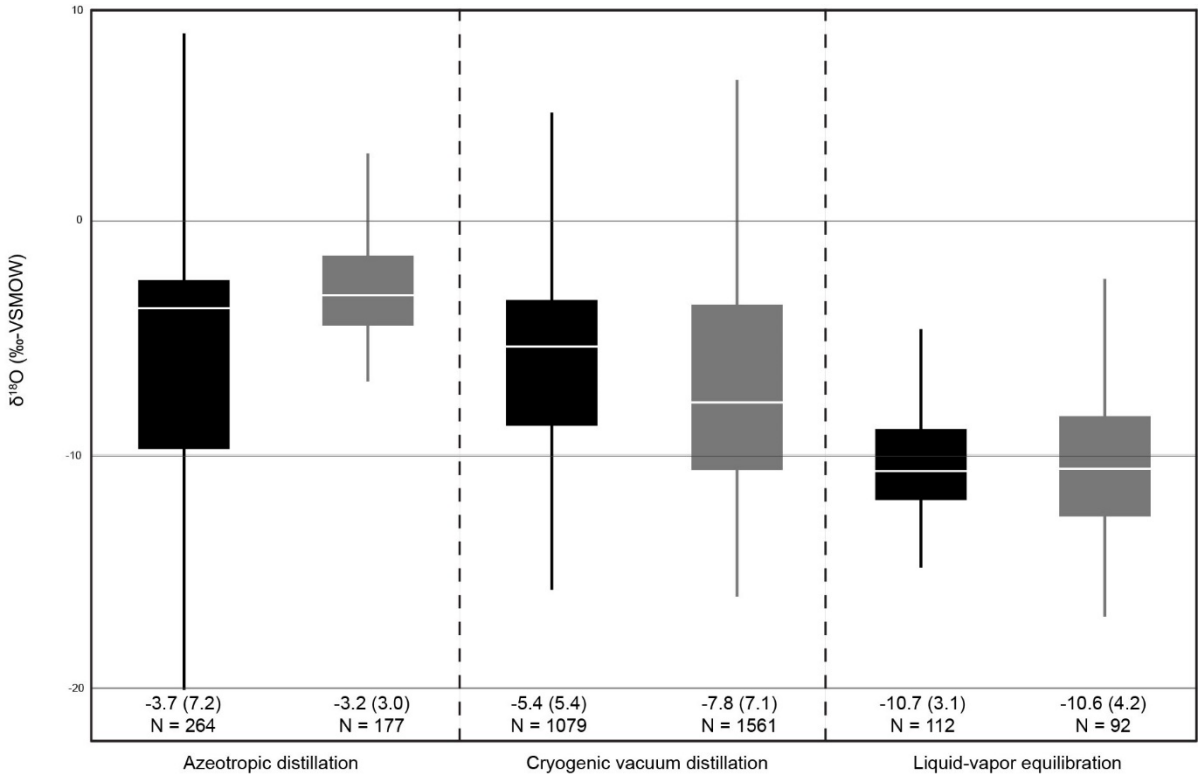

Figure 3.8. Global map of plant xylem water *precipitation offsets*.

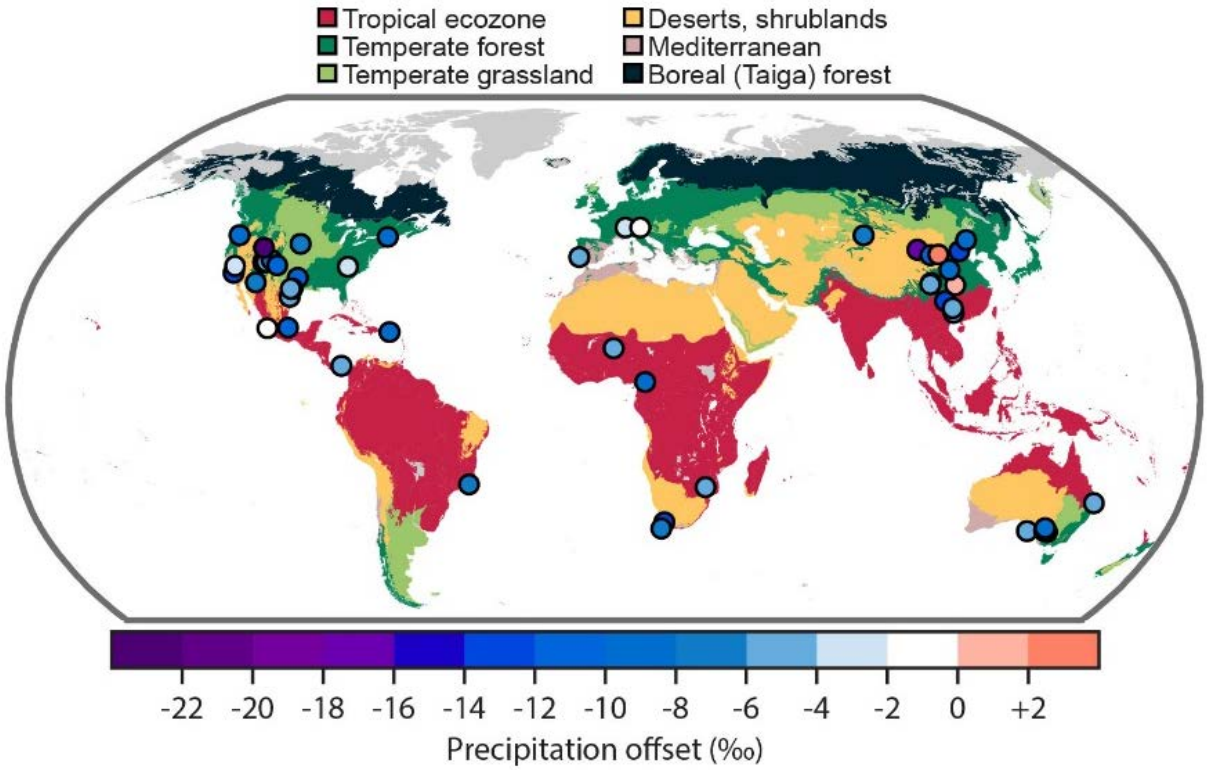

CHAPTER 4

GROUNDWATER USE BY PLANTS NOT WIDESPREAD GLOBALLY

Status: Minor revision

Submitted: March 2016

Citation: Evaristo, J. and J. J. McDonnell (in revision), Groundwater use by plants not widespread globally, *(Nature) Scientific Reports*.

4.1 Abstract

The degree of groundwater use by plants has not yet been synthesized worldwide. Here we present evidence, derived from a global compilation of xylem and groundwater dual stable isotope (δ^2H and $\delta^{18}O$) information, that groundwater use is limited to 12±5% of ~4000 plants (mostly trees) globally across 126 sites and 9 terrestrial biomes; this calculation is in stark contrast to that made using the standard single isotope analysis of these data that suggests global use of groundwater by plants is widespread (41±45%). This finding highlights the importance of using both isotopes in plant water uptake studies and consequently the more limited use of groundwater by plants than is assumed in the largely single isotope dominated literature.

4.2 Main Text

The stable isotopes of water are powerful, non-invasive tools for tracing water sources for plants[1]. Since root water uptake is generally a non-fractionating process[2, 3], the isotopic composition ($\delta^2H/\delta^{18}O$) of xylem (i.e. plant stem) water should reflect that of its source within the rooting zone. This fundamental understanding of water uptake and transport from roots to shoots underlies the utility of stable isotopes in plant water uptake investigations. While many site-based studies have now been completed, a global synthesis of these data has not yet been made.

Here we use a compiled database of groundwater (n = 6964) and xylem water isotopes from 3,898 plant samples (trees n = 3,162; shrubs n = 622; others n = 114), representing 275 species (angiosperms n = 245; gymnosperms n = 30), and 126 sites across 9 terrestrial biomes (Figure 4.1 inset) to reveal the global picture of groundwater use by plants. Where dual isotope was used in the source paper (hereafter "dual isotope method"), we quantify the number of xylem samples that are consistent with groundwater (see Methods). Using a modification to the method used by ref. 4, we develop an index for groundwater use by plants:

$$\text{xylem-groundwater connectivity} = [\delta^2\text{H} - a \cdot \delta^{18}\text{O} - b]/S \quad (4.1)$$

where δ^2H and δ^{18}O are isotopic composition of xylem water at each study site, a and b are the slope and y intercept, respectively, calculated from measurements of δ^{18}O and δ^2H of groundwater, and S is one standard deviation measurement uncertainty. A xylem-groundwater connectivity value of zero means strong coupling between xylem and groundwater (that is, groundwater use); a xylem-groundwater connectivity value farther from zero suggests decoupling (that is, soil water use).

Globally, Figure 4.1 shows a "high" connectivity (median, interquartile range) between groundwater and precipitation (3.2, 4.7), and a "low" connectivity between xylem and groundwater (12, 13). This finding supports recently reported studies on widespread ecohydrological separation – the water that supplies plant transpiration is different from the water that recharges groundwater and replenishes streamflow[4, 5].

We also calculate the coefficient of variation (CV) of xylem-groundwater connectivity at the species (n = 121), genus (n = 77), and biome (n = 9) level (Figure 4.2a). The CVs of xylem-groundwater connectivity across intra-specific, intra-genus, and intra-biome groupings are not significantly different (oneway ANOVA, P = 0.22); post hoc tests (Tukey–Kramer honest significant difference) show no significant difference between each grouping: species-genus (P = 0.97), species-biome (P = 0.22), genus-biome (P = 0.19). These results illustrate that the variability in xylem-groundwater connectivity is not related to species, genera, and biomes represented by the plants in our database.

Grouping into angiosperms (n = 46) and gymnosperms (n = 12), however, shows that angiosperms exhibit greater offset from zero than gymnosperms (z-value = -2.1; $P < 0.05$)

(Figure 4.2b). Greater offset from zero in angiosperms than in gymnosperms supports the interpretation that gymnosperms have access to deeper subsurface water sources than angiosperms at the aggregated scale of our analysis. The CV of xylem-groundwater connectivity amongst angiosperms is also higher (86%) than amongst gymnosperms (66%). This finding supports the understanding related to key anatomical differences between the two groups[6]: xylem vessels (angiosperms) allow for more varied sizes and thicknesses than tracheids (gymnosperms); and greater number of parenchyma cells in angiosperms[7].

Our findings run counter to the traditional approach for quantifying groundwater use by plants using either δ^2H or $\delta^{18}O$ where xylem water δ^2H or $\delta^{18}O$ is "matched" to that of groundwater (the "single isotope method"). Recent studies have shown that the single isotope analysis is problematic[4] because the physical process of evaporation[8] has a disproportionately greater effect on $\delta^{18}O$ than on δ^2H. This means that either isotope may provide different information on potential water sources of plant water uptake[9]. Figure 4.3a interrogates our global database of published papers between 1991 and 2015 that use either δ^2H or $\delta^{18}O$ (hereafter "single isotope method"). This is quantified via direct interpolation (e.g. refs. 10, 11) and/or the use of mixing models (e.g. ref. 12). Figure 4.3a shows that using the single isotope method with our global dataset, 41±45% (median 19%, interquartile range 100%) of xylem values are consistent with groundwater use. Using the dual isotope method (e.g. ref. 13) (Figure 4.3b), only 8% (within 25th and 75th percentiles) and 16% (within 10th and 90th percentiles) of plants in the database are consistent with use of groundwater. While single isotope mixing models[12] may be useful in other applications (e.g. trophic and animal foraging studies), the single isotope approach for plant water uptake can lead to potentially unrealistic source water identification.

Overall, our results illustrate that groundwater use by plants (mostly trees in our global database) is not as widespread as is increasingly being argued in the literature[14]. Our finding that most trees rely on soil water may have several implications including greater vulnerability to drought impacts across scales[15] – from impaired growth after drought stress at plant and ecosystem scales to uncertainties in modeling climate-vegetation feedbacks at global scales[16]; less impact on river discharge at catchment scales than the case might be with widespread groundwater use[17]; and a rethinking on approaches used in afforestation schemes and silvicultural systems that place emphasis on species selection and groundwater use[18].

4.3 Methods

4.3.1 Data compilation and treatment

We searched the published literature for water stable isotope papers (hereafter "source papers") in ecology and hydrology. Where single isotope (δ^2H or $\delta^{18}O$) was used in a source paper, we compiled percent groundwater use by vegetation either from direct interpolation method or from reported mixing model results (e.g. IsoSource, after ref. 12). Where dual isotopes were used in a source paper, we used equation (1) to calculate the "offset" (xylem-groundwater connectivity) of a xylem water value from the groundwater line. The groundwater line (see slope and intercept parameters in Table S1) is calculated from measurements of $\delta^{18}O$ and δ^2H of groundwater at a site[19]. *S* in equation (1) is one standard deviation measurement uncertainty ($S = [(\delta^2H \text{ analytical error})^2 + (a \cdot \delta^{18}O \text{ analytical error})^2]^{0.5}$). We then defined upper and lower bounds of groundwater use if a xylem-groundwater connectivity value falls within the 10^{th} and 90^{th} percentiles and within the 25^{th} and 75^{th} percentiles of groundwater nonparametric data density space, respectively. We employed species-level accounting in establishing groundwater use by plants. This approach enabled us to test for effects not only at a site level but also at other categories of interest (e.g. species, genus, biome, etc.).

4.4 Publication bias

Any meta-analysis is prone to publication bias (i.e. the file-drawer problem). This is a function, by and large, of the inherent propensity of many journals to not publish negative results. A meta-analysis such as this contribution, therefore, may not be immune to such publication bias in the most fundamental sense. Nevertheless, in the treatment of the data where we sought to quantify the degree of groundwater use by vegetation, we suggest that publication bias is not likely to drive our main conclusions. Our method for literature search did not discriminate against any studies in a particular environment. That is, we compiled as many single- and dual-isotope papers as we could find between 1991 and 2015 using standard indexing databases (ISI Web of Science and Scopus) without prejudice to papers from any physiographic setting (e.g. arid/semi-arid, humid tropical climates, etc.) While our literature search was exhaustive, we could not

discount the possibility that we may have missed some papers in the literature. Given the extent of our search that encompasses 9 terrestrial biomes and 275 species (angiosperms n = 245; gymnosperms n = 30) across 126 sites, however, we suggest that our compiled database – the largest to date in the literature – is global-in-scale and representative of the current state-of-knowledge that is decipherable in a meta-analysis of this nature.

4.5 Taxonomic and biome effects on groundwater use

To assess whether species, genus, or terrestrial biome classification has an effect on xylem-groundwater connectivity (i.e. groundwater use), we calculated the coefficient of variation (CV) of respective categories (Figure 4.2a). We also compared the xylem-groundwater connectivity differences based on embryophyte classification (primarily angiosperms and gymnosperms) (Figure 4.2b). Because xylem-groundwater connectivity as an index of groundwater use is based on dual isotopes, we considered only source papers that met this criterion in the analysis made in Figure 4.2. Approximately 90% of taxonomic information in our database were referenced from National Center for Biotechnology Information (NCBI http://www.ncbi.nlm.nih.gov/taxonomy).

4.6 Transition Statement

This chapter quantified the degree of groundwater use by vegetation via meta-analysis of published literature on water stable isotopes in plant-water relations. Heretofore, isotope-based evidence of groundwater use by vegetation has been dispersed in the literature. In light of global-in-scale lines of evidence for ecohydrological separation, the publication of this chapter is timely because (1) it addressed some of the questions surrounding the implications of ecohydrological separation on the role of groundwater in sustaining vegetation, and (2) it strengthened the foundation upon which a search for the mechanistic underpinnings of ecohydrological separation would be based. The aforementioned points were the central research questions pursued in the following chapter.

4.7 Author Contributions

J.E. designed the study, compiled the data set, and conducted the statistical analyses. J.E. wrote the first paper draft. J.J.M. edited and commented on the manuscript and contributed to the text in later iterations.

4.8 References

1. Ehleringer, J. R. & Dawson, T. E. Water uptake by plants: perspectives from stable isotope composition. *Plant, Cell Environ.* **15**, 1073-1082 (1992).
2. Zimmermann, U. *et al*. Tracers determine movement of soil moisture and evapotranspiration. *Science* **152**, 346-347 (1966).
3. Dawson, T. E. & Ehleringer, J. R. Streamside Trees that do Not use Stream Water. *Nature* **350**, 335-337 (1991).
4. Evaristo, J., Jasechko, S. & McDonnell, J. J. Global separation of plant transpiration from groundwater and streamflow. *Nature* **525**, 91-+ (2015).
5. Good, S. P., Noone, D. & Bowen, G. Hydrologic connectivity constrains partitioning of global terrestrial water fluxes. *Science* **349**, 175-177 (2015).
6. Anderegg, W. R. L. Spatial and temporal variation in plant hydraulic traits and their relevance for climate change impacts on vegetation. *New Phytol.* **205**, 1008-1014 (2015).
7. Miguel Olano, J., Arzac, A., Garcia-Cervigon, A. I., von Arx, G. & Rozas, V. New star on the stage: amount of ray parenchyma in tree rings shows a link to climate. New Phytol. **198**, 486-495 (2013).
8. Craig, H. Isotopic variations in meteoric waters. *Science* **133**, 1702-1703 (1961).
9. McDonnell, J. J. The two water worlds hypothesis: ecohydrological separation of water between streams and trees? WIREs Water **1**, 323–329 (2014).
10. Ishshalom, N., Sternberg, L. D. L., Ross, M., Obrien, J. & Flynn, L. Water Utilization of Tropical Hardwood Hammocks of the Lower Florida Keys. *Oecologia* **92**, 108-112 (1992).

11. Chimner, R. A. & Cooper, D. J. Using stable oxygen isotopes to quantify the water source used for transpiration by native shrubs in the San Luis Valley, Colorado USA. *Plant Soil* **260**, 225-236 (2004).

12. Phillips, D. L. & Gregg, J. W. Source partitioning using stable isotopes: coping with too many sources. *Oecologia* **136**, 261-269 (2003).

13. Goldsmith, G. R. *et al*. Stable isotopes reveal linkages among ecohydrological processes in a seasonally dry tropical montane cloud forest. *Ecohydrology* **5**, 779-790 (2012).

14. Fan, Y. Groundwater in the Earth's critical zone: Relevance to large-scale patterns and processes. *Water Resour. Res.* **51**, 3052-3069 (2015).

15. Anderegg, L. D. L., Anderegg, W. R. L., Abatzoglou, J., Hausladen, A. M. & Berry, J. A. Drought characteristics' role in widespread aspen forest mortality across Colorado, USA. *Global Change Biol.* **19**, 1526-1537 (2013).

16. Reichstein, M. *et al*. Climate extremes and the carbon cycle. *Nature* **500**, 287-295 (2013).

17. McJannet, D. L., Vertessy, R. A. & Clifton, C. A. Observations of evapotranspiration in a break of slope plantation susceptible to periodic drought stress. *Tree Physiol.* **20**, 169-177 (2000).

18. Fritzsche, F. *et al*. Soil-plant hydrology of indigenous and exotic trees in an Ethiopian montane forest. *Tree Physiol.* **26**, 1043-1054 (2006).

19. Jasechko, S. *et al*. The pronounced seasonality of global groundwater recharge. *Water Resour. Res.* **50**, 8845-8867 (2014).

Figure 4.1: Nonparametric density contour plot of xylem, groundwater, and precipitation connectivity (unitless index). Contour lines are quantiles. Connectivity between xylem (i.e. stem) water (n = 1460) and groundwater (y-axis) (n = 6964) and between groundwater and precipitation (x-axis). Values are calculated using equation (1), expressed in absolute values and rescaled for comparison. Inset map shows sites (*n* = 126) of source papers and number of xylem samples (*n* = 3,898) in the meta-analysis (map generated using ArcMap 10.2; http://services.arcgisonline.com/arcgis/rest/services/World_Street_Map/MapServer).

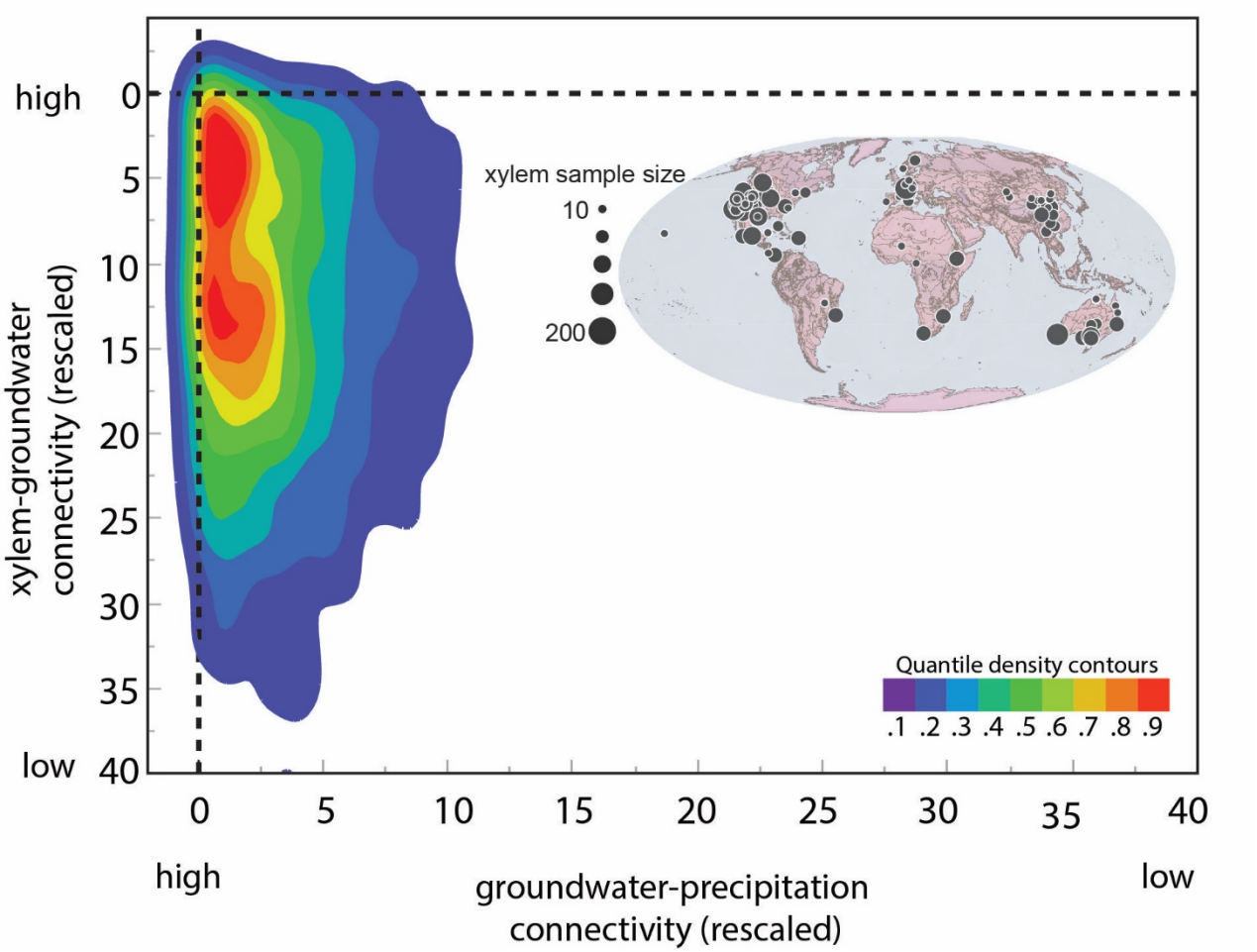

Figure 4.2: Xylem-groundwater connectivity. **a**, Intra-specific, intra-genus, and intra-biome coefficient of variation (CV) of xylem-groundwater connectivity; **b**, xylem-groundwater connectivity between angiosperms and gymnosperms. Box in box plots bounds the interquartile range (IQR) divided by the median; whiskers extend to a maximum of 1.5 × IQR beyond the box. Numbers below bars in 2a indicate the sample size of respective groupings; numbers below bars in 2b represent the number of angiosperms and gymnosperms used in the analysis. Different letters denote statistical significance at $P < 0.05$; same letters denote no statistical significance.

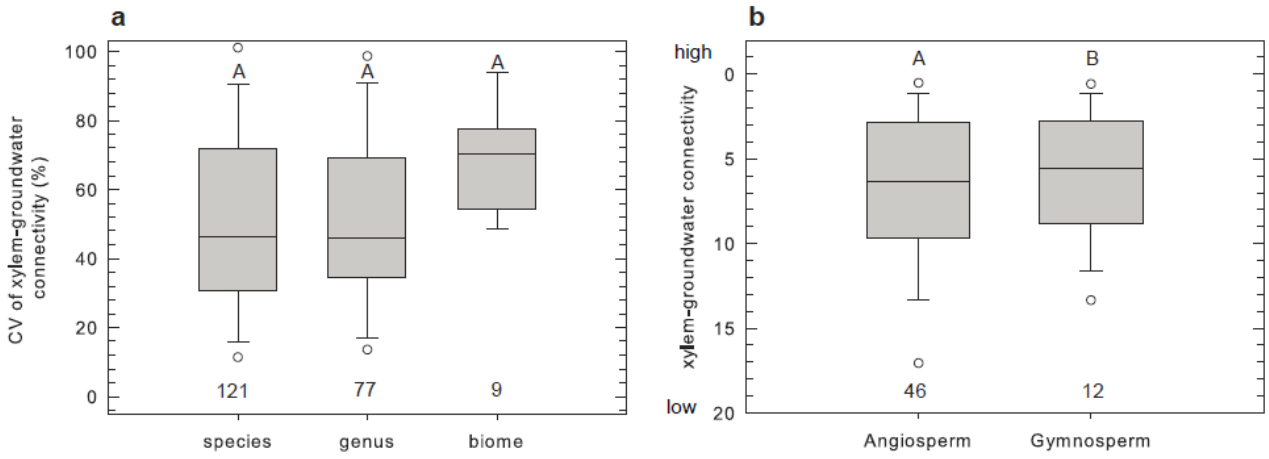

Figure 4.3: Single- versus dual-isotope method in inferring sources of plant water uptake. **a**, single isotope method (sites *n* = 126; xylem *n* = 3,898); **b**, dual isotope method (sites *n* = 67; xylem *n* = 1,460). Map of 16 terrestrial biomes delineated by The Nature Conservancy http://www.nature.org. Map was generated using ArcMap 10.2 (http://services.arcgisonline.com/arcgis/rest/services/World_Street_Map/MapServer) based on data reported by 98 source papers between 1991 and 2015.

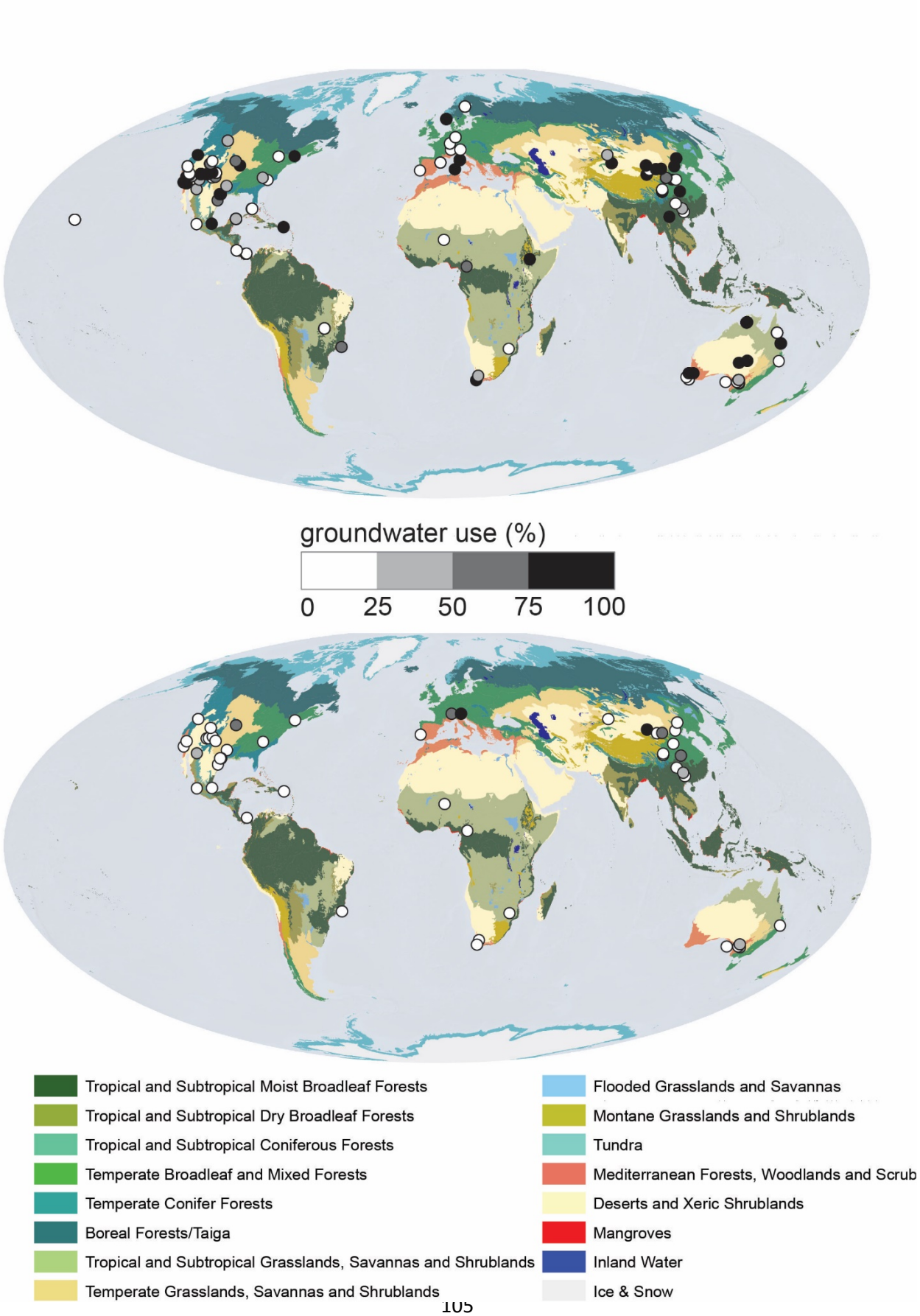
groundwater use (%)
0
25
50
75
100
Tropical and Subtropical Moist Broadleaf Forests
Tropical and Subtropical Dry Broadleaf Forests
Tropical and Subtropical Coniferous Forests
Temperate Broadleaf and Mixed Forests
Temperate Conifer Forests
Boreal Forests/Taiga
Tropical and Subtropical Grasslands, Savannas and Shrublands
Temperate Grasslands, Savannas and Shrublands
Flooded Grasslands and Savannas
Montane Grasslands and Shrublands
Tundra
Mediterranean Forests, Woodlands and Scrub
Deserts and Xeric Shrublands
Mangroves
Inland Water
Ice & Snow

CHAPTER 5

SOURCE APPORTIONMENT IN THE CRITICAL ZONE: CHARACTERIZING THE FLUXES AND AGE DISTRIBUTION OF SOIL WATER, PLANT WATER AND DEEP PERCOLATION

Status: To be submitted (October 2016)

Citation: Evaristo, J., J. J. McDonnell, Kim, M., van Haren, J., Pangle, L., Harman, C.J., and Troch, P.A. *Water Resources Research*

5.1 Abstract

Determining the ages and sources of water that supply transpiration and groundwater recharge is a major challenge in ecohydrology. Compounding such difficulty are recent lines of evidence showing widespread ecohydrological separation whereby transpiration water is different from the relatively more mobile water in soils, groundwater, and streams. Such an assertion has been met with varied reactions from the water resources community. Of the many outstanding questions surrounding ecohydrological separation, one overarching question is explored in this paper: is ecohydrological separation a separation in time or in space? That is, transpiration might be taking place at a time and space in the subsurface different from groundwater recharge. Here we take a holistic view of transit times at the ecosystem level. We present new results from the 35000-m^3 mesocosm, Biosphere 2-Tropical Rainforest (B2-TRF) biome. We test the null hypothesis that the ecohydrological system is tightly connected in that transpiration and groundwater recharge are sourced from the same storage volume (L^3) at comparable average water flux (L^3 T^{-1}), thus, having similar mean transit times. We performed a 10-week drought and then added 66 mm of labelled rainfall with 152‰ δ^2H distributed over four events (mean 16.5 mm per event). This was followed by a total of 87 mm of rainfall (-60‰ δ^2H) distributed over 13 events that were spaced every 2-3 days. Our results show that mean transit times through the individual ecohydrological domains (groundwater recharge and plant transpiration) were highly preferential: groundwater recharge was 3-7 times younger (~10 days) than transpired

water (range 24-71 days). The "age" of transpired water showed strong dependence on species and was strongly linked to water transport driving force (difference between soil matric potential and midday leaf water potential). We also partitioned tree water uptake via roots by using a mixing model implemented in a Bayesian inference framework. During drought, our results show that the fraction of mobile water in xylem increased exponentially (mean 0.50, range 0.26-0.78) with driving force. In contrast, immediately after rewetting, almost 90% (±2%) of water in xylem came from the top 40 cm of the soil profile before decreasing to 70% (±16%) and 60% (±20%) seven and 14 days after the first rainfall, respectively. The fraction of mobile water in xylem post drought, therefore, decreased (mean 0.21, range 0.08-0.34), suggesting a switch to soil matrix water. Overall, our findings underline two key discoveries: (1) mobile water fraction in xylem increases with water transport driving force, underlining species-level control; (2) transpiration flux is older than groundwater recharge flux. The latter discovery is consistent with a perceptual (qualitative) model whereby transpiration and groundwater recharge fluxes are sourced from separate storage volumes and sampled at markedly different average sampling flux. Our study is the first to measure and quantify what was referred heretofore as the "missing exit age" of transpiration.

5.2 Introduction

Water uptake by vegetation (i.e. transpiration) returns almost half of precipitation that falls on the Earth's critical zone (Schlesinger and Jasechko, 2014). The ages and sources of transpiration water, from hillslope-catchment to continental scales, however, are poorly understood. Determining the ages and sources of transpiration water, and stream water, is important because of recent global-in-scale evidence showing widespread ecohydrological separation (Evaristo *et al*., 2015; Good *et al*., 2015). Ecohydrological separation (also known colloquially as the *two water worlds* hypothesis; McDonnell, 2014) posits that the water used by vegetation is different from the "more mobile" water in soils, groundwater and streams. A similar phenomenon was also recently reported using nitrate isotopes (*two nitrate worlds*) (Hall *et al.*, 2016), thereby supporting the idea that water/nutrient uptake by vegetation and groundwater recharge/nutrient export to streams are separated. Indeed, if ecohydrological separation is real, then the implications for quantifying transit times in streams using current approaches that assumed a

well-mixed critical zone are profound, since ecohydrological separation is synonymous with an acutely non-well mixed subsurface.

Originally reported in the Pacific Northwest, USA (Brooks *et al*., 2010) and later in various sites in the tropics and elsewhere (Goldsmith *et al*., 2012; Evaristo *et al*., 2016; Hervé-Fernández *et al.*, 2016), the *two water worlds* hypothesis has been met with much informed skepticism (e.g. Geris *et al*., 2015; Tetzlaff *et al*., 2015) and constructive criticism (e.g. Sprenger *et al.*, 2016). In cases where benefit of the doubt was given to the hypothesis (Bowen 2015; Brooks 2015; Bowling *et al.*, 2016) questions pertain to the purported mechanisms proposed by the original and later authors. Of the many outstanding questions surrounding ecohydrological separation, one overarching question is explored in this paper: *is ecohydrological separation a separation between transpiration and mobile soil water in time or a separation in space?*

Earlier research on the *two water worlds* hypothesis carried the implicit suggestion that transpiration flux is older than the more mobile water pool. This runs counter to most catchment modeling studies that suggest that evapotranspiration fluxes are younger (Hrachowitz *et al*., 2013, 2015; Harman, 2015). This time aspect involves quantifying the mean transit time (MTT) from corresponding transit time distribution (TTD) of subsurface water and transpiration. But no studies have yet quantified the transit time of transpired water[1] or the transit time of the low mobility water[2]. Of course, in steady state conditions, MTT is the ratio between storage volume (L^3) and average water flux ($L^3\,T^{-1}$). Catchment *transit time* is the time that a water parcel spends from input as rainfall to output as streamflow or transpiration water (also known as "exit age"). In rainfall-runoff literature, the shape of streamwater TTDs and associated MTT provide insights on catchment behavior with implications for runoff generation, nutrient export, and contaminant fate and transport (Kirchner *et al*., 2000; McDonnell *et al*., 2010; Hrachowitz *et al.*, 2016).

While streamwater MTT and TTD has been, and continues to be, the source of much active research (McGuire and McDonnell, 2015) the other piece of the exit age distribution—namely plant transpiration—has until now been neglected. Soulsby *et al*. (2015) note that "estimating the age distribution of evaporated waters remains a fundamental research need in order to quantify the total exit age of waters leaving a catchment". Nevertheless, the only work in this regard are a

[1] Except for *residence time* studies that used D_2O label injection directly into trees. See later Discussion.
[2] Except for a recent study using tritium (Zhang *et al.,* in review, *Hydrological Processes*).

few studies in the plant ecophysiology literature (e.g. James *et al*. 2003) where within-tree D_2O labelling has been done to estimate tracer velocity and ages. James *et al*. (2003) have reported tree water ages for two tropical species in Panama that ranged between 2 days (*Cordia alliodora*) and 22 days (*Anacardium excelsum*). A similar range was reported by Meinzer *et al*. (2006) for two coniferous (Douglas fir and western hemlock) species in southwestern WA, USA, while Gaines *et al*. (2016) reported a range between 5 and 22 days for four tree species in PA, USA. While these data suggest marked variability, no work has yet explored plant water age, soil water age and streamflow experimentally. Such work is key not only for understanding mixing and source apportionment in the critical zone, but also for testing the time based (if any) aspects of *ecohydrological separation.*

TTDs and MTTs, however, are not measured *per se* but rather inferred from conservative geochemical tracers (e.g. Cl^-, ^{18}O, ^{2}H) in inputs and outputs. The inferential nature of TTD modeling implies, with all its simplifying assumptions (see Kirchner 2016), that the shape of a TTD can be assumed—although recent work has called for catchment scale labelling experiments to define experimentally the TTD (McDonnell and Beven, 2014; Klaus *et al*., 2015).

While experimental and modeling work in rainfall-runoff TTD are now common practice (McGuire and McDonnell, 2015), rarely, if ever, has the "TTD tracer toolbox" contained rainfall-transpiration tracer parameterization. Similarly, when water transport studies included isotope labeling in vegetation (e.g. James *et al*., 2003; Meinzer *et al*., 2006; Gaines *et al*., 2016), they lacked the typically high-resolution sampling in rainfall-runoff experiments (McGuire and McDonnell, 2006), let alone comparison to whole-catchment travel times with explicit labeling and tracking of root water uptake sources (Soulsby *et al*., 2015).

Beyond time, the space aspect of ecohydrological separation entails quantifying the source proportions of the isotopic signal that is integrated in the xylem (i.e. plant stem) water. Approaches in plant source water identification using water stable isotopes generally fall under two main categories: process based mixing (PBM) models and simple linear mixing (SLM) models (Ogle *et al*., 2014). PBM models (e.g. RAPID by Ogle et al., 2004; Ogle et al., 2014) integrate stable isotope data and a biophysical model into a Bayesian framework. Where two or three water sources are identified, traditional SLM models may prove sufficient for explicit

representation of sources via simple mass balance (e.g. Thorburn and Walker, 1994; Brunel *et al*., 1995).

In the simplest case where xylem water may represent an integrated signal of two sources, the proportional contribution of each source may be resolved using a single isotope in a two-source system of mass balance equation (Dawson 1993; Phillips and Ehleringer, 1995):

$$\delta_{xyl} = f_A\delta_A + f_B\delta_B \quad (5.1)$$

where δ_{xyl} is plant xylem water (either δ^2H or δ^{18}O), and the proportions (f_A, f_B) of sources (summing to 1) with isotopic signatures (δ_A, δ_B), respectively.

In many if not most cases, however, the number of possible sources far exceeds the number of isotopes in the system, that is:

$$\delta_{xyl} = f_A\delta_A + f_B\delta_B + f_C\delta_C + \cdots f_n\delta_n \quad (5.2)$$

In such an underdetermined system, where the number of sources is greater than the number of isotopes plus one, the most widely used approach to date is a simple linear, Visual Basic-based program and iterative algorithm called IsoSource (Phillips and Gregg, 2003). Notwithstanding the widespread use of IsoSource in systems with multiples sources, the method can only provide a range of feasible (not likely) solutions. The lack of a robust statistical foundation of an iterative approach, therefore, boosts the case for an alternative method that frames the mixing model atop a solid statistical (i.e. Bayesian) formulation. In this study, we quantify the source water proportions in xylem ("mixture") water by using an algorithm implemented in a Bayesian framework (Parnell *et al*., 2010).

So how can we evaluate and quantify these time- and space-based components of ecohydrological separation when boundary conditions in natural catchments are unknown and largely unknowable? In general, experiments that allow for high degree of control over environmental variables at useful space and time scales are needed. What is needed going forward to characterize sources, flowpaths and exit time distributions is some combination of the degree of control typical in growth chamber scale experiments with something like a field-based experiment where the representative elementary volume of the critical zone domain is large enough to contain a sufficient range of heterogeneity and thereby satisfy scale requirements. But

such scales then come at a cost of not being able to control experimental variables. Here we take advantage of the 27 m tall, 1936 m^2 mesocosm Biosphere 2-Tropical Rainforest (B2-TRF) biome that represents a total volume of 35000 m^3. The B2-TRF has soils that vary from 1-3 m with 23 dominant tree species where much basic ecosystem work has already been done (Scott 1999; Leigh *et al*., 1999; Rascher *et al*. 2004; Rosolem *et al*., 2010). As such the B2-TRF biome represents the ideal scale at which to address fundamental aspects of water sources, flowpaths, and transit times through the critical zone, enabling controlled experiments to be designed and implemented at the biome scale, but with complete boundary controls. Here we present new results from a 10-week drought experiment where we induce water stress on 4 tree species (n = 8) and then add 66 mm of labelled rainfall with 152 ‰ deuterated water distributed over four events. We follow the label with a total of 87 mm of rainfall (-60‰) distributed over 13 events, spaced every 2-3 days. Over the course of this 9-month experiment we test the null hypothesis that the ecohydrological system is tightly connected in that water forming groundwater recharge and plant transpiration is sourced from a common pool. Alternatively, if labelled water taken up via roots is the same as the water that contributes to groundwater recharge (and eventual routing to streams), then their "ages" (i.e. mean transit times) and by extension sources in the subsurface, should be the same. Our specific questions include:

a. What is the nature of source water apportionment in time and space by B2-TRF trees and how is it affected by drought and rewetting?

b. What are the relative transit times of plant water and deep percolation water?

c. What soil- and plant-level factors control the sources, flowpaths and age distribution of water in the critical zone?

5.3 Materials and Methods

5.3.1 Biosphere 2 Tropical Rainforest

Biosphere 2 (B2) is a large-scale Earth science facility near Tucson (Arizona, USA). It consists of five biomes, including the tropical rainforest (B2-TRF) biome where we conducted this study. Constructed between 1990 and 1991, the B2-TRF is a 1936 m^2 mesocosm with a total volume of

35000 m^3. The distance between the lowest soil level and the highest point in the enclosed, pyramidal glass structure is ~27 m. Rainfall, humidity, and temperature inside the B2-TRF are controlled to reflect climatic conditions that are comparable to natural rainforests (Leigh et al., 1999).

Artificial rainfall, applied every 3-4 days, is delivered via and distributed equally over four sections of overhead sprinklers. During normal conditions (i.e. without an ongoing experiment), the B2-TRF receives an annual rainfall of ~1300 mm (3.6 mm d^{-1}) with relatively constant δ^2H and $\delta^{18}O$ values (mean ±1SD) of -60.2 ±4.2 and -8.3 ±0.75 ‰, respectively. Rainfall amounts are monitored through in line flow meters before the water enters the rainforest. Operating in "flow through mode" where drier air is vented through the system and humidity fixed between 70-85%, an inversion layer exists above the mean canopy level resulting in two distinct daytime humidity regimes. Turbulence is negligible suggesting that most mass and energy transfer are driven largely by mass transfer (Arain *et al.*, 2000). Rainfall events take place usually during nighttime so that isotopic enrichment of throughfall and interception via evaporation water are minimal.

The plant community consists of a mix of trees, vines and herbs designed to mimic a tropical rainforest (Leigh *et al*. 1999). The plants were derived from multiple locations closely representing a pan-tropical distribution. The largest trees currently reach to ~25 m in height and ~50 cm in diameter. This study focuses on soil water, deep percolation and five tree species (described in detail below), and their partitioning of water sources and its drivers during and after a controlled drought. We derived the total, ecosystem-level transpiration amount from meteorological conditions, particularly vapor density (g m^{-3}), and by systematically accounting for airflow injection and water loss to the flow through system. This study places emphasis on the use of water stable isotopes as well as soil moisture and water potential measurements. For a detailed study with emphasis on atmospheric forcing and vegetation response at the B2-TRF, the interested reader is directed to Rosolem *et al.*, (2010).

5.3.2 Environmental monitoring and sampling

There are three soil pits at the B2-TRF, with depths varying between 1 and 3 m. The four walls of each soil pit are fixed by an acrylic glass (Plexiglas). Holes were made into the Plexiglas walls

to accommodate instrumentation and sampling. Volumetric water content (VWC) was determined by measuring the dielectric constant of the soil using capacitance/frequency domain technology (5TM Decagon Devices WA, USA), and was calibrated with the gravimetric method. Soil water potential was measured at the same depths (15, 25, 55, 65, 100, 130, 150 cm) with recording tensiometers (T4e UMS GmbH Germany). T4e measurement range is between +100 and -85 kPa with an accuracy ±0.5 kPa.

We collected rainfall (throughfall) samples during one, seven, and six events in February, June, and July 2014, respectively, before the drought. Seepage samples (representing "zero tension" groundwater recharge) from collector pipes that drain the overlying mesocosm were also collected during the same times as for rainfall sampling and at higher frequency during post-drought (rewetting). We sampled for soil water isotopes weekly by collecting bulk soil samples (three replicates each) at 15, 25, 35, 55, 100, 130, 250 cm. Although each soil pit was covered by a 1.5-cm thick metal sheet when no sampling was performed, care was taken during each sampling by scraping ~3cm of soil off the face of the wall at respective depths. This was done to ensure that we were not sampling for evaporatively enriched soil water at the soil face.

Weekly stem ("xylem") water samples were taken from the part of stems with mature bark closest to the main branch (following Dawson, 1993) to minimize the effect of evaporative enrichment by water loss through unsuberized stems. Stem samples were collected (three replicates each) using clipping just below canopy height via bosun's chair from five canopy species: *Ceiba pentandra* (N=2, DBH=36 and 53 cm), *Clitoria racemosa* (N=4, DBH=29±3 cm), *Hura crepitans* (N=1, DBH=45 cm), *Hibiscus elatus* (N=1, DBH=28 cm), and *Pterocarpus indicus* (N=1, DBH=24 cm).

Water from bulk soil and stem samples were extracted using cryogenic vacuum distillation method. Isotope analysis of all stem water samples were performed using isotope ratio mass spectrometry at the University of Victoria (Alberta Innovates - Technology Futures) due to possible spectral contamination of plant water. Isotope analysis of bulk soil, rainfall, and seepage water samples were performed using isotope ratio infrared spectroscopy (LGR OA-ICOS CA, USA) at McDonnell Watershed Hydrology Lab. Laboratory precision at both University of Victoria and McDonnell Lab was ±1‰ and ±0.2‰ δ^2H and $\delta^{18}O$, respectively.

5.3.3 Soil and tree measurements

We described the rooting profile by averaging the maximum rooting depth visible from the four walls of each soil pit. Consistent with an earlier survey of the B2-TRF (Rosolem *et al*., 2010), we found no roots below 65 cm, with the highest fraction found at the top 15-20 cm of the soil profile (Figure 5.2). For our purposes in this paper, we set 60 cm as the maximum rooting depth. We then compared the isotopic composition ($\delta^{18}O$) of bulk soil water at respective sampling depths within each moisture period (drought and post drought). Finding no statistical difference in $\delta^{18}O$ of bulk soil across depths within a moisture period ($P>0.05$ Tukey's HSD), we discretized the soil profile into three depth groups 10-20, 20-40, and 50-60 cm by averaging the isotopic composition of bulk soil water from 15, 25-35, and 55 cm, respectively (Figure 5.2). Mean and range of bulk soil $\delta^{18}O$ and VWC, as well as soil textural composition at respective depths are also shown in Figure 5.2.

To be able to calculate the driving force for water transport, we measured predawn and midday leaf water potential (MPa) of *C. racemosa* and *H. elatus* by cutting three 20-cm long branches and using a pressure chamber (PMS, Albany, Oregon). These measurements were made on 29 Jul, 05 Aug, 11 Aug, and 09 Sep. Leaf water potential of *H. crepitans* was also measured on 29 July. Midday driving force (where transpiration is most active) for water transport was calculated by taking the difference between corresponding soil water potential and midday leaf water potential.

5.3.4 Drought and rewetting experiment

To be able to assess the possible changes in source water apportionment in the dominant canopy species, we performed a drought experiment by closing all the water valves going into the rainforest. The drought lasted for 68 days between 23 July and 29 September 2014. During rewetting that began 30 September 2014, we introduced a 99.5% deuterium oxide (D_2O) label (Cambridge Isotopes, Cambridge, MA, USA) into the sprinkler ("rainfall") system. A total of 66 mm of labelled rainfall with 152‰ δ^2H was distributed over four events (mean 16.5 mm per event) including the 30 Sep rain: 01 Oct, 05 Oct, 07 Oct. This was followed by a total of 87 mm of rainfall (-60‰ δ^2H) distributed over 13 events that were spaced every 2-3 days.

5.3.5 Isotope mass balance calculation

Major components of the water balance at the B2-TRF include rainfall (P), soil water (S), subsoil drainage or "seepage" (L), interception (I), soil evaporation (ε), and root water uptake (T). We know the mass and isotopic composition associated with each component of the water balance except for I. The isotope mass balance was formulated as:

$$m_{\mathrm{P}} + m_{\mathrm{i}} = m_{\mathrm{L}} + m_{\mathrm{I}} + m_{\mathrm{f}} + m_{\varepsilon} + m_{\mathrm{T}} \quad (5.3)$$

and

$$\delta_{\mathrm{P}} x_{\mathrm{P}} + \delta_{\mathrm{i}} x_{\mathrm{i}} = \delta_{\mathrm{L}} x_{\mathrm{L}} + \delta_{\mathrm{I}} x_{\mathrm{I}} + \delta_{\mathrm{f}} x_{\mathrm{f}} + \delta_{\varepsilon} x_{\varepsilon} + \delta_{\mathrm{T}} x_{\mathrm{T}} \quad (5.4)$$

where m_{x} is mass, δ_{x} is the isotopic composition and the subscript *x* represents the fraction of corresponding component in the water balance. Soil water mass is represented by subscripts *i* and *f* to indicate the initial soil water mass *i* prior to rainfall and the final soil water mass *f*. δ_{i} and δ_{f} were calculated using the weighted isotopic composition at each soil layer (following Sutanto *et al*., 2012):

$$\delta_i = \delta_f = \frac{\sum_{j=1}^{n} (\delta_{sj} \cdot z_j \cdot \theta_j)}{\bar{\theta} \cdot z_{total}} \quad (5.5)$$

where *n* is the number of soil layer, δ_{sj} is the isotopic composition at corresponding layer *j*, z_{j} is the corresponding depth at layer *j*, θ_{j} is the soil water content at layer *j*, $\bar{\theta}$ is the average soil water content, and z_{total} is total depth. For purposes of closing the water balance, we considered three depths: 25, 65 and 150 cm.

The unknown variable in the water balance x_{I} was calculated as derived from Equation (5.6):

$$x_{\mathrm{I}} = \frac{\delta_{\mathrm{P}} x_{\mathrm{P}} - \delta_{\mathrm{L}} x_{\mathrm{L}} - \delta_{\mathrm{f}} x_{\mathrm{f}} - \delta_{\varepsilon} x_{\varepsilon} - \delta_{\mathrm{T}} x_{\mathrm{T}} + \delta_{\mathrm{i}} x_{\mathrm{i}}}{\delta_{\mathrm{I}}} \quad (5.6)$$

δ_{ε} was calculated following Craig and Gordon (1965) with parameters derived from a pan evaporation experiment that we conducted inside the B2-TRF. The isotope mass balance was solved during the four weeks (25 Jun-23 Jul 2014) that we have data prior to drought onset.

5.3.6 Modeling

5.3.6.1 Root water uptake and Bayesian inference

We determined the source water proportions in xylem ("mixture") water by using a simple linear mixing model implemented in a Bayesian framework. We employed the SIAR (stable-isotope analysis in R) Bayesian mixing model statistical package (Parnell *et al*., 2010) to determine the most likely proportion of xylem water from various depths in the soil profile using Markov Chain Monte Carlo (MCMC) methods. We discretized the soil profile following the three soil depth groups ("sources") as shown in Figure 5.2. We identified a fourth source in the model called "mobile" water. During the drought, the value of mobile water was set as the seepage water prior to the onset of drought (-60.2 ±4.2‰ δ^2H, -8.3 ±0.8‰ δ^{18}O). Seven sampling time points, spanning the entire 68 days (~10 weeks) of drought, were included in the model run: 29 Jul, 05 Aug, 11 Aug, 09 Sep, 16 Sep, 23 Sep, and 29 Sep.

During rewetting, the values of mobile water were the corresponding seepage water values in the following eight sampling time points, spanning 70 days (10 weeks) post-drought: 30 Sep, 02 Oct, 07 Oct, 14 Oct, 21 Oct, 28 Oct, 04 Nov, and 09 Dec. The model was run with 500 000 iterations (discarding the first 50 000) and a source water's most likely contribution (i.e. the mean of the posterior distribution of the MCMC simulation) to xylem water was obtained. The SIAR method was an appropriate treatment of our data because the proximity between our bulk soil water values across the soil profile was relatively small. Evaristo *et al.*, (in review) showed that a Bayesian approach constrains the uncertainty estimates better than a simple mass balance approach (e.g. Brunel *et al.*, 1995) when maximizing the difference between sources is not possible. The validity of our approach in combining the bulk soil water values from two or more sources also leads to more constrained and less diffuse solutions (Phillips *et al.*, 2014) than if we assigned sources with statistically insignificant differences.

5.3.6.2 Transit time distribution

The differences in time scales of transport dynamics towards each outflux could be revealed by examining transit time distributions (TTDs). We used the observed breakthrough curves (BTCs) associated with the fluxes to estimate the TTDs. In this study, we estimated MTT by assuming

that the TTD $h(\tau)$ follows the widely-used two-parameter gamma distribution (Kirchner *et al.*, 2000, 2010):

$$h(\tau) = \frac{\tau^{\alpha-1}}{\beta^{\alpha}\Gamma(\alpha)} e^{-\tau/\beta} = \frac{\tau^{\alpha-1}}{(\bar{\tau}/\alpha)^{\alpha}\Gamma(\alpha)} e^{-\alpha\tau/\bar{\tau}} \quad (5.7)$$

where α and β are the shape and scale parameters, respectively; τ is the transit time, and $\bar{\tau} = \alpha\beta$ is the mean transit time.

We applied time-invariant TTD modeling to characterize the transit times of outfluxes. This approach was done to estimate "rough" transit times associated with each outflux and their relative differences. A key assumption in this approach is that flow pathways – towards seepage, soil water recharge, or transpiration – do not vary in time, and therefore the partitioning of the labelled water particles into each outflux are not a function of time. Time-invariant TTDs were estimated by fitting a specific form of TTDs to model the observed BTCs by convolving the distributions with the injection concentration time-series (Maloszewski and Zuber, 1982). The widely-used two-parameter gamma distribution (Kirchner *et al.*, 2000, 2010) was chosen arbitrarily, and scaling parameter was also applied to consider the mass-recovery issue which is inevitable in practice, especially, in this type of a complex system. We note that a problem in closing the tracer mass balance is inherent in the time-invariant TTD modeling; thus, the scaling parameter is not guaranteed to be consistent with the physical mass recovery ratios. Parameters (three for each BTC – shape, scale, and scaling) were estimated in a Bayesian way to consider its uncertainty using the DREAM (DiffeRential Evolution Adaptive Metropolis; Vrugt *et al.*, 2009) algorithm.

5.4 Results

5.4.1 Environmental conditions

Pre-drought meteorological conditions, particularly temperature and vapor pressure deficit (VPD), at 13 m above the forest floor were (mean ±1SD) 29 ±7°C and 1.2 ±0.2 kPa, respectively. At 1 m above the forest floor temperature was 25 ±2°C and VPD was 0.3 ±0.1 kPa. During the drought, temperature at both levels and VPD at 13m were similar to pre-drought conditions, except for VPD at 1 m above the forest floor which was 0.4 ±0.2 kPa. Post-drought

temperature was 24 ±3°C and 26 ±5°C at 1 m and 13 m, respectively. VPD was similar to pre-drought levels over the course of the record (Figure 5.1 top panel).

Total ecosystem transpiration pre-drought ranged between 900 and ~2700 kg d^{-1} (1733 ±389 kg d^{-1}). During the drought, ecosystem-level transpiration decreased to between 100 and ~1500 kg d^{-1} (877 ±319 kg d^{-1}). Transpiration amount recovered slightly during the first two weeks following rewetting (similar to early and mid-drought levels) but maintained at subdued levels (635 ±296 kg d^{-1}) over the course of the record (Figure 5.1 middle panel).

Soil volumetric water content (VWC) at 25 cm pre-drought ranged between 0.26 and 0.31 cm^3 cm^{-3} (0.28 ±0.01 cm^3 cm^{-3}) (Figure 5.1 bottom panel). During the drought, VWC at 25 cm decreased to between 0.20 and 0.26 cm^3 cm^{-3} (0.22 ±0.02 cm^3 cm^{-3}). VWC at 25 cm began to recover to pre-drought levels ~8 days following rewetting. It fully recovered (i.e. stabilized) to pre-drought levels at ~14 days. Water content at 65 cm pre-drought ranged between 0.15 and 0.16 cm^3 cm^{-3}. During the drought, this decreased to between 0.11 and 0.15 cm^3 cm^{-3} (0.13 ±0.01 cm^3 cm^{-3}). Like water content at 25 cm, VWC at 65 cm began to recover to pre-drought levels ~8 days following rewetting and stabilized at ~14 days. Soil water potential (SWP) pre-drought ranged between -3 and -2 kPa (~20-30 cm H_2O). During the drought, this decreased to between -77 and -3 kPa (~30-785 cm H_2O). SWP recovered to pre-drought levels ~ 14 days following rewetting.

5.4.2 Source water apportionment by trees

Results from Bayesian inference modeling showed that the fraction of mobile water in xylem (represented by “zero tension” seepage water pre-drought) increased steadily through the drought from 0.33 ±0.09 on 29 Jul to 0.69 ±0.12 on 16 Sep. Thereafter, the mobile water fraction in xylem decreased to 0.52 ±0.16 on 23 Sep and 0.30 ±0.09 immediately prior to rewetting on 29 Sep (Figure 5.3a). Over the course of the drought, the fraction of mobile water in xylem for all four tree species was not statistically different from each other ($P>0.05$, Tukey-Kramer HSD), ranging from 0.21 to 0.78.

The fraction of mobile water in xylem (represented by “zero tension” seepage water during rewetting) also increased somewhat steadily through the rewetting from 0.08 ±0.01 on 30 Sep to

0.37 ±0.05 on 09 Dec. These values, however, were smaller and statistically different ($P<0.01$, Tukey-Kramer HSD) from the drought. Like during the drought, inter-specific differences in mobile water fraction in xylem were not statistically different ($P>0.90$, Tukey-Kramer HSD), ranging from 0.08 to 0.42.

These trends in the fraction of mobile water in xylem during the 68-day drought and 70-day rewetting (as illustrated in Figure 5.3) were effectively the inverse of the trends in soil water contribution to xylem. That is, there was a steadily decreasing contribution from all three depth sources in the bulk soil during the drought, and a steadily increasing contribution from all bulk soil sources during rewetting. The relative contributions of bulk soil sources during the drought were not statistically different from each other, suggesting that all three sources contributed equally likely to xylem. Nevertheless, immediately after rewetting (30 Sep), almost 90% (±2%) of water in xylem came from the top 40 cm of the soil profile before decreasing to 70% (±16%) and 60% (±20%) seven and 14 days after the first rainfall, respectively.

We note that one of the five tree species, *Pterocarpus indicus*, was not included in the Bayesian source water apportionment model. *P. indicus*, showed persistent use of "stream water", a small body of open water at B2-TRF that meanders around the mound where *P. indicus* is planted.

5.4.3 Soil water retention and driving force

The soil water retention curve (10 Jul-25 Sep) is shown in Figure 5.4 through the dry down. An empirical model fit after Brooks and Corey (1964) best explained the data ($R^2=0.98$, AIC=-198.4). The last two data points that slightly deviated from the model on the matric suction axis reflected the tensiometer detection limit as the T4e instrument approached its maximum range (~85 kPa). Nevertheless, Figure 5.4 shows a water retention curve that is characteristic of a loamy substrate.

Following the insights from the Bayesian mixing model suggesting that root water uptake took place mostly from the top 40 cm of the soil profile, we found a nonlinear relationship between the fraction of mobile water in xylem of each tree species and VWC. Figure 5.5 shows that the fraction of mobile water in xylem increased as soil water content decreased. A three-parameter exponential model best described the data. The model's asymptote 0.22 [0.17, 0.27 95% C.I.]

reflected the threshold whereby each source in the four-source Bayesian mixing model was equally likely. Stated differently, because such threshold reflects bulk soil water contribution, only the values above the confidence limits of this threshold may be considered as sourced from mobile water with much greater likelihood than bulk soil water. This can be extended by juxtaposing Figure 5.5 over the Bayesian isotope mixing model results in Figure 5.3. For example, *C. racemosa* in Figure 5.5 has four data points above the threshold 0.21 [0.10, 0.34 95%C.I.]. The region to which these observations are located coincides with the four weeks in Figure 5.3 (i.e. columns 3-6) when mobile water contribution to *C. racemosa* was significantly greater than bulk soil water.

Figure 5.6 shows the calculated difference between soil water potential and midday leaf water potential (i.e. driving force) at four corresponding times during the drought. There was a nonlinear, exponential relationship (R^2=0.86) between the fraction of mobile water in xylem and driving force (MPa). Conversely to the case in Figure 5.5, the fraction of mobile water in xylem increased as driving force increased. Nevertheless, a threshold-like trend similar to Figure 4.5 is also apparent in Figure 5.6 represented by a three-parameter exponential. The best-fit model's asymptote was 0.22 [0.06, 0.38 95% C.I.], representing the threshold below which bulk soil water dominated over mobile water. The corresponding measurements above this threshold corresponded to 60% (±15%) contribution from mobile water for *C. racemosa* and 70% (±15%) for *H. elatus*. As the drought proceeded and soil water potential decreased from -2.9 kPa (-0.003 MPa, 30 cm H_2O) to -7.4 kPa (-0.007 MPa, 75 cm H_2O), leaf water potential also decreased correspondingly (albeit in a species-specific manner). For example, when soil water potential was -2.9 kPa, leaf water potential was -527 kPa (-0.53 MPa, 5371 cm H_2O) for *C. racemosa*, while it was -320 kPa (-0.32 MPa, 3263 cm H_2O) for *H. elatus*. At the lowest point in soil water potential value of -7.4 kPa, leaf water potential was -1170 kPa (-1.17 MPa, 11931 cm H_2O) for *C. racemosa*, while it was -743 kPa (-0.74 MPa, 7580 cm H_2O) for *H. elatus*.

5.4.4 Transit time, flow velocity and mass balance

The time-scale differences among the waters that traveled through the different flow pathways (and indeed ended up in different outfluxes) were significant (Figure 5.7). In terms of mean transit time, the mean for the seepage flow was the lowest and was around 230 h (~9.6 days).

The mean transit times for *C. racemosa* and *H. elatus* were quite similar to each other, 610 h (~25 days) and 650 h (~27 days), respectively. *H. crepitans* transpired much older water than all the others, with a transpiration flux mean transit time of around 1700 h (~71 days). Values of TTD shape parameter α for seepage, *H. elatus*, *C. racemosa*, and *H. crepitans* were 0.30, 0.80, 1.0, and 2.3, respectively. We note that we excluded *C. pentandra* in TTD modeling because we did not detect any uptake of the tracer in the tree; that is, xylem δ^2H remained relatively unchanged before, during, and after the drought at -56 (±4.5) ‰. *P. indicus* was excluded in TTD modeling for the same reason that it was excluded in Bayesian source water apportionment model, that is, persistent use of "stream water" at all stages of the experiment.

Figure 5.8 shows a plot where calculated tracer velocity (done by dividing tree height with mean TT) is plotted against midday driving force. Results for three tree species in this study and four tree species in Gaines *et al*. (2016) are presented in the same plot for comparison. It can be shown that *H. crepitans* had the lowest tracer velocity and midday driving force, while *C. racemosa* had the highest midday driving force although its tracer velocity is comparable to *H. elatus*.

When soil water storage was in presumed steady state prior to onset of drought, results from our isotope mass balance calculations showed the following: initial soil water mass (51%) and total rainfall input mass (49%). Losses are partitioned into seepage (6%), interception (27%), soil water (51%), soil water evaporation (~4%), and transpiration (13%).

5.5 Discussion

Much of our analysis has relied on water stable isotopes and the assumption that they are useful tools in tracing and partitioning various components of the water cycle, as others have done (e.g. Ehleringer and Dawson, 1992; Gibson and Edwards, 2002; Jasechko *et al*., 2013; Coenders-Gerrits *et al.*, 2014; Jameel *et al*., 2016). And, because of their conservative nature, they are affected mainly by physical processes that are relatively well understood (Friedman 1953; Dansgaard 1964). The general assumption that root water uptake, in most environments, is a non-fractionating process has been shown to be valid in both laboratory (Wershaw *et al.*, 1966; Thorburn *et al.*, 1993) and field (White *et al*., 1985) settings. Exceptions to this rule, however,

have been reported in certain environments (Lin and Sternberg, 1992; Ellsworth and Williams, 2007; Evaristo *et al*., in review). Notwithstanding the long history in the use of water stable isotopes in root water uptake studies, dating back to the seminal work of Dawson and Ehleringer (1991), its *descriptive power* in hydrological models is still in its infancy. At the B2-TRF, transpiration accounts for 13% of the water balance (1.4 mm d^{-1}). Owing to small evaporative demand under the dense canopy of B2-TRF (4% or 0.4 mm d^{-1}), T/ET is estimated at 79%. This value is well within the 70 ±14% range of estimates in tropical rainforests (Schlesinger and Jasechko, 2014; Good *et al.*, 2015). Although the uncertainties associated with our isotope mass balance estimates are likely to be non-trivial, we note that the magnitude and relative proportions of each component are within expectations. For example, despite our lack of actual measurement for interception, our approach showed that interception accounts for 27% (2.9 mm d^{-1}) of the water balance. This is well within the 2-5 mm d^{-1} range as estimated by the analytical model of De Groen (2002), and comparable to 3.3 mm d^{-1} estimated by Schellekens *et al*. (2000) for a mature Tabonuco forest in northeast Puerto Rico.

5.5.1 How does our study differ from earlier D_2O labeling experiments?

The transit time of water in our monitored trees was 24-71 days. Others have indeed explored the time it takes for xylem water to ascend the tree stem using deuterated water. James *et al.* (2003) reported tree water ages in this way for two tropical species in Panama that ranged between 2 days (*Cordia alliodora*) and 22 days (*Anacardium excelsum*). A similar range was reported by Meinzer *et al*. (2006) for two coniferous (Douglas fir and western hemlock) species in southwestern WA, USA, while Gaines *et al*. (2016) reported a range between 5 and 22 days for four tree species in PA, USA. While transit times for two of our tree species here (*C. racemosa* and *H. elatus*) are comparable to these earlier studies, we know of no earlier labeling study that have reported transit times as long as 71 days (*H. crepitans*).

Moreover, the method that we used to estimate tree water transit time is different to most tree-based injection work. Heretofore, tree water transit time was estimated based on the time it takes for the label to reach 10% of maximum tracer concentration in the leaves (from the point of tracer injection either at the base of the tree or in the trunk) and return to within 5% of baseline deuterium concentration (e.g. Gaines *et al*., 2016). None of these earlier studies included D_2O

labelling in rainfall and tracer breakthrough in soils or in streams. To the best of our knowledge, our study is:

1. the first to use D_2O label and follow its evolution (i.e. breakthrough) in seepage (groundwater recharge), soils (soil water recharge), and trees (RWU)
2. the first to sample stem water for isotopes at such high frequency
3. the first to apply the time-invariant TTD modeling in stem water isotopes, let alone over an extended period of over six months

We suggest that our rainfall labeling approach represents the plant water uptake system better than tree-based injection methods because it can "follow the water" from input as rainfall through to water uptake via roots. Equally noteworthy was our use of Bayesian inference methods in quantifying the sources of water used by trees during and after a prolonged drought. This means that we not only identified tracer breakthrough in the tree, we also quantified root water uptake sources in the subsurface, as we now describe below.

5.5.2 Ecohydrological determinism in the critical zone?

By applying a root water uptake (RWU) source apportionment model implemented in a Bayesian framework and by estimating "water ages" based on transit time distribution (TTD) modeling, we were able to provide the first unequivocal evidence of ecohydrological separation in space and in time, respectively. The main advantage of the Bayesian inference approach used here is that unlike previous work that has had to rely on the "offset" of a water sample from the local meteoric water line (e.g. Evaristo *et al.*, 2015), or in earlier mixing model capabilities providing only "point estimates" (e.g. Brunel *et al.*, 1995), here we have a labeled source whose uncertainties as it is partitioned into various reservoirs prior to root water uptake are fully accounted for. The main advantage of the TTD modeling used here over tree-based injection work is that we have a full catchment description of transit times not only in trees but also in soils and seepage (proxy for groundwater recharge).

The Bayesian model of RWU sources showed that the fraction of mobile water in the stem is a nonlinear function of soil-to-leaf driving force (Fig. 6). The driving force, in turn, is a composite

function of soil texture and species-specific patterns. Such species-level control over soil-to-leaf driving force translates to tree water transit times. For example, when soil matric potential was -0.007 MPa (75 cm H_2O), leaf water potential for *C. racemosa* was -1.17 MPa (11931 cm H_2O), and therefore greater driving force (1.16 MPa) and shorter mean transit time. In contrast, leaf water potential was -0.74 MPa (7580 cm H_2O) for *H. elatus*, and therefore relatively smaller driving force (0.74 MPa) and longer transit time. Our leaf water potential data during the drought and TTD model results post-drought suggest species-specific patterns that span both extremes in moisture periods. Our leaf water potential trends are also consistent with drought and post-drought data for the same tree species in an earlier study at B2-TRF (Rascher *et al*., 2004). Nonetheless, one overarching question remains: *why did trees use mobile water when soils became drier, and why did the same trees not use mobile water when soils became wetter?*

Evaristo *et al.* (2015) proposed a conceptual mixing model (following Hrachowitz *et al.*, 2013) informed only by the degree of separation between "more mobile" and "less mobile" waters – the line-conditioned excess (LCE) of Landwehr and Coplen (2006). The LCE parameter is not applicable in the B2-TRF because of (1) a rainfall isotopic composition that stays relatively constant all year round; and, (2) very limited evaporative demand (0.4 mm d^{-1}). Both factors lead to little natural variation of isotopic composition thereby making the dual isotope approach, upon which the LCE parameter is derived, not applicable (Brunel *et al.*, 1995). The B2-TRF system, therefore, is an ideal setup for a mechanistic assessment of ecohydrological separation. This is because RWU sources can be identified mainly on the basis of a xylem water's "proximity" to its possible sources, without the potential complications in interpretation due to isotopic enrichment effects of soil water evaporation.

During rewetting, the dimensionless mixing coefficient $C_{M,i}$(equation 28 in Hrachowitz *et al.*, 2013) that is informed only by changes in soil moisture, may explain our results in conceptual terms. That is, as the soil is wets-up, the resultant decrease in soil matrix suction leads to increasingly smaller proportions of tracer infiltrating the soil matrix, and thus increasingly greater proportions of the D_2O label (new water) being routed to preferential flow pathways. The high flow velocities in preferential flow pathways results in earlier breakthroughs in seepage and therefore shorter mean transit times (~10 days) than soil matrix water that is taken up by roots

(25-71 days). Indeed, our soil matric potential measurements fully recovered to pre-drought levels (~20-30 cm H_2O) ~14 days after the first post-drought rainfall.

During drought, we hypothesize a converse mechanism whereby during dry-down due to root water uptake, the resultant and increasingly negative matric potential gradients in the rhizosphere would have directed the mobile water from pockets of larger pore spaces into refilling the site(s) of root water uptake in the soil matrix (Carminati *et al.*, 2010). Following the Hrachowitz *et al*. (2013) model, such a drying condition would result in a higher dynamic mixing coefficient between the "refilling" mobile water that contributes to root water uptake and resident matrix water. Such matrix water in the early ecohydrological separation work was referred to as "tightly bound water" (Brooks *et al*., 2010). These findings support the idea that antecedent soil moisture conditions and species-level response *determine* the partitioning between a "more mobile" and a "less mobile" water source for both vegetation and groundwater recharge.

5.5.3 On the physical meaning of 'tightly bound water'

The first paper on ecohydrological separation by Brooks *et al*. (2010) first introduced the phrase "tightly bound water" to describe the soil matrix water that is used by trees. Our study enabled us to clarify some of the implications of the so-called "tightly bound water" by providing evidence based on our soil and leaf water potential data, and Bayesian model of root water uptake sources. The positive nonlinear relationship between fraction of mobile water in xylem and soil-to-leaf driving force (Fig. 6) demonstrates that soil matric potential is only one piece of this puzzle. For example, at matric potential -2.9 kPa (~30 cm H_2O) mobile water in xylem was 25% in both *C. racemosa* and *H. elatus*. As drought progressed and at a more negative matric potential of -7.5 kPa (~76 cm H_2O), mobile water in xylem was 67% and 27% in *C. racemosa* and *H. elatus*, respectively. This suggests that access to mobile water, during soil dry-down depended on the extent with which a species compensated for a decrease in soil matrix potential (i.e. the soil-to-leaf driving force). Following Darcy's law, sap flow Q is related to transport driving force ΔP by hydraulic conductance K; that is, $Q = K \cdot \Delta P$ (Smith and Sperry, 2014). At a given Q, K is reduced as ΔP increases. Although we lack Q measurements, the decrease in leaf water potential for a given soil matric potential (increased ΔP) during drought could, in theory, lead to reduced K and greater risks for embolism (Wheeler *et al.*, 2013; Smith and Sperry, 2014). This is not a

surprise but rather simply demonstrates that *C. racemosa* was more “water stressed" than *H. elatus*. What is surprising and novel is the suggestion that such an increase in ΔP and reduction in K is associated with greater fraction of mobile water in xylem. These results suggest (and this is what we emphasize in this section) that there is no tightly bound water *sensu* root water uptake. While cryogenic vacuum distillation method for soil water extraction represents suction pressures as high as $3x10^{-8}$ MPa (Orlowski *et al*., 2015), this should not be interpreted as the region of suction pressures that drive water ascent in trees. “Tightly bound water” in the sense of Brooks *et al*. (2010), therefore, was a misnomer that we hope has been clarified by these results.

5.5.4 On the isotopic similarity between soil mobile water and groundwater

In natural field settings, an increase in the fraction of mobile water in xylem would be associated with, or interpreted as, preferential uptake of saturated zone water (or groundwater) as soil water potential decreases, for example, during drought (Barbeta *et al.*, 2015). Our results (Fig. 5) are consistent with the latter except that this mobile water source is not synonymous to a groundwater source in natural field settings. Firstly, there is no “groundwater”, no fully saturated zone at the B2-TRF. Soil texture at the B2-TRF could not support a capillary rise greater than ~16 cm (Fig. 4) Secondly, maximum rooting depth at the B2-TRF is ~60 cm while soil depth ranges between 1 and 3 m. If the B2-TRF had a fully saturated zone, then our results would have supported an interpretation in favor of capillary flow, that is, “upward, vertical refilling” of soil matrix water from the saturated zone. This would have resulted from root water uptake induced negative potentiometric gradients as drought progressed. We rule out this possibility here. Instead, we suggest that the increase in the use of mobile water during drought when soil matric potential was low (≅16% v/v water content) resulted from refilling of rhizosphere water by diffused mobile water pockets in the bulk soil. Thus, we suggest caution in interpreting root water uptake of groundwater in field observations unless it can be established that the depth to the water table and/or capillary fringe exceeds the maximum rooting depth (Naumburg *et al.*, 2005).

5.5.5 On ecohydrological separation in time and space

The work presented here is the first evidence of ecohydrological separation that addresses the question whether or not the *two water worlds* is a separation in space or in time. As Bowen (2015) asked: "…the relative roles of physical and temporal segregation remain unclear. Do plants draw water from different parts of the soil matrix from groundwater recharge, or do plant withdrawals happen at a different time from groundwater recharge?"

Results from our Bayesian model of root water uptake sources support an interpretation of ecohydrological separation in space. Model results show that use of preferential flow ("more mobile") water increased through the drought (as soil matric potential decreased), and that use of soil matrix ("less mobile") water increased during rewetting (as soil matric potential recovered). If we qualify ecohydrological separation as vegetation using low mobility, soil matrix water over high mobility, preferential flow water (*sensu* Brooks *et al*., 2010), then our results suggest that there was greater ecohydrological separation during wet-up than during dry-down. This is (conceptually) consistent with the dynamic partial mixing mechanism of Hrachowitz *et al*. (2013) in that the dynamic active storage below the root zone dominates preferential flow, while the dynamic passive storage around the root zone dominates soil matrix water. Notwithstanding, some nuances are apparent. Our results provide evidence of species-level control with respect to the fraction of more mobile water in xylem, in that leaf water potential differentially compensated for the drop in soil matric potential to be able to maintain water transport.

Results from our time-invariant TTD modeling suggest a "time based segregation", that is, the water taken up by roots is older than seepage water by a factor of three to seven. The value of shape parameter α for seepage (0.30) is at the lower end of the 0.3-0.7 range reported in many catchments in nature (Godsey *et al*., 2010; Kirchner and Neal, 2013; Aubert *et al*., 2014), representing rapid tracer release in seepage flux and subsequent lower tracer concentrations ~8 weeks after the first labelled rainfall. α was larger in *H. elatus* (0.80) and *C. racemosa* (1.0) with the latter representing an exponential. The larger α in *H. elatus* and *C. racemosa* implies lesser variability in transit times of these outfluxes than in seepage. Consequently, skewness ($2/\sqrt{\alpha}$) and kurtosis ($6/\alpha$) were smaller in both species than in seepage. While we know of no study to date that used time-invariant TTD modeling for xylem, the shape factors for *H. elatus* and *C. racemosa* fell well within the range of typical rainfall-runoff catchment TTDs (Kirchner, 2016).

Notwithstanding, the differences in MTT is not trivial – seepage flux being one-fourth of the average MTT for both species. Even more surprising is *H. crepitans* with α that rises to a peak after a long 6-week delay thereby approximating a normal distribution.

If we qualify ecohydrological separation strictly as a time-based segregation (*sensu* Bowen 2015), then these MTT differences between seepage and transpiration fluxes may be interpreted as sampling of water from the same subsurface storage volume that differed only in average sampling flux. That is, transpiration water flux being slower than seepage flux by a factor of three to seven. An alternative interpretation, as discussed earlier, might be sampling of water from different subsurface compartments – transpiration from passive storage around the root zone (soil matrix water), seepage from active storage below the root zone (preferential flow water) – and different average sampling flux. The latter alternative explanation is more consistent with our definition of ecohydrological separation in this study, underpinned by the modeling approaches employed herein.

While the broad family of gamma distributions for TT has been used widely elsewhere with success (Kirchner et al., 2000; Godsey *et al.*, 2010; Jasechko *et al.*, 2016; Kirchner 2016), our adoption of the gamma distribution here is our first attempt at estimating transit times in a time invariant way. Future TT modeling work will consider time variability, caused by unsteady fluxes and time-varying flow pathways (Harman and Kim, 2014; Harman 2015; Kim *et al.*, 2016).

5.6 Conclusions

We present an assessment of ecohydrological separation by performing controlled drought and rainfall rewetting experiment at the Biosphere 2-Tropical Rainforest biome – a scale that is representative of a real world critical zone but with known and controlled boundary conditions (Figure 5.9). Our Bayesian mixing model of root water uptake sources show that transpiration is derived from soil matrix water and is different from the mobile water component in soils, particularly during wet-up. During dry-down, mobile water fraction in xylem increases as driving force increases, the latter explained mainly by species-level control that compensates for a decrease in soil matric potential. Our time-invariant transit time distribution modeling of xylem

water and deep percolation all show that the water taken up by roots is older than seepage ("groundwater recharge") water by a factor of three to seven. One possible explanation for these age differences is sourcing of transpiration and seepage water from the same storage volume but at markedly different average sampling flux. The Bayesian root water uptake and time-invariant TTD modeling results presented here, however, are consistent with a perceptual (qualitative) model whereby transpiration is sourced from soil matrix (determined by antecedent moisture states and species-specific control) at a markedly different average sampling flux. The latter perceptual model may be implemented with future transit time modeling approaches that could account for unsteady fluxes and time-varying flow pathways.

5.7 Acknowledgments

All data from this study are available for collaborative use by anyone interested; contact J. Evaristo for information on data access (jaivime.evaristo@usask.ca). We thank the following undergraduate research assistants for their help during the pre-drought and drought stages of the experiment: Meghan McDonnell, Ietza Gonzalez Silva, Fatima Olmos Flores and Daniel Espinosa Ruiz). We thank Maggie Heard, Sara Jane Harders, John Adams, Kim Land, and all staff and crew at Biosphere 2 for their invaluable support during the conduct of this experiment. Finally, we thank Kim Janzen and Cody Millar in McDonnell Lab (Univ. of Saskatchewan, SK, Canada) for logistical and lab support; and Gibson Lab (Univ. of Victoria, BC, Canada) for mass spec analysis. J. Evaristo thanks Saskatchewan Innovation and Opportunity Scholarship (Government of Saskatchewan) and Graduate Research Fellowship (School of Environment and Sustainability) for research funding.

5.8 Author Contributions

J.E designed the study, collected the samples, and conducted all data analysis and modeling except for transit time modeling which was performed by C.J.H and M.K. J.E. wrote the paper. J.J.M., J.vH., P.A.T. and L.P. edited and commented on the manuscript and contributed to the text in later iterations.

5.9 References

1. Arain, M., W. Shuttleworth, B. Farnsworth, J. Adams, and O. Sen (2000), Comparing micrometeorology of rain forests in Biosphere-2 and Amazon basin, *Agric. For. Meteorol., 100*, 273-289.

2. Aubert, A. H., J. W. Kirchner, C. Gascuel-Odoux, M. Faucheux, G. Gruau, and P. Merot (2014), Fractal Water Quality Fluctuations Spanning the Periodic Table in an Intensively Farmed Watershed, *Environ. Sci. Technol., 48*, 930-937.

3. Barbeta, A., M. Mejia-Chang, R. Ogaya, J. Voltas, T. E. Dawson, and J. Penuelas (2015), The combined effects of a long-term experimental drought and an extreme drought on the use of plant-water sources in a Mediterranean forest, *Global Change Biol., 21*, 1213-1225.

4. Bowen, G. (2015), HYDROLOGY The diversified economics of soil water, *Nature, 525*, 43-44.

5. Bowling, D. R., E. S. Schulze, and S. J. Hall (2016), Revisiting streamside trees that do not use stream water: Can the two water worlds hypothesis and snowpack isotopic effects explain a missing water source?, *Ecohydrology*, n/a-n/a.

6. Brooks, J. R., H. R. Barnard, R. Coulombe, and J. J. McDonnell (2010), Ecohydrologic separation of water between trees and streams in a Mediterranean climate, *Nature Geosci., 3*, 100-104.

7. Brooks, J. R. (2015), Water, bound and mobile, *Science, 349*, 138-139.

8. Brooks, R.H., and A.T. Corey (1964), Hydraulic properties of porous media, Hydrology Papers, No.3, Colorado State University, Fort Collins, Colorado.

9. Brunel, J. P., G. R. Walker, and A. K. Kennettsmith (1995), Field Validation of Isotopic Procedures for Determining Sources of Water used by Plants in a Semiarid Environment, *Journal of Hydrology, 167*, 351-368.

10. Carminati, A., A. B. Moradi, D. Vetterlein, P. Vontobel, E. Lehmann, U. Weller, H. -. Vogel, and S. E. Oswald (2010), Dynamics of soil water content in the rhizosphere, *Plant Soil, 332*, 163-176.

11. Coenders-Gerrits, A. M. J., R. J. van der Ent, T. A. Bogaard, L. Wang-Erlandsson, M. Hrachowitz, and H. H. G. Savenije (2014), Uncertainties in transpiration estimates, *Nature, 506*, E1-E2.

12. Craig, H., and L. I. Gordon (1965), Deuterium and oxygen 18 variations in the ocean and marine atmosphere, in Stable Isotopes in Oceanographic Studies and Paleotemperatures, edited by E. Tongiorgi, pp. 9– 130, Lab. Geologia Nucleare, Pisa, Italy.

13. Dansgaard, W. (1964), Stable Isotopes in Precipitation, *Tellus, 16*, 436-468.

14. Dawson, T. E. (1993), Hydraulic lift and water use by plants: implications for water balance, performance and plant-plant interactions, *Oecologia, 95*, 565-574.

15. Dawson, T. E. and J. R. Ehleringer (1991), Streamside Trees that do Not use Stream Water, *Nature, 350*, 335-337.

16. De Groen, M.M. (2002), Modelling interception and transpiration at monthly time steps; introducing daily variability through Markov chains. PhD thesis, IHE-Delft, Swets & Zeitlinger, Lisse, The Netherlands.

17. Ehleringer, J. R. and T. E. Dawson (1992), Water uptake by plants: perspectives from stable isotope composition, *Plant, Cell Environ., 15*, 1073-1082.

18. Ellsworth, P. Z. and D. G. Williams (2007), Hydrogen isotope fractionation during water uptake by woody xerophytes, *Plant Soil, 291*, 93-107.

19. Evaristo, J., S. Jasechko, and J. J. McDonnell (2015), Global separation of plant transpiration from groundwater and streamflow, *Nature, 525*, 91-94.

20. Evaristo, J., J. J. McDonnell, M. A. Scholl, L. A. Bruijnzeel, and K. P. Chun (2016), Insights into plant water uptake from xylem-water isotope measurements in two tropical catchments with contrasting moisture conditions, *Hydrol. Process., 30*, 3210-3227.

21. Evaristo, J. McDonnell, J.J., and Clemens, J. (In Review) "Plant source water identification using stable isotopes: A critical evaluation". *New Phytologist*

22. Friedman, I. (1953), Deuterium content of natural waters and other substances, *Geochim. Cosmochim. Acta, 4*, 89-103.

23. Gaines, K. P., F. C. Meinzer, C. J. Duffy, E. M. Thomas, and D. M. Eissenstat (2016), Rapid tree water transport and residence times in a Pennsylvania catchment, *Ecohydrology*, n/a-n/a.

24. Geris, J., D. Tetzlaff, J. McDonnell, J. Anderson, G. Paton, and C. Soulsby (2015), Ecohydrological separation in wet, low energy northern environments? A preliminary assessment using different soil water extraction techniques, *Hydrol. Process., 29*, 5139-5152.

25. Gibson, J. J. and T. W. D. Edwards (2002), Regional water balance trends and evaporation-transpiration partitioning from a stable isotope survey of lakes in northern Canada, *Global Biogeochem. Cycles, 16*, 1026.

26. Godsey, S. E. et al. (2010), Generality of fractal 1/f scaling in catchment tracer time series, and its implications for catchment travel time distributions, *Hydrol. Process., 24*, 1660-1671.

27. Goldsmith, G. R., L. E. Muñoz-Villers, F. Holwerda, J. J. Mcdonnell, H. Asbjornsen, and T. E. Dawson (2012), Stable isotopes reveal linkages among ecohydrological processes in a seasonally dry tropical montane cloud forest, *Ecohydrology, 5*, 779-790.

28. Good, S. P., D. Noone, and G. Bowen (2015), Hydrologic connectivity constrains partitioning of global terrestrial water fluxes, *Science, 349*, 175-177.

29. Hall, S. J., S. R. Weintraub, and D. R. Bowling (2016), Scale-dependent linkages between nitrate isotopes and denitrification in surface soils: implications for isotope measurements and models, *Oecologia*, 1-11.

30. Harman, C. J. (2015), Time-variable transit time distributions and transport: Theory and application to storage-dependent transport of chloride in a watershed, *Water Resour. Res., 51*, 1-30.

31. Harman, C. J. and M. Kim (2014), An efficient tracer test for time-variable transit time distributions in periodic hydrodynamic systems, *Geophys. Res. Lett., 41*, 1567-1575.

32. Hervé-Fernández, P., C. Oyarzún, C. Brumbt, D. Huygens, S. Bodé, N. E. C. Verhoest, and P. Boeckx (2016), Assessing the “two water worlds” hypothesis and water sources for native and exotic evergreen species in south-central Chile, *Hydrol. Process.*, n/a-n/a.

33. Hrachowitz, M., H. Savenije, T. A. Bogaard, D. Tetzlaff, and C. Soulsby (2013), What can flux tracking teach us about water age distribution patterns and their temporal dynamics?, *Hydrology and Earth System Sciences, 17*, 533-564.

34. Hrachowitz, M., P. Benettin, B. M. van Breukelen, O. Fovet, N. J. K. Howden, L. Ruiz, Y. van der Velde, and A. J. Wade (2016), Transit times—the link between hydrology and water quality at the catchment scale, *Wiley Interdisciplinary Reviews: Water, 3*, 629-657.

35. Hrachowitz, M., O. Fovet, L. Ruiz, and H. H. G. Savenije (2015), Transit time distributions, legacy contamination and variability in biogeochemical 1/f(alpha) scaling: how are hydrological response dynamics linked to water quality at the catchment scale?, *Hydrol. Process., 29*, 5241-5256.

36. Jameel, Y., S. Brewer, S. P. Good, B. J. Tipple, J. R. Ehleringer, and G. J. Bowen , Tap water isotope ratios reflect urban water system structure and dynamics across a semiarid metropolitan area, *Water Resour. Res.*, n/a-n/a.

37. James, S., F. Meinzer, G. Goldstein, D. Woodruff, T. Jones, T. Restom, M. Mejia, M. Clearwater, and P. Campanello (2003), Axial and radial water transport and internal water storage in tropical forest canopy trees, *Oecologia, 134*, 37-45.

38. Jasechko, S., J. W. Kirchner, J. M. Welker, and J. J. McDonnell (2016), Substantial proportion of global streamflow less than three months old, *Nat. Geosci., 9*, 126-129.

39. Jasechko, S., Z. D. Sharp, J. J. Gibson, S. J. Birks, Y. Yi, and P. J. Fawcett (2013), Terrestrial water fluxes dominated by transpiration, *Nature, 496*, 347-350.

40. Kirchner, J. W. (2016), Aggregation in environmental systems - Part 1: Seasonal tracer cycles quantify young water fractions, but not mean transit times, in spatially heterogeneous catchments, *Hydrology and Earth System Sciences, 20*, 279-297.

41. Kirchner, J. W. and C. Neal (2013), Universal fractal scaling in stream chemistry and its implications for solute transport and water quality trend detection, *Proc. Natl. Acad. Sci. U. S. A., 110*, 12213-12218.

42. Kirchner, J. W., D. Tetzlaff, and C. Soulsby (2010), Comparing chloride and water isotopes as hydrological tracers in two Scottish catchments, *Hydrol. Process., 24*, 1631-1645.

43. Kirchner, J., X. Feng, and C. Neal (2000), Fractal stream chemistry and its implications for contaminant transport in catchments, *Nature, 403*, 524-527.

44. Klaus, J., K. P. Chun, K. J. McGuire, and J. J. McDonnell (2015), Temporal dynamics of catchment transit times from stable isotope data, *Water Resour. Res., 51*, 4208-4223.

45. Landwehr, J. and T. Coplen (2006), Isotopes in Environmental Studies, 132-135.

46. Leigh, L., T. Burgess, B. Marino, and Y. Wei (1999), Tropical rainforest biome of Biosphere 2: Structure, composition and results of the first 2 years of operation, *Ecol. Eng., 13*, 65-93.

47. Lin G. and L.S.L. da Sternberg (1993), Hydrogen isotopic fractionation by plant roots during water uptake in coastal wetland plants. In: Ehleringer JR, Hall AE, Farquhar GD (eds) Stable isotopes and plant carbon-water relations. Academic Press Inc., New York, pp 497–510

48. Malozewski, P. and A. Zuber (1982), Determining the Turnover Time of Groundwater Systems with the Aid of Environmental Tracers .1. Models and their Applicability, *Journal of Hydrology, 57*, 207-231.

49. McDonnell, J. J. (2014), The two water worlds hypothesis: ecohydrological separation of water between streams and trees?, *WIREs Water, 1*, 323-329.

50. McDonnell, J. J. and K. Beven (2014), Debates-The future of hydrological sciences: A (common) path forward? A call to action aimed at understanding velocities, celerities and residence time distributions of the headwater hydrograph, *Water Resour. Res., 50*, 5342-5350.

51. McDonnell, J. J. et al. (2010), How old is streamwater? Open questions in catchment transit time conceptualization, modelling and analysis, *Hydrol. Process., 24*, 1745-1754.

52. McGuire, K. J. and J. J. McDonnell (2006), A review and evaluation of catchment transit time modeling, *Journal of Hydrology, 330*, 543-563.

53. McGuire, K. J. and J. J. McDonnell (2015), Tracer advances in catchment hydrology, *Hydrol. Process., 29*, 5135-5138.

54. Meinzer, F., J. Brooks, J. Domec, B. Gartner, J. Warren, D. Woodruff, K. Bible, and D. Shaw (2006), Dynamics of water transport and storage in conifers studied with deuterium and heat tracing techniques, *Plant Cell and Environment, 29*, 105-114.

55. Naumburg, E., R. Mata-Gonzalez, R. Hunter, T. Mclendon, and D. Martin (2005), Phreatophytic vegetation and groundwater fluctuations: A review of current research and application of ecosystem response modeling with an emphasis on Great Basin vegetation, *Environ. Manage., 35*, 726-740.

56. Ogle, K., R. Wolpert, and J. Reynolds (2004), Reconstructing plant root area and water uptake profiles, *Ecology, 85*, 1967-1978.

57. Ogle, K., C. Tucker, and J. M. Cable (2014), Beyond simple linear mixing models: process-based isotope partitioning of ecological processes, *Ecol. Appl., 24*, 181-195.

58. Oleson, K. W., et al. (2010), Technical description of version 4.0 of the Community Land Model, NCAR Tech. Note NCAR/TN-4781STR, National Center for Atmospheric Research, Boulder, Colo.

59. Parnell, A. C., R. Inger, S. Bearhop, and A. L. Jackson (2010), Source Partitioning Using Stable Isotopes: Coping with Too Much Variation, *PLoS One, 5*, e9672.

60. Phillips, D. L. and J. W. Gregg (2003), Source partitioning using stable isotopes: coping with too many sources, *Oecologia, 136*, 261-269.

61. Phillips, D. L., R. Inger, S. Bearhop, A. L. Jackson, J. W. Moore, A. C. Parnell, B. X. Semmens, and E. J. Ward (2014), Best practices for use of stable isotope mixing models in food-web studies, *Can. J. Zool., 92*, 823-835.

62. Phillips, S. L. and J. R. Ehleringer (1995), Limited Uptake of Summer Precipitation by Bigtooth Maple (Acer-Grandidentatum Nutt) and Gambels Oak (Quercus-Gambelii Nutt), *Trees-Structure and Function, 9*, 214-219.

63. Rascher, U. et al. (2004), Functional diversity of photosynthesis during drought in a model tropical rainforest - the contributions of leaf area, photosynthetic electron transport and stomatal conductance to reduction in net ecosystem carbon exchange, *Plant Cell and Environment, 27*, 1239-1256.

64. Rosolem, R., W. J. Shuttleworth, X. Zeng, S. R. Saleska, and T. E. Huxman (2010), Land surface modeling inside the Biosphere 2 tropical rain forest biome, *Journal of Geophysical Research-Biogeosciences, 115*, G04035.

65. Schellekens, J., L. A. Bruijnzeel, F. N. Scatena, N. J. Bink, and F. Holwerda (2000), Evaporation from a tropical rain forest, Luquillo Experimental Forest, eastern Puerto Rico, *Water Resour. Res., 36*, 2183-2196.

66. Schlesinger, W. H. and S. Jasechko (2014), Transpiration in the global water cycle, *Agric. For. Meteorol., 189*, 115-117.

67. Scott, H. (1999), Characteristics of soils in the tropical rainforest biome of Biosphere 2 after 3 years, *Ecol. Eng., 13*, 95-106.

68. Smith, D. D. and J. S. Sperry (2014), Coordination between water transport capacity, biomass growth, metabolic scaling and species stature in co-occurring shrub and tree species, *Plant Cell and Environment, 37*, 2679-2690.

69. Soulsby, C., C. Birkel, and D. Tetzlaff (2016), Characterizing the age distribution of catchment evaporative losses, *Hydrol. Process., 30*, 1308-1312.

70. Sprenger, M., H. Leistert, K. Gimbel, and M. Weiler (2016), Illuminating hydrological processes at the soil-vegetation-atmosphere interface with water stable isotopes, *Rev. Geophys.*, n/a-n/a.

71. Sutanto, S. J., J. Wenninger, A. M. J. Coenders-Gerrits, and S. Uhlenbrook (2012), Partitioning of evaporation into transpiration, soil evaporation and interception: A comparison between isotope measurements and a HYDRUS-1D model, *Hydrol. Earth Syst. Sci., 16*, 2605-2616.

72. Tetzlaff, D., J. Buttle, S. K. Carey, M. H. J. van Huijgevoort, H. Laudon, J. P. McNamara, C. P. J. Mitchell, C. Spence, R. S. Gabor, and C. Soulsby (2015), A preliminary assessment of water partitioning and ecohydrological coupling in northern headwaters using stable isotopes and conceptual runoff models, *Hydrol. Process., 29*, 5153-5173.

73. Thorburn, P. J. and G. R. Walker (1994), Variations in stream water uptake by Eucalyptus camaldulensis with differing access to stream water, *Oecologia, 100*, 293-301.

74. Thorburn, P. J., G. R. Walker, and J. P. Brunel (1993), Extraction of Water from Eucalyptus Trees for Analysis of Deuterium and O-18 - Laboratory and Field Techniques, *Plant Cell and Environment, 16,* 269-277.

75. Vrugt, J. A., C. J. F. ter Braak, C. G. H. Diks, B. A. Robinson, J. M. Hyman, and D. Higdon (2009), Accelerating Markov Chain Monte Carlo Simulation by Differential Evolution with Self-Adaptive Randomized Subspace Sampling, *International Journal of Nonlinear Sciences and Numerical Simulation, 10,* 273-290.

76. Wershaw R.L., I. Friedman, and S.J. Heller (1966), Hydrogen isotope fractionation of water passing through trees. In Advances in Organic Geochemistry, ed. F Hobson, M Speers, pp. 55-67. New York: Pergamon

77. Wheeler, J. K., B. A. Huggett, A. N. Tofte, F. E. Rockwell, and N. M. Holbrook (2013), Cutting xylem under tension or supersaturated with gas can generate PLC and the appearance of rapid recovery from embolism, *Plant Cell and Environment, 36,* 1938-1949.

78. White J.W.C., E.R. Cook, J.R. Lawrence, and W.S. Broecker (1985), The deuterium to hydrogen ratios of sap in trees: implications for water sources and tree ring deuterium to hydrogen ratios. Geochim. Cosmochim. Acta 49:237-46

79. Zhang, Z., Si, B., Li, Z., Evaristo, J., McDonnell, J.J. (In Review) “Tritium analysis shows that apple trees transpire 29 yr old bound water”. *Hydrological Processes.*

Figure 5.1 – Environmental conditions during the study period. Gray shaded area represents drought period (23 Jul-29 Sep 2014). Top panel is 15-min resolution vapor pressure deficit (VPD) at 13 m (top subplot) and 1m (bottom subplot) above the forest floor. Black solid curves in each subplot represent simple moving average smoothed and centered at 200 (window size). Middle panel is ecosystem-level transpiration mount; left axis is daily total in kg (gray curves); right axis are 15 min totals (filled yellow circles), error bars represent 1 SD. Bottom panel is soil water content (left axis) and soil matric potential (right axis) at 25 and 65 cm.

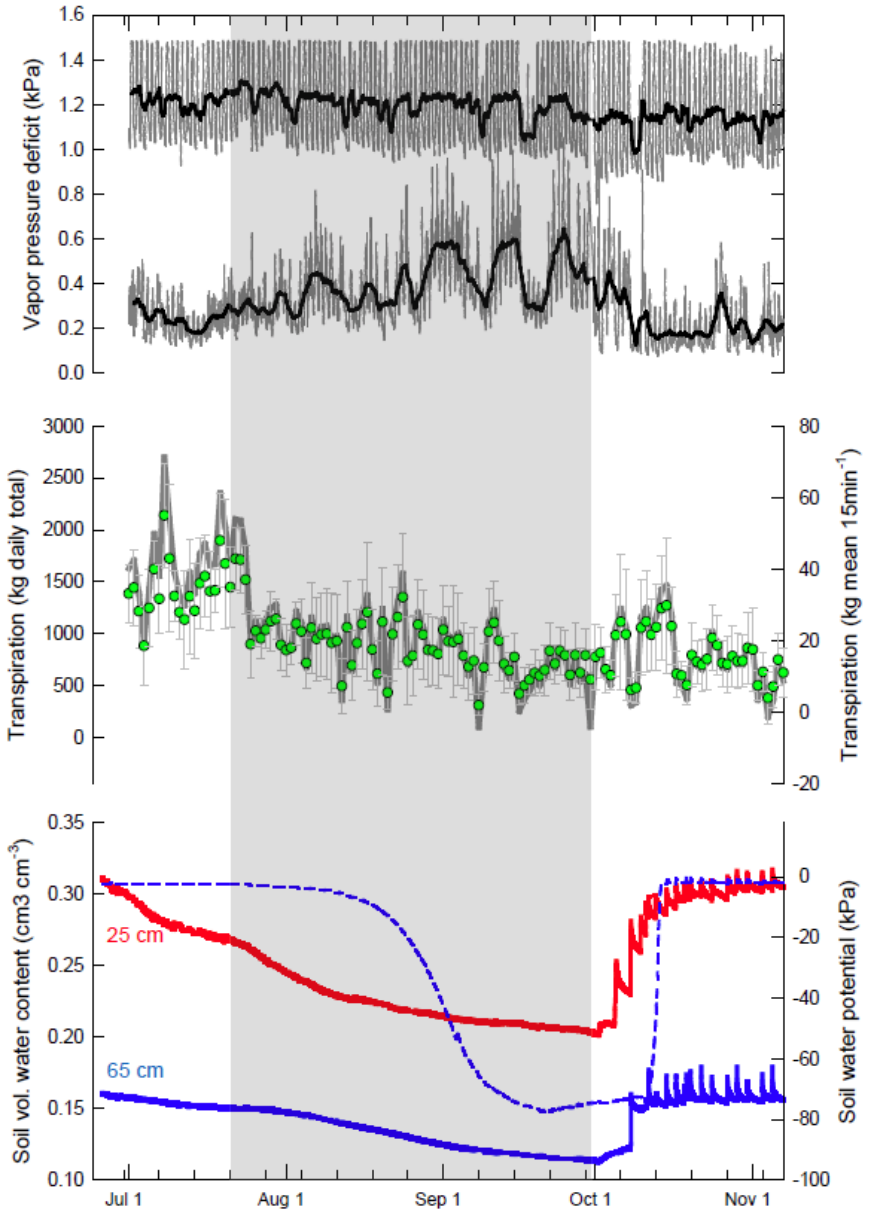

Figure 5.2 – Summary of bulk soil water isotope and volumetric water content during and after drought. Left panel shows a schematic of root fraction distribution following Rosolem *et al*. (2010). Middle and right panels show bulk soil water isotope ($\delta^{18}O$) and soil volumetric water content profiles, respectively, during and after drought (error bars represent ranges) Also shown are particle size fractions (mean ±1SD).

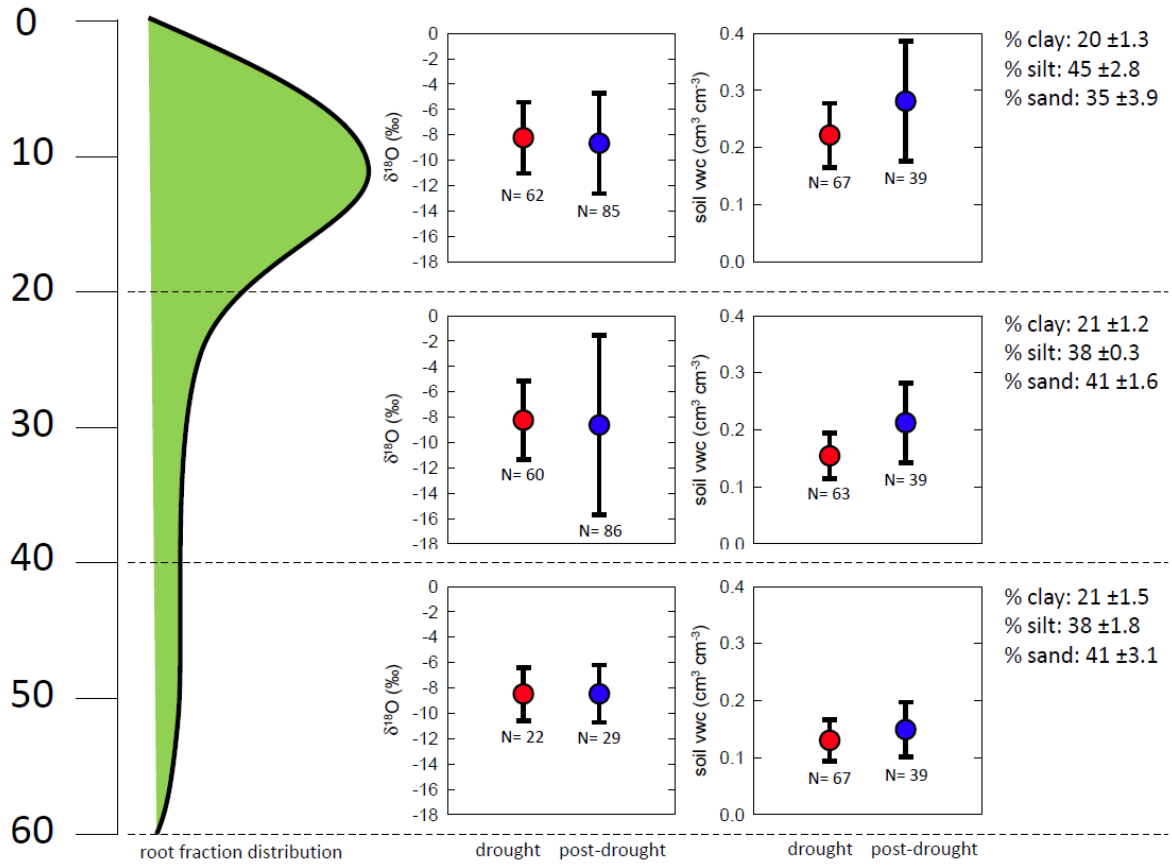

Figure 5.3 – Source water partitioning using Bayesian mixing model during drought (a) and post-drought (b). Numbers below each column correspond to week of sampling. Drought: 29 Jul, 05 Aug, 11 Aug, 09 Sep, 16 Sep, 23 Sep, 29 Sep. Post-drought: 30 Sep, 02 Oct, 07 Oct, 14 Oct, 21 Oct, 28 Oct, 04 Nov, 09 Dec. Error bars represent 1 SD.

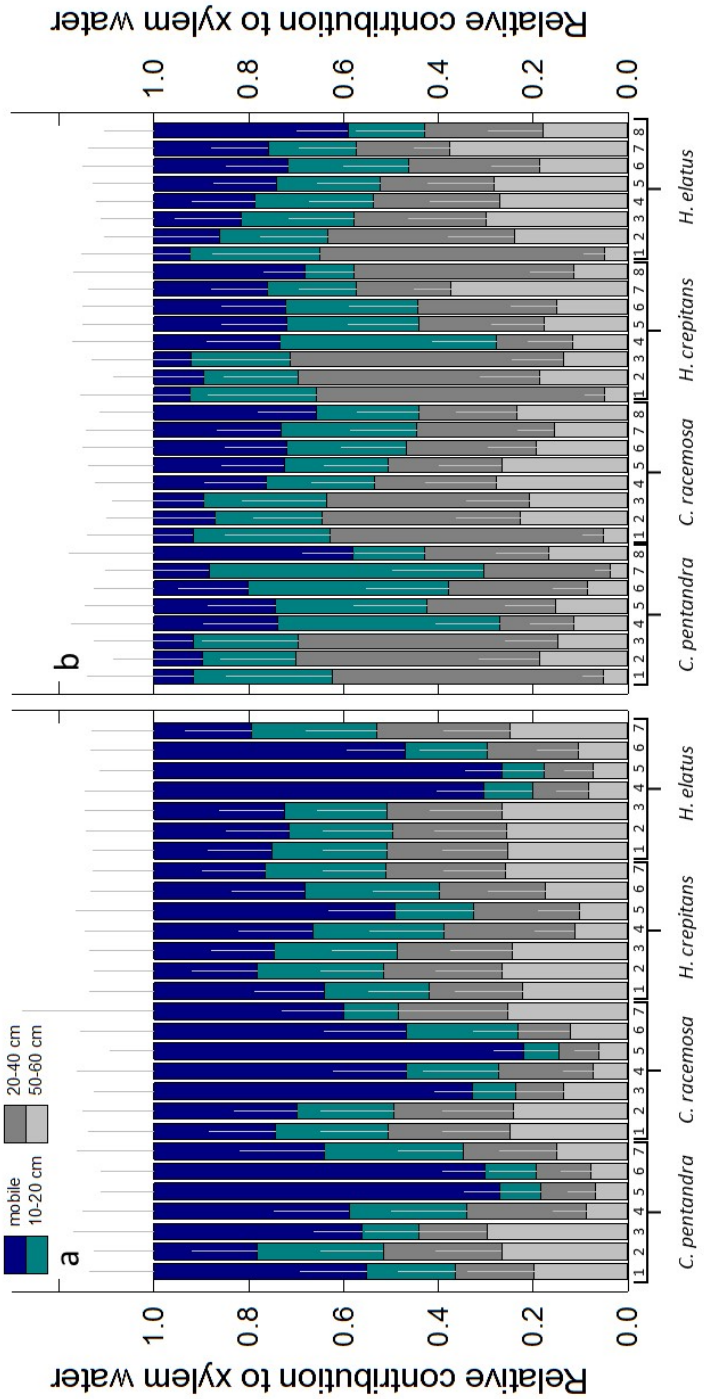

Figure 5.4 – Soil moisture retention curve at 65cm.

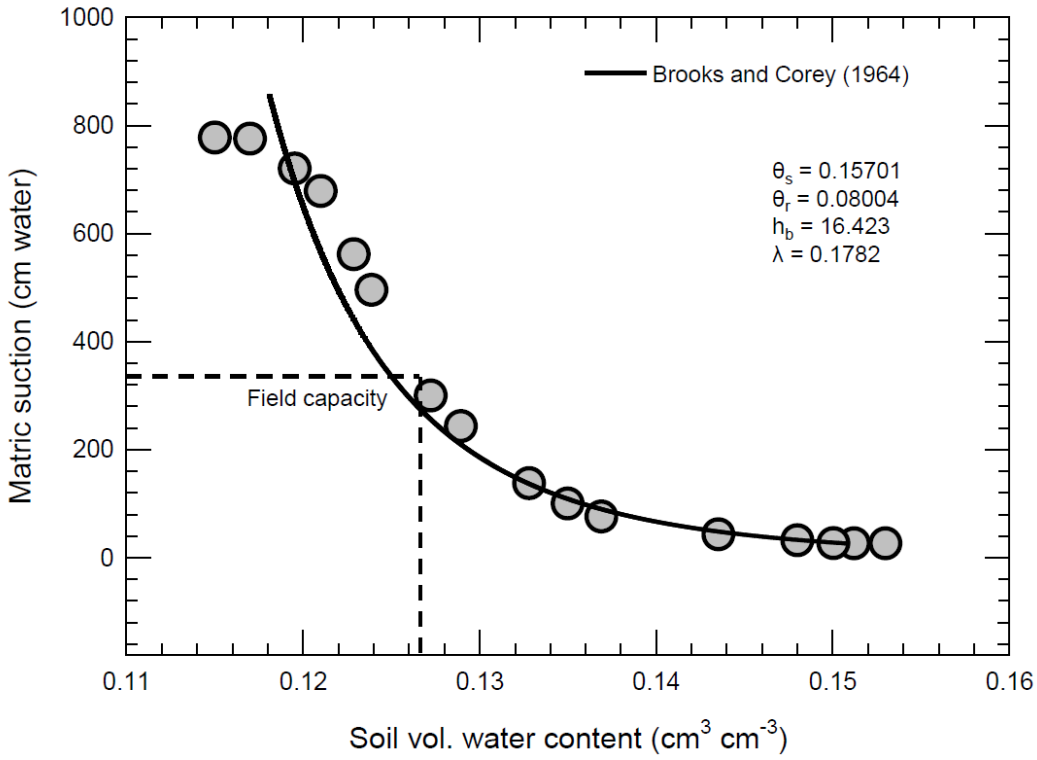

Figure 5.5 – Fraction of mobile water in xylem versus soil volumetric water content during and after drought. Error bars represent 1 SD.

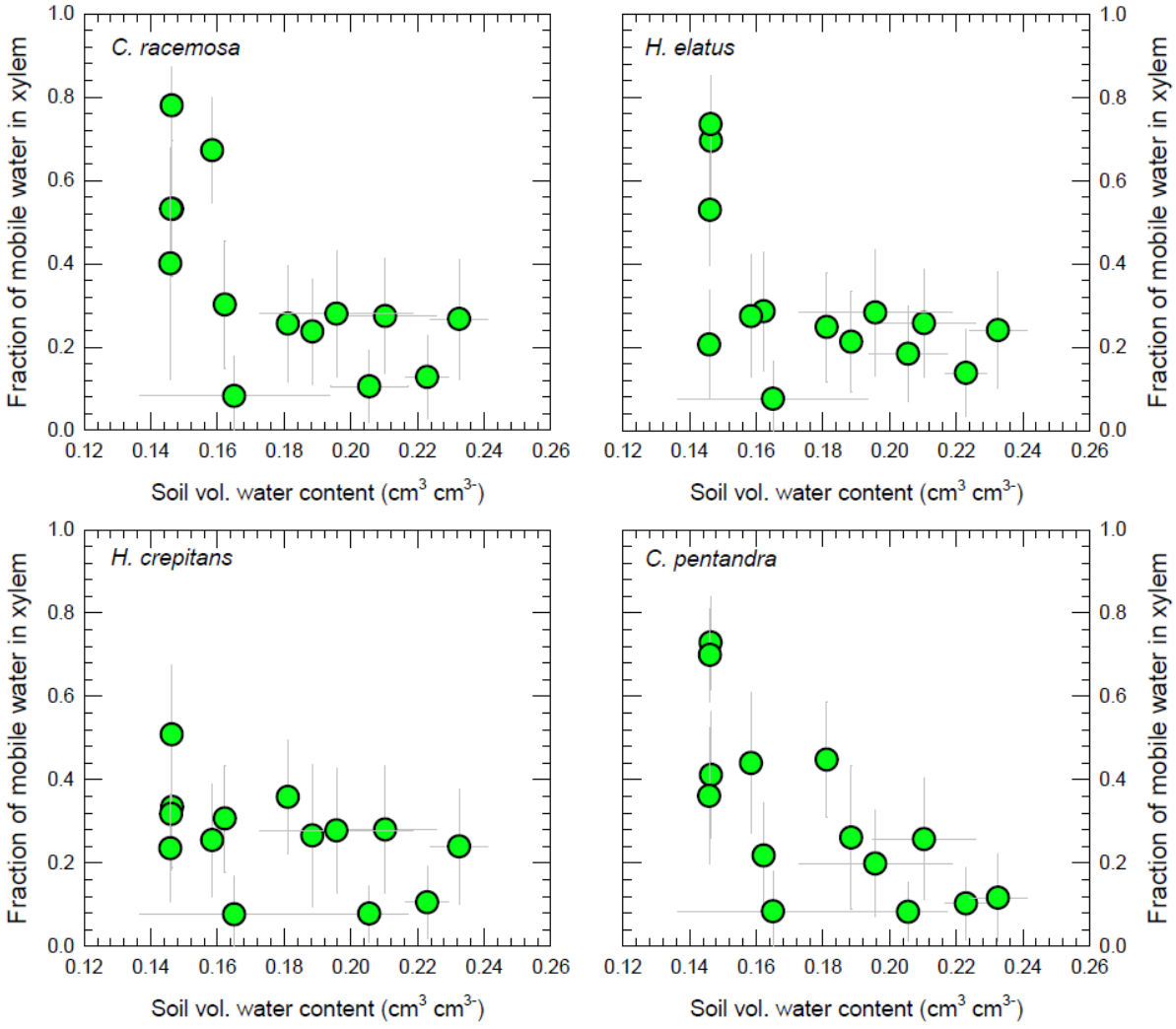

Figure 5.6 – Fraction of mobile water in xylem versus water transport driving force (difference between soil matric potential and leaf water potential) during drought. Best-fit is a three-parameter exponential with an asymptote, scale, and growth factors. Error bars represent 1SD.

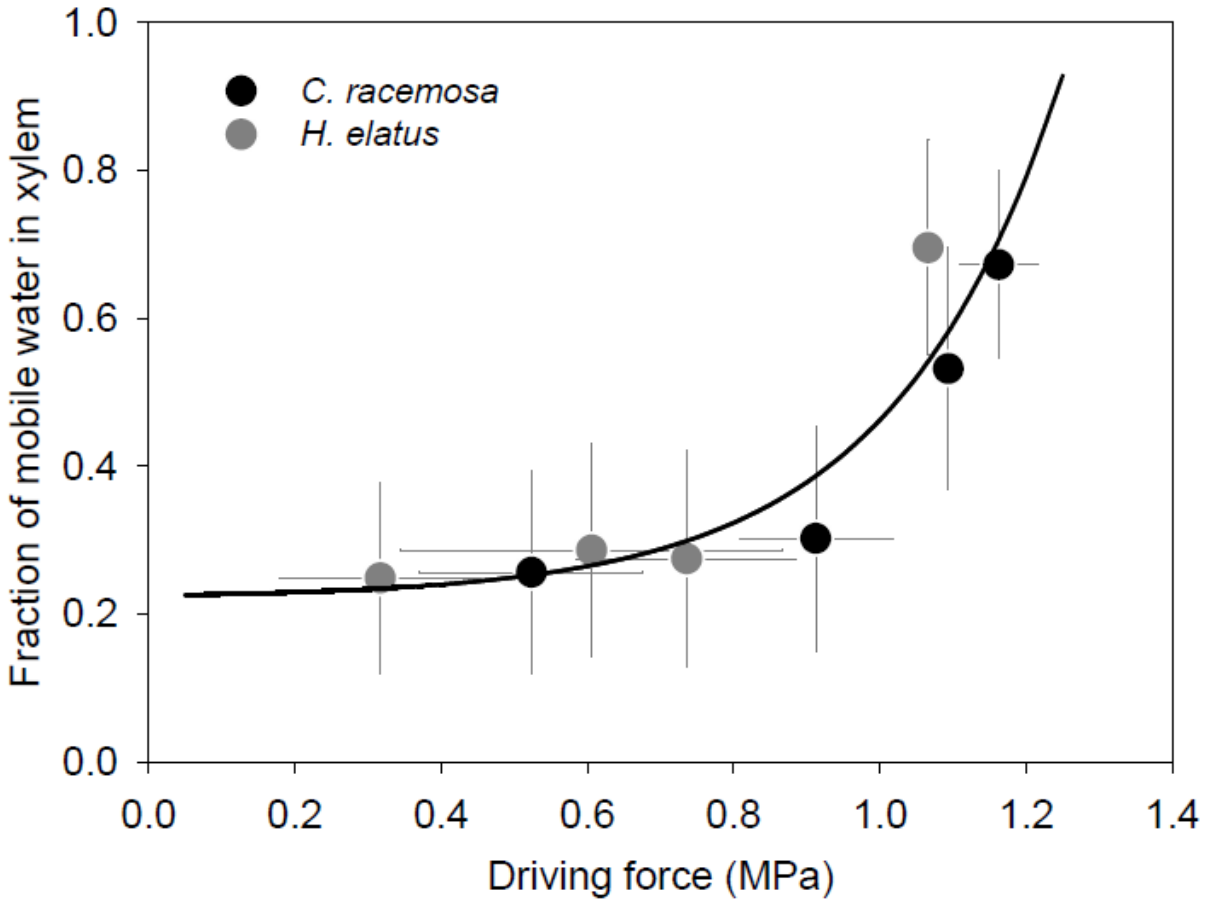

Figure 5.7 – Time-invariant transit time distribution (TTD) modeling. Shaded area shows four rainfall events with a D_2O label. Middle inset shows CDFs and four subplot insets are model parameters derived from DREAM (DiffeRential Evolution Adaptive Metropolis; Vrugt *et al.*, 2009) algorithm.

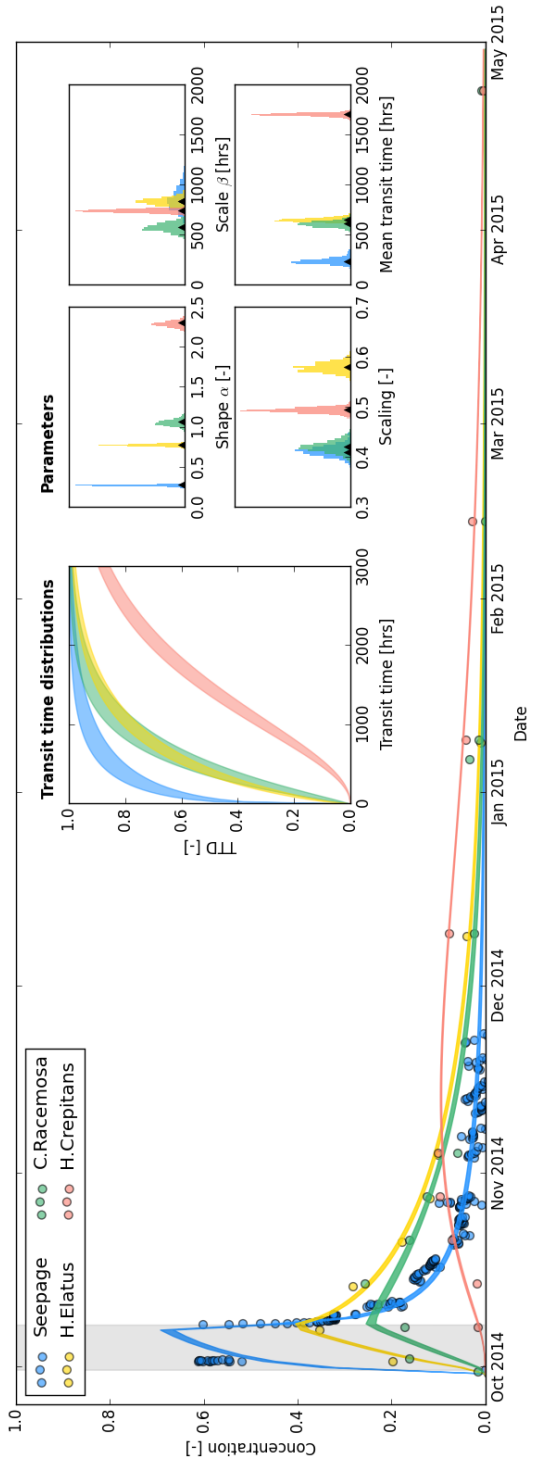

Figure 5.8 – Tracer velocity (tree height divided by mean transit time) versus water transport driving force for three tree species in this study. Also shown are data from four tree species in Gaines *et al*. (2016). Best-fit is linear, 95% confidence limits represented by gray dashed lines.

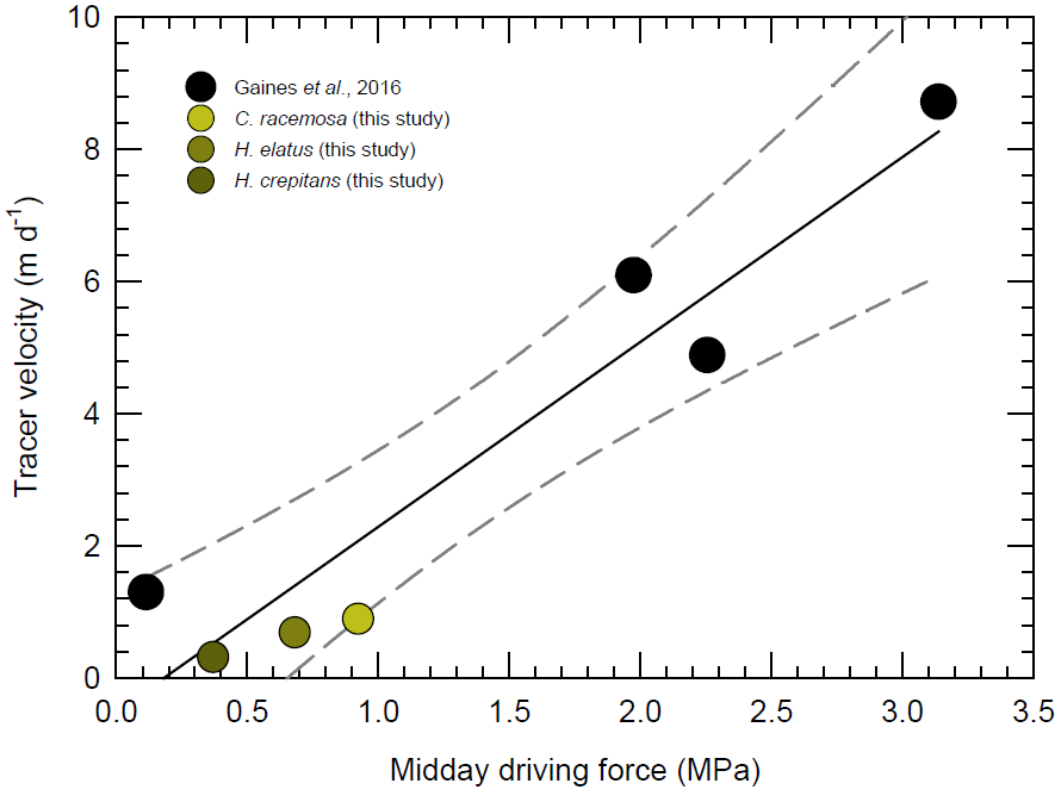

Figure 5.9 – Summary schematic illustration of the study during and after drought. θ and ψ represent soil volumetric water content ($cm^3\ cm^{-3}$) and water potential (MPa), respectively. δ-f_{mobile} represents fraction on mobile water in xylem from the Bayesian model of root water uptake sources. Values within brackets are ranges. Ages are derived from the time-invariant TTD model; $age_{gw\ recharge} \equiv$ seepage.

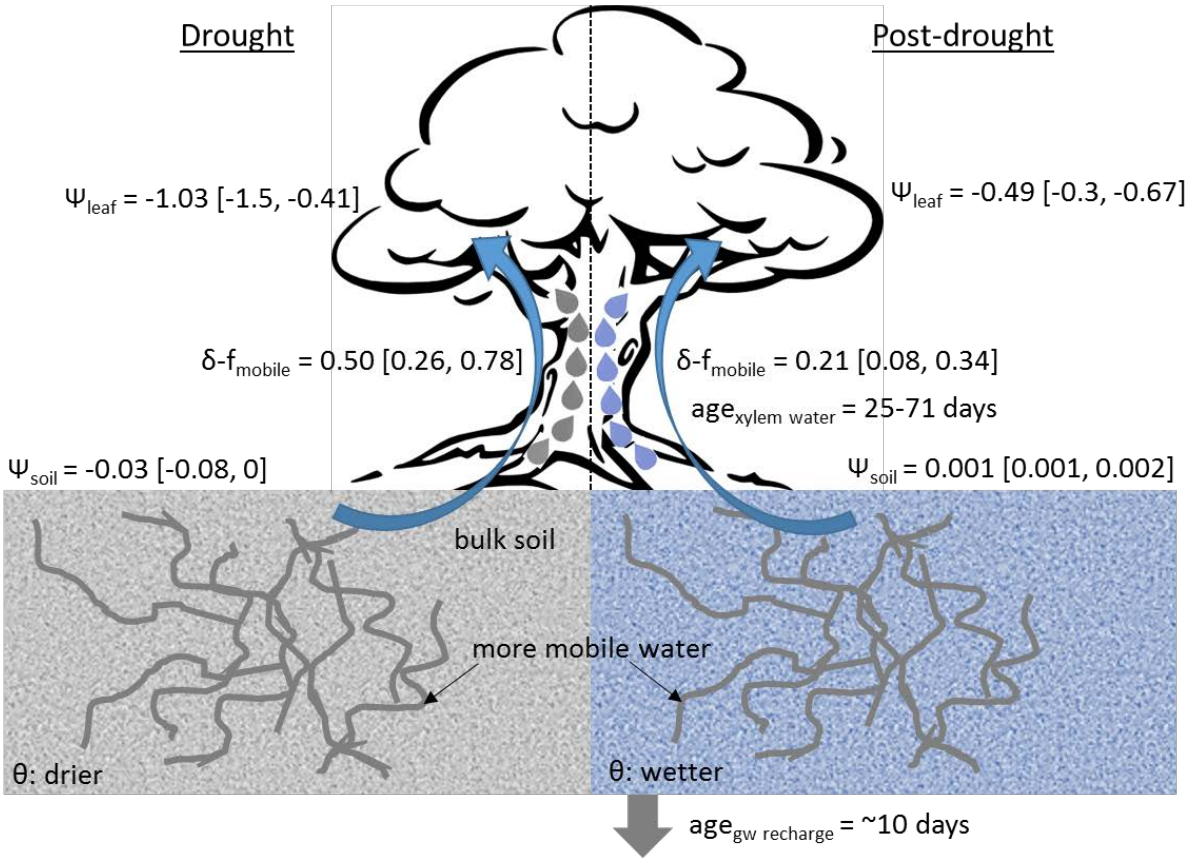

CHAPTER 6

CONCLUSION

The water balance (precipitation = runoff – evapotranspiration) is one of environmental science's simplest and most important equations. Water drives most physical and biogeochemical reactions at the landscape scale. Understanding the cycling of water is fundamental to human infrastructure and ecosystem services and predictions of future water security. While hydrologists have studied the water balance for over a century, recent work on ecohydrological separation has suggested that one piece of the water balance—evapotranspiration (the sum of evaporation and plant transpiration) is separated from the more mobile cycling of water that forms groundwater recharge and streamflow generation. The basic research questions explored over the course of my PhD education were directed towards achieving greater clarity and understanding of the phenomenon that is ecohydrological separation.

Originally reported in the Pacific Northwest, USA (Brooks *et al*., 2010) and later in various sites in the tropics and elsewhere (Goldsmith *et al*., 2012; Evaristo *et al*., 2016; Hervé-Fernández *et al*., 2016), ecohydrological separation (*two water worlds*) is now recognized as a widespread phenomenon (Evaristo *et al*., 2015; Good *et al*., 2015). A similar phenomenon (*two nitrate worlds*) pertaining to nitrogen cycling (Hall *et al*., 2016) supports the idea that water/nutrient uptake by vegetation and groundwater recharge/nutrient export to streams are separated. Prior to these recent advances in our understanding of ecohydrological separation, however, it was initially assumed that the phenomenon might be related to the temporal phasing between hydrologic activity (e.g. rainfall/snowmelt) and ecological activity (i.e., primary productivity) (Phillips, 2010). My work in Puerto Rico (Chapter 2, Evaristo *et al*., 2016, *Hydrological Processes*) provided evidence disproving the latter. That is, ecohydrological separation might be related less to ecosystem-scale temporal phase differences between hydrology (i.e. precipitation inputs) and ecology (i.e. primary productivity and water uptake by vegetation) than with the

fundamental processes that drive soil drying – e.g. soil water evaporation, root water uptake, and drainage.

Having been able to demonstrate that ecohydrological separation was present in the less seasonal settings of Puerto Rico, my meta-analysis work (Chapter 3, Evaristo *et al*., 2015, *Nature*) provided a global-in-scale evidence supporting ecohydrological separation, transcending large-scale differences in physiographic settings including species, seasonality and biome. Indeed, the same global-in-scale conclusion was supported by a study using remotely sensed vapor isotopic data (Good *et al*., 2015). Implicit in the global-in-scale demonstration of ecohydrological separation, however, was the research question on the degree of groundwater use by vegetation. My work on a global synthesis of published literature (Chapter 4, Evaristo and McDonnell, in revision, *Nature Scientific Reports*), specifically quantifying the prevalence of groundwater use by vegetation, provided evidence that groundwater use was not as widespread as increasingly being assumed in the literature. Among others, our finding that most trees rely on soil water may have several implications including greater vulnerability to drought impacts across scales – from impaired growth after drought stress at plant and ecosystem scales to uncertainties in modeling climate-vegetation feedbacks at global scales; less impact on river discharge at catchment scales than the case might be with widespread groundwater use; and a rethinking on approaches used in afforestation schemes and silvicultural systems that place emphasis on species selection and groundwater use. This wide range of implications notwithstanding, in view of ecohydrological separation, this work addressed some of the questions surrounding the implications of ecohydrological separation on the role of groundwater in sustaining vegetation. Moreover, it strengthened the foundation upon which a search for the mechanistic underpinnings of ecohydrological separation would be based.

Indeed, my PhD research work culminated in a mechanistic assessment of ecohydrological separation (Chapter 5, Evaristo *et al*. for submission). Achieved by performing a controlled drought and rainfall experiment at the Biosphere 2-Tropical Rainforest biome (Arizona, USA), our results showed that transpiration water was derived from soil matrix water and was different from the mobile water component in soils, particularly during wet-up period. During dry-down,

mobile water fraction in xylem increased as the driving force of root water uptake increased, which was explained mainly by species-level control that compensated for a decrease in soil matric potential. Our time-invariant transit time distribution modeling of xylem water and deep percolation all showed that the water taken up by roots was older than seepage ("groundwater recharge") water by a factor of three to seven. These results are consistent with a perceptual (qualitative) model whereby transpiration water is sourced from soil matrix (determined by antecedent moisture states and species-specific control) at a markedly different average sampling flux. I propose that the latter perceptual model may be implemented with future transit time modeling approaches that could account for unsteady fluxes and time-varying flow pathways. McDonnell (2014) issued a call to the ecohydrology community for the design of experiments that would elucidate the controls on ecohydrological separation. The culmination of my PhD work provided in this Biosphere 2 experiment provides the first detailed evidence of ecohydrological separation at the scale of an ecosystem.

The results condensed in this PhD thesis embody a significant advance in the field of ecohydrological research. I was able to demonstrate the generality of ecohydrological separation and quantify the degree of groundwater use by vegetation. I was also able to reveal the possible and likely controls behind the partitioning of subsurface water between root water uptake and groundwater recharge. These advances go against a century of research in the hydrological sciences where mixing in the subsurface and translatory flow are assumed, and high mobility water linked to flow and transport is often the focus of plant water uptake.

Indeed, the implications of ecohydrological separation are manifold. In rainfall-runoff modeling and water balance studies, ecohydrological separation implies that research using chemical or isotopic tracers to partition water sources for streamflow may be missing a significant part of the soil water balance related to transpiration and soil water evaporation. Transpiration and soil water evaporation are non-trivial components of the water balance (Jasechko *et al*., 2013). Good *et al*. (2015) showed that while evapotranspiration fluxes comprised ~52% of the global terrestrial water budget, my findings at the Biosphere 2-Tropical Rainforest biome (Chapter 5, Evaristo *et al*. for submission) show that the age of transpiration water could be older than

groundwater recharge. Together these recent discoveries suggest that model estimates of transit times (i.e. “ages” of water in a catchment), informed mainly by tracers in precipitation and streams, may represent only the “younger” component of water that enters and leaves a watershed. Ecohydrological separation suggests that a full accounting of tracer fluxes, including transpiration and soil matrix water, is needed to be able to simulate the high temporal variability of streamflow and large uncertainties in transpiration flux estimates. The former has direct implications for stormflow generation models; the latter has a wide range of applications, including understanding and predicting the long-term response of vegetation to episodic droughts.

Finally, ecohydrological separation has direct implications for soil biogeochemistry as well as nutrient use and export. As demonstrated by recent findings of Hall *et al*. (2016), ecohydrological separation also calls into question our fundamental understanding of nutrient fate and transport in soils. Similar to the implications of ecohydrological separation in rainfall-runoff studies, our view of nutrient export into streams may be biased towards the “younger” component of the nutrient mix that is relatively disconnected from the older component associated with nutrient use by vegetation. In applied terms, ecohydrological separation may call into question current irrigation and nutrient application schemes that rely on assumptions based on a “well mixed” soil water system. Emerging irrigation techniques like partial root drying and regulated deficit irrigation hold great potential for improving water and nutrient use efficiency within the framework of ecohydrological separation.

These scientific advances notwithstanding, we face a myriad of technological challenges for improving the ways with which we interrogate ecohydrological processes at various scales. Techniques for in-situ, high-frequency measurements of liquid and vapor isotopes in the unsaturated zone (e.g. Volkmann and Weiler, 2014) hold great potential for improving the models used in subsurface water fluxes. The range of pore sizes amenable to current extraction techniques (10^{-5}<range>10^{-1} m), however, is orders of magnitude greater than the scales that may be relevant to water uptake by roots (10^{-5}<diameter<10^{-3} m) and/or fungal hyphae (10^{-6}<diameter<10^{-5} m) (Smith *et al*., 2010). Moreover, the destructive nature of sampling related to

these extraction techniques eliminates the opportunity to account for effects on soil properties by soil microfauna and microflora (Hallett *et al*., 2013) and vice versa (Hallett *et al*., 2009; Kravchenko *et al*., 2013). Given the spatio-temporal incongruence between our soil water extraction techniques and plant (root/mycorrhizal) water uptake mechanisms, we need to develop fundamentally new water extraction approaches.

Nevertheless, future research should build on the information synthesized in this body of scholarly work. Explicit representation of ecohydrological separation in hydrological and water chemistry models is an obvious next step, in addition to addressing the aforementioned technological challenges. These hold great potential for future discoveries. The application of ecohydrological separation found in my PhD research has implications that span a wide range of research, from improving the efficiency of water and nutrient applications in agricultural systems to better quantification of runoff generation, nutrient retention and export, and pollutant fate and transport.

6.1 References

1. Brooks, J. R., H. R. Barnard, R. Coulombe, and J. J. McDonnell (2010), Ecohydrologic separation of water between trees and streams in a Mediterranean climate, *Nature Geosci.*, *3*, 100-104.

2. Evaristo, J., S. Jasechko, and J. J. McDonnell (2015), Global separation of plant transpiration from groundwater and streamflow, *Nature*, *525*, 91-94.

3. Evaristo, J., J. J. McDonnell, M. A. Scholl, L. A. Bruijnzeel, and K. P. Chun (2016), Insights into plant water uptake from xylem-water isotope measurements in two tropical catchments with contrasting moisture conditions, *Hydrol. Process.*, *30*, 3210-3227.

4. Evaristo, J., and J. J. McDonnell (In Revision), “Groundwater use by plants not widespread globally". *Nature (Scientific Reports)*

5. Evaristo, J., J.J. McDonnell, M. Kim, J. van Haren, L. Pangle, C. Harman, P. Troch (For Submission), “Source apportionment in the critical zone: Characterizing the fluxes and age distribution of soil water, plant water and deep percolation”. *Water Resources Research*

6. Goldsmith, G. R., L. E. Muñoz-Villers, F. Holwerda, J. J. Mcdonnell, H. Asbjornsen, and T. E. Dawson (2012), Stable isotopes reveal linkages among ecohydrological processes in a seasonally dry tropical montane cloud forest, *Ecohydrology*, *5*, 779-790.

7. Good, S. P., D. Noone, and G. Bowen (2015), Hydrologic connectivity constrains partitioning of global terrestrial water fluxes, *Science*, *349*, 175-177.

8. Hall, S. J., S. R. Weintraub, and D. R. Bowling (2016), Scale-dependent linkages between nitrate isotopes and denitrification in surface soils: implications for isotope measurements and models, *Oecologia*, 1-11.

9. Hallett, P. D., D. S. Feeney, A. G. Bengough, M. C. Rillig, C. M. Scrimgeour, and I. M. Young (2009), Disentangling the impact of AM fungi versus roots on soil structure and water transport, *Plant Soil*, *314*, 183-196.

10. Hallett, P. D., K. H. Karim, A. G. Bengough, and W. Otten (2013), Biophysics of the Vadose Zone: From Reality to Model Systems and Back Again, *Vadose Zone J.*, *12*.

11. Hervé-Fernández, P., C. Oyarzún, C. Brumbt, D. Huygens, S. Bodé, N. E. C. Verhoest, and P. Boeckx (2016), Assessing the “two water worlds” hypothesis and water sources for native and exotic evergreen species in south-central Chile, *Hydrol. Process.*, n/a-n/a.

12. Jasechko, S., Z. D. Sharp, J. J. Gibson, S. J. Birks, Y. Yi, and P. J. Fawcett (2013), Terrestrial water fluxes dominated by transpiration, *Nature*, *496*, 347-350.

13. Kravchenko, A., H. -. Chun, M. Mazer, W. Wang, J. B. Rose, A. Smucker, and M. Rivers (2013), Relationships between intra-aggregate pore structures and distributions of Escherichia coli within soil macro-aggregates, *Appl. Soil Ecol.*, *63*, 134-142.

14. McDonnell, J. J. (2014), The two water worlds hypothesis: ecohydrological separation of water between streams and trees?, *WIREs Water*, *1*, 323-329.

15. Phillips, F. M. (2010), Hydrology: Soil-water bypass, *Nature Geoscience*, *3*, 77-78.

16. Smith, S. E., E. Facelli, S. Pope, and F. A. Smith (2010), Plant performance in stressful environments: interpreting new and established knowledge of the roles of arbuscular mycorrhizas, *Plant Soil, 326,* 3-20.

17. Volkmann, T. H. M. and M. Weiler (2014), Continual in situ monitoring of pore water stable isotopes in the subsurface, *Hydrol. Earth Syst. Sci., 18,* 1819-1833.